

Review

Photoinduced intermolecular hydrogen atom transfer reactions in organic synthesis

Hui Cao,^{1,2} Xinxin Tang,¹ Haidi Tang,^{1,2} Ye Yuan,¹ and Jie Wu^{1,2,*}

SUMMARY

Hydrogen-atom transfer (HAT) provides straightforward methods to generate open-shell radical intermediates from R-H (R = C, Si, etc.) bonds and offers unique opportunities for green and sustainable synthesis. Traditional HAT protocols required harsh conditions and relied on the use of harmful reagents such as Cl₂ and peroxides. An emerging strategy is photoinduced intermolecular HAT, in which transformations can be driven by photocatalysis under mild conditions. In recent years, photoinduced intermolecular HAT reactions have seen substantial development of their versatility, efficiency, and selectivity. This review summarizes recent advances (up to December 2020) in this rapidly expanding research area. The representative examples provided are classified according to the active species responsible for hydrogen atom abstraction. The reactivity, selectivity, and established transformations for each type of active species are briefly summarized. This review aims to provide guidance for the application of photoinduced HAT in R-H functionalization reactions and to inspire further progress in this research area.

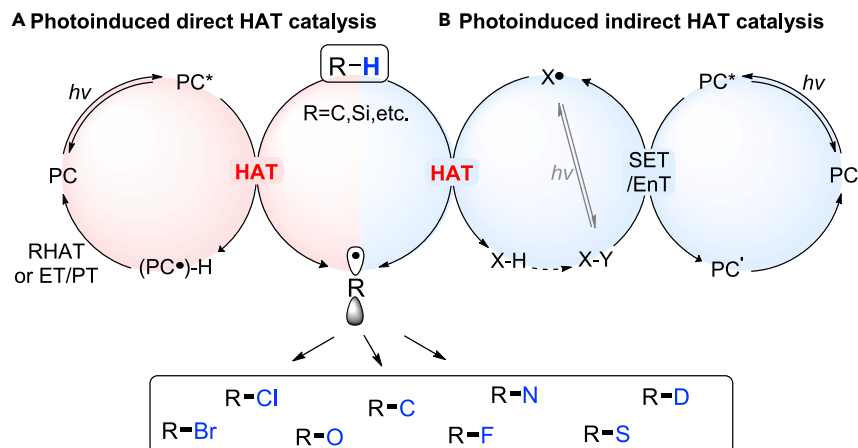
INTRODUCTION

Hydrogen atom transfer (HAT) is defined as the concerted transfer of a proton and an electron from one group to another in a single kinetic step.¹ Over a century of research has highlighted the importance of HAT in diverse processes ranging from hydrocarbon combustion, atmospheric chemistry, and oxidative degradation to enzymatic and biomimetic catalysis.¹ Since R-H bonds (R = C, Si, etc.) are ubiquitous in organic substrates, the direct functionalization of R-H bonds would offer an array of new approaches to the construction and late-stage derivatization of complex molecules.² In this regard, HAT, in an intermolecular fashion, enables straightforward activation of R-H bonds without the need for pre-functionalization or installation of a directing group. It thus represents one of the most atom- and step-economic approaches for R-H functionalizations. Traditionally, intermolecular HAT reactions rely on the use of stoichiometric reagents under harsh conditions. For example, Cl₂ is used for the chlorination of alkanes through ultraviolet (UV) light or high-temperature initiation. In the past decades, much effort has been dedicated to intermolecular HAT through transition metal catalysis (along with the use of peroxides),³ iodine catalysis,⁴ photocatalysis,⁵ electrocatalysis,⁶ and enzymatic catalysis.⁷ With light as an unlimited and traceless energy source, photoinduced HAT catalysis meets the requirements of green chemistry and sustainable synthesis. Compared with photoinduced single electron transfer (SET) catalysis,⁸ photoinduced HAT can activate substrates without the limitation of redox potentials.

This review provides a concise overview of the latest developments of photoinduced intermolecular HAT catalysis (up to December 2020). Applications in asymmetric

The bigger picture

The direct functionalization of unactivated R-H (R = C, Si, etc.) bonds can facilitate and expedite the synthesis of natural products, pharmaceuticals, and agrochemicals. Photoinduced intermolecular hydrogen atom transfer (HAT) catalysis is an appealing approach toward this goal. There has been growing interest in photoinduced intermolecular HAT in the last decade, and this has led to the development of atom- and step-economic synthetic protocols using abundant feedstocks as starting materials. In drug discovery, late-stage C-H functionalization based on photoinduced intermolecular HAT provides access to structural analogs of targets without the need for *de novo* synthesis. In material science, photoinduced HAT reactions offer new handles for material synthesis and post-modification. Photoinduced HAT catalysis has become a ubiquitous and prevailing research area in synthetic chemistry.



Scheme 1. Two different strategies to achieve R-H bond activation through photoinduced intermolecular HAT catalysis

(A) Direct HAT process.

(B) Indirect HAT process.

catalysis, heterogeneous catalysis, material synthesis, and modification are described. The reactivity and selectivity of different HAT catalysts as well as the established transformations are summarized. General guidance on the use of photoinduced HAT catalytic systems for various R-H bond functionalizations is provided. The greenness, efficiency, tunability, and versatility of photoinduced intermolecular HAT catalysis promise to provide a powerful weapon for the synthetic community.

Photoinduced intramolecular HAT reactions in which the reactivity and selectivity differ from intermolecular HAT are not included in this review.⁹ Although closely related, proton-coupled electron transfer (PCET) processes are not covered, as they are guided by different principles.¹⁰ In addition, examples in which the HAT event does not involve the activation of R-H substrates, such as photoinduced alkene hydrofunctionalizations using thiol as a hydrogen atom donor, are not included.¹¹

Mechanisms of photoinduced intermolecular HAT reactions

The activation of R-H bonds through photoinduced intermolecular HAT can occur through two different pathways. The first, shown in [Scheme 1A](#), is direct HAT catalysis, where a photocatalyst (PC) (e.g., benzophenone, neutral eosin Y), upon light excitation and intersystem crossing to an excited triplet state (PC*), directly abstracts an H atom from the R-H substrate. The catalytic cycle subsequently proceeds through a reverse HAT (RHAT) to an intermediate generated in the reaction. Alternatively, the photocatalyst can be regenerated through consecutive electron transfer (ET) and proton transfer (PT) processes.

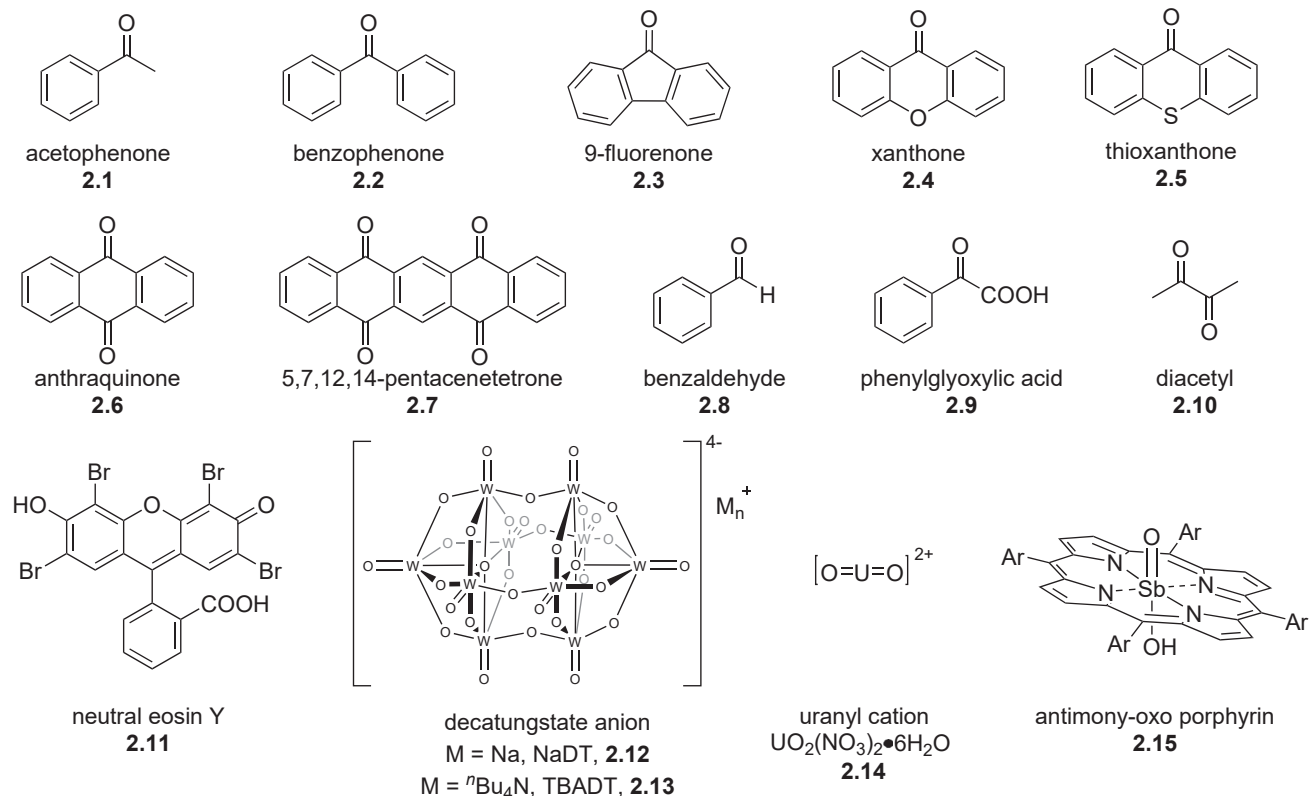
The second mode, shown in [Scheme 1B](#), is the indirect HAT process, in which the excited photocatalyst (PC*) activates another co-catalyst (X-Y) via SET or energy transfer (EnT), and the generated abstractor, X•, promotes the subsequent HAT process. When X-H (e.g., thiol, benzoic acid, amide, and hydrogen chloride) is employed as the co-catalyst, PC* undergoes a reductive quenching process and the generated PC' species is subsequently oxidized to its ground state. The co-catalyst X-H can also be regenerated after the HAT event. In the case of an oxidative quenching or EnT process, regeneration of the co-catalyst X-Y (Y ≠ H) is difficult; hence, a stoichiometric amount of X-Y (e.g., peroxide, persulfate) is usually employed. In

¹Department of Chemistry, National University of Singapore, 3 Science Drive 3, Singapore 117543, Singapore

²National University of Singapore (Suzhou) Research Institute, 377 Lin Quan Street, Suzhou Industrial Park, Suzhou, Jiangsu 215123, China

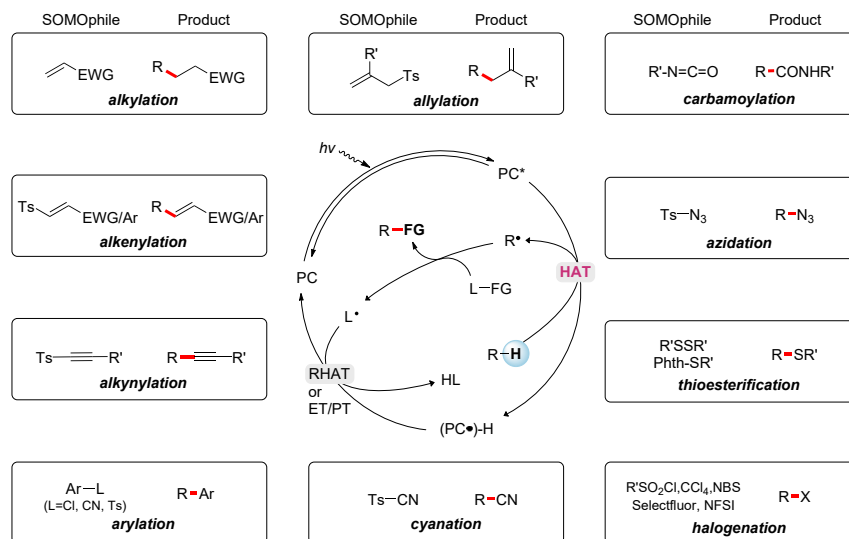
*Correspondence: chmjie@nus.edu.sg

<https://doi.org/10.1016/j.cheecat.2021.04.008>



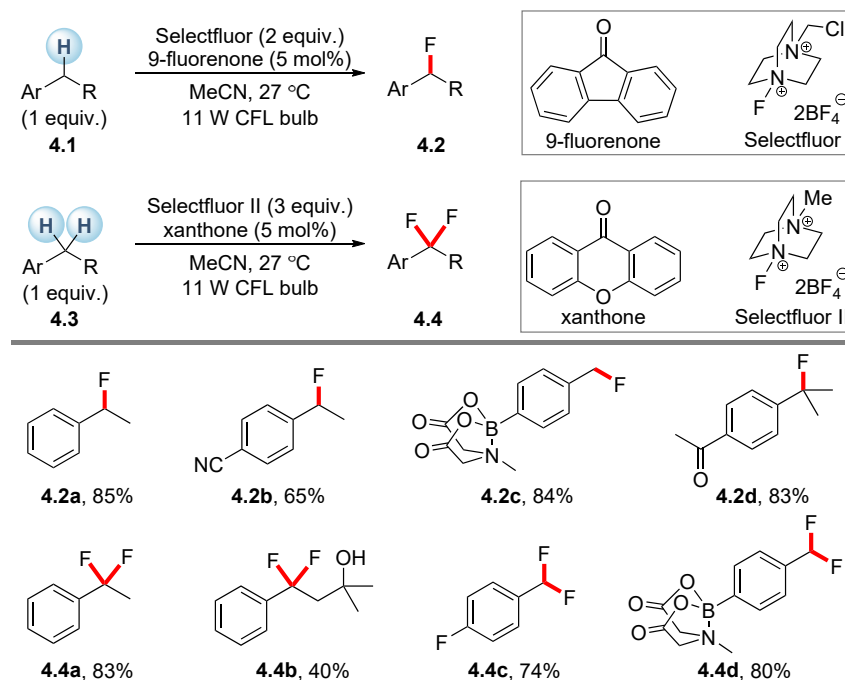
Scheme 2. Representative direct HAT photocatalysts

In addition to the SET and EnT pathways, the direct photoexcitation of the HAT reagent X-Y (Y ≠ H) to generate an abstractor X· has also been reported. With their similarity to EnT processes and the stoichiometric use of X-Y reagents, these examples are classified into indirect HAT modes.



Scheme 3. Photoinduced direct HAT reactions with representative SOMOphiles

EWG, electron-withdrawing group; Ts, tosyl; Ar, aryl; FG, functional group.

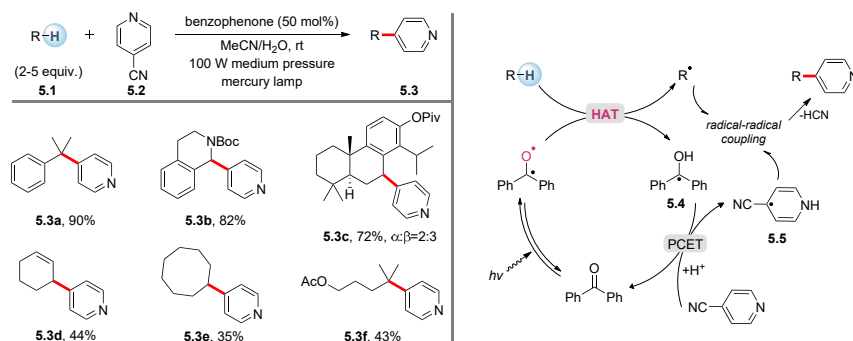


Scheme 4. Photoinduced benzylic monofluorination and difluorination

The rate of hydrogen abstraction from an R-H bond by abstractor X· depends on the strength of the bond broken (R-H), the strength of the bond being formed (X-H), polar effects in the transition state, and steric effects.¹² Once generated, the active open-shell R· species can be subjected to numerous transformations, including the formation of R-D, R-C, R-N, R-O, R-F, R-S, R-Cl, and R-Br bonds. To clearly show the reactivity and selectivity of different abstractors, these transformations are classified in this review according to the active species responsible for the HAT.

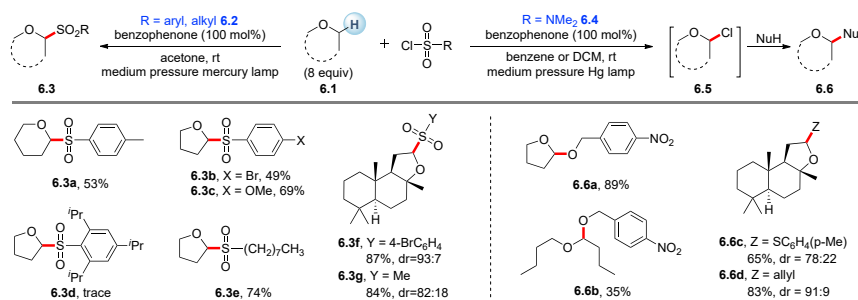
PHOTOINDUCED DIRECT HAT CATALYSIS

Representative direct HAT photocatalysts are shown in [Scheme 2](#). The photocatalysts available for photoinduced direct HAT chemistry include aromatic ketones and carbonyl compounds such as benzaldehyde (2.8), diacetyl (2.10), neutral eosin



Scheme 5. Photoinduced 4-pyridination of C(sp³)-H bonds

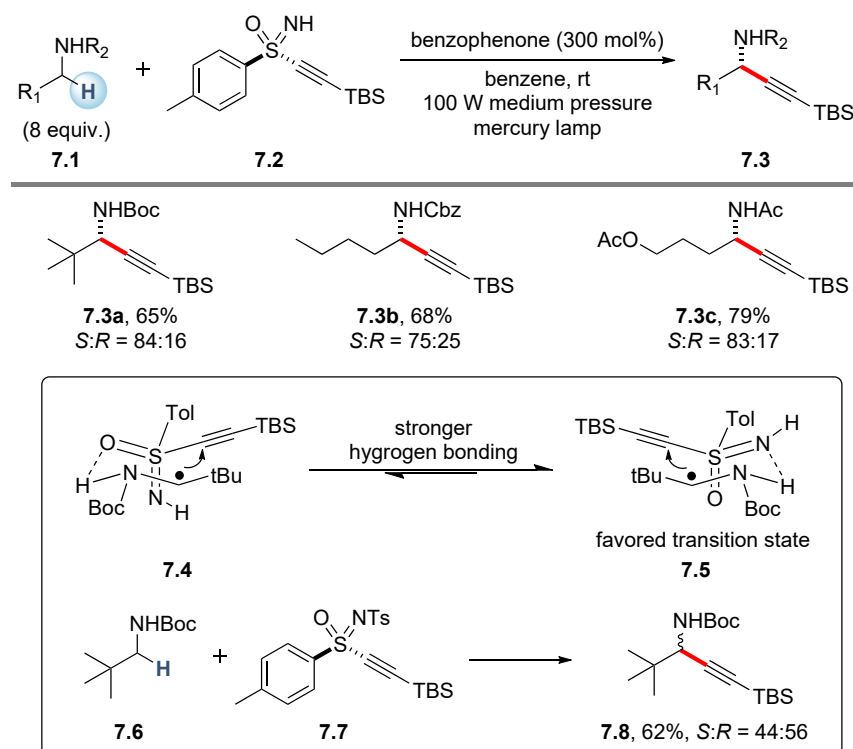
Boc, tert-butyloxycarbonyl; Piv, pivalic.



Scheme 6. Sulfonation and chlorination of ether α -C-H bonds by using different SOMophiles

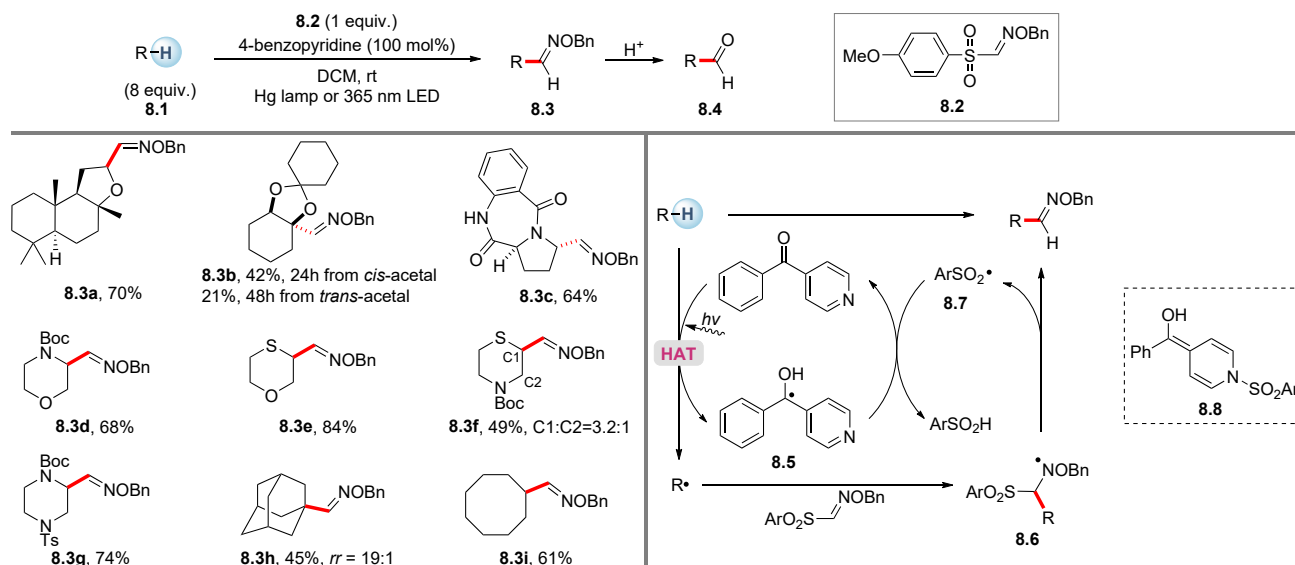
Y (2.11), the decatungstate anion [W₁₀O₃₂]⁴⁻ (2.12, 2.13), the uranyl cation [UO₂]²⁺ (2.14), and antimony-oxo porphyrin (2.15).

The direct HAT photocatalysts share some common features: (1) an oxo group in the structure, (2) an easily accessible triplet state with a sufficiently long lifetime (generally >10 ns), and (3) the formation of an electrophilic oxygen center in the excited state, which is capable of abstracting H atoms from substrates. With these features, various reactions of R-H bonds with radical acceptors (SOMophiles; SOMO stands for singly occupied molecular orbital) have been developed, including alkylation, alkenylation, alkynylation, arylation, allylation, cyanation, carbamoylation, azidation, thioesterification, and halogenation (Scheme 3). In a general mechanism, the radical R· that is produced by HAT from an R-H bond could undergo radical addition, possibly followed by elimination of a leaving radical L·, or radical substitution. The



Scheme 7. Photoinduced enantioselective alkynylation of C(sp³)-H bonds

TBS, tert-butyldimethylsilyl; Cbz, carboxybenzyl; Ac, acetyl; Tol, p-tolyl.



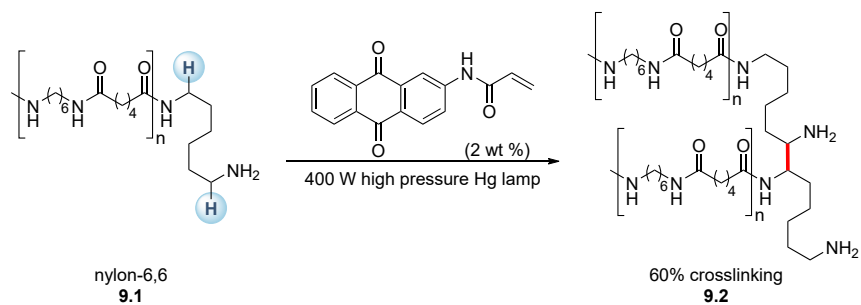
Scheme 8. Photoinduced formal formylation of C(sp³)-H bonds
Bn, benzyl.

newly generated radical could complete the photocatalytic cycle through a RHAT process or sequential ET/PT process. Alternatively, the photocatalytic cycle could be turned over by external oxidants (e.g., air) in the net-oxidative reactions. In an effort to be insightful rather than exhaustive, selected representative direct HAT reactions with SOMOphiles are highlighted in this section.

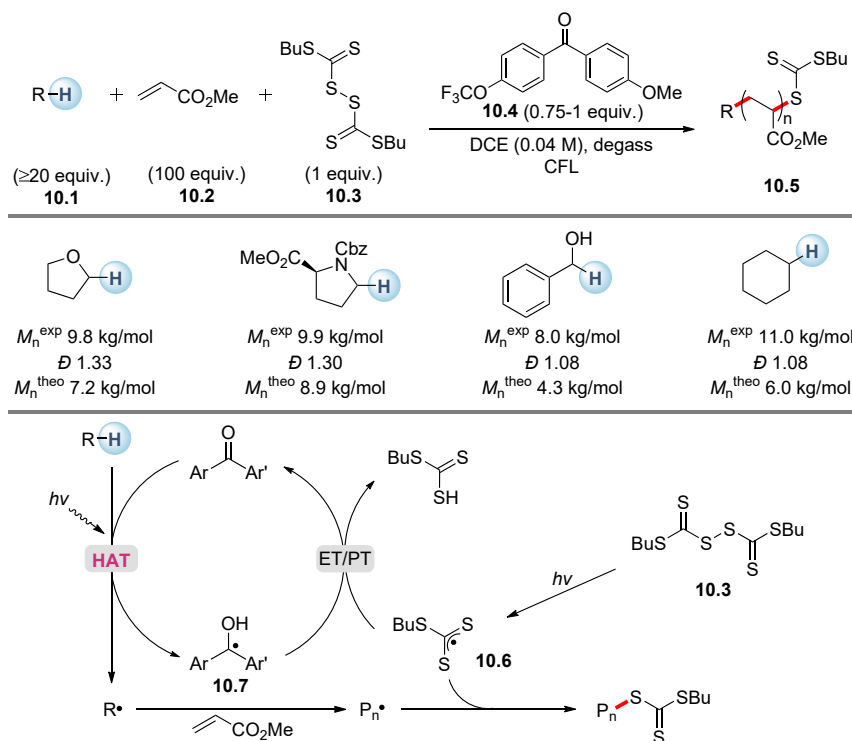
Aromatic ketone and aromatic ketone derivatives

Upon excitation with light, aromatic ketones can undergo rapid and efficient intersystem crossing (e.g., benzophenone, $K_{ISC} \sim 10^{11} \text{ s}^{-1}$, $\Phi_{ISC} = 1.0$), because their $S_1(n, \pi^*)$ and $T_1(\pi, \pi^*)$ are close in energy.¹³ The hydrogen-atom-abstracting ability of triplet aromatic ketones has been known since the birth of photochemistry.¹⁴ The ketyl radical intermediate derived from triplet aromatic ketones after abstracting H could undergo irreversible dimerization to form a pinacol product due to the relatively slow RHAT process. A high loading of aromatic ketone photocatalysts was generally required to offset this problem.

The HAT ability of photoexcited aromatic ketones was put to use by Chen and co-workers, who demonstrated selective benzylic C-H fluorination using 1 equiv of



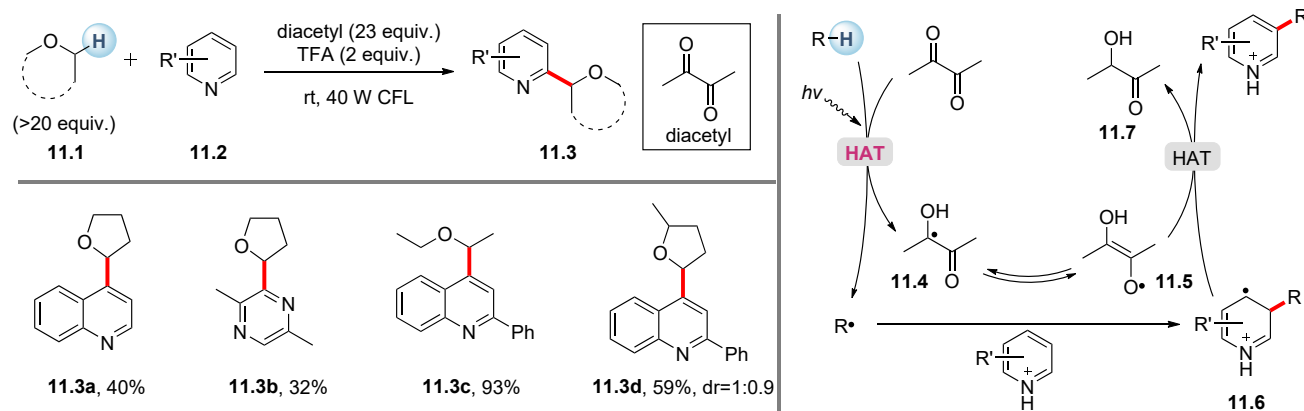
Scheme 9. Photoinduced cross-linking of nylon-6,6



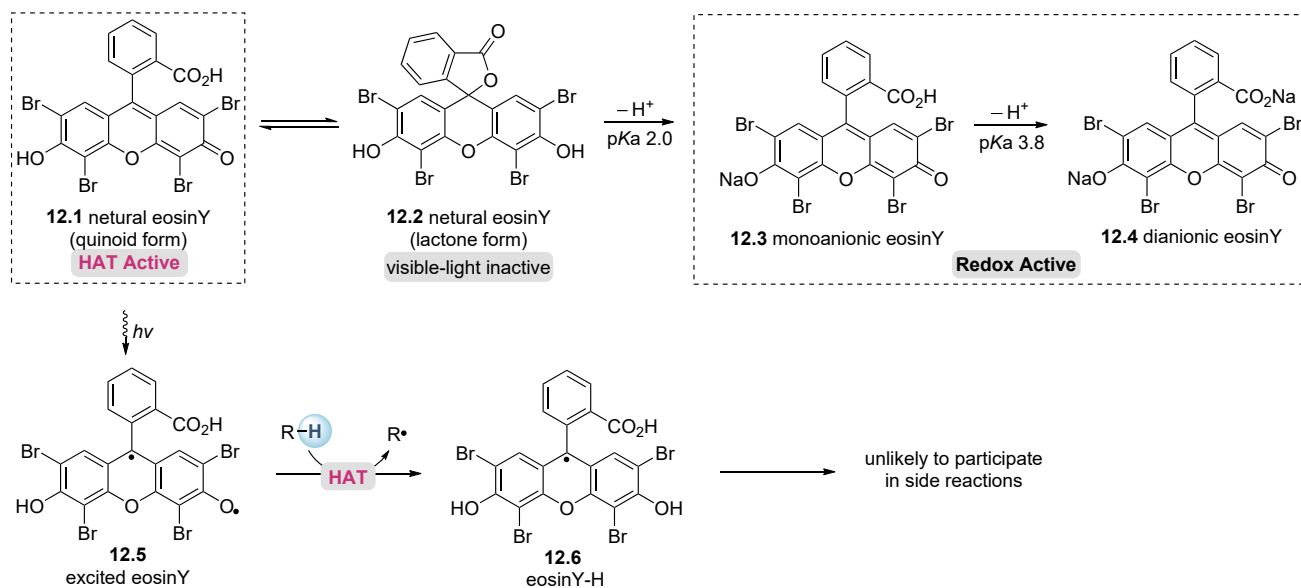
Scheme 10. Photoinduced polymerization grafting from C-H bonds

Bu, *n*-butyl.

the C-H substrate (Scheme 4).¹⁵ With 9-fluorenone as the direct HAT photocatalyst and Selectfluor (1-chloromethyl-4-fluoro-1,4-diazoniabicyclo[2.2.2]octane bis(tetrafluoroborate)) as the fluorination reagent, high yields of the monofluorinated products were obtained. Interestingly, switching 9-fluorenone and Selectfluor to xanthone and Selectfluor II (*N*-fluoro-*N*'-methyl triethylenediamine bis(tetrafluoroborate)), respectively, resulted in exclusive benzylic C-H difluorination. Under the same conditions, 9-fluorenone gave only 2% of **4.4a** and 62% of the monofluorinated **4.2a**. The authors suggested that the more electron-rich xanthone was more reactive toward HAT and thus could overcome the deactivating effect of the first fluorination.

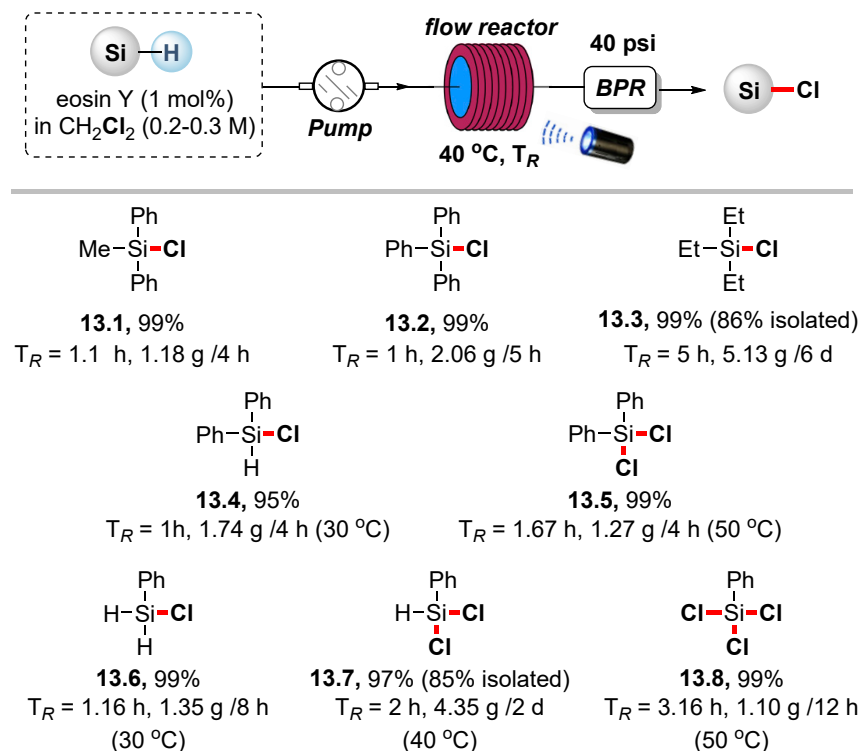


Scheme 11. Diacetyl as a direct HAT photosensitizer in Minisci alkylation



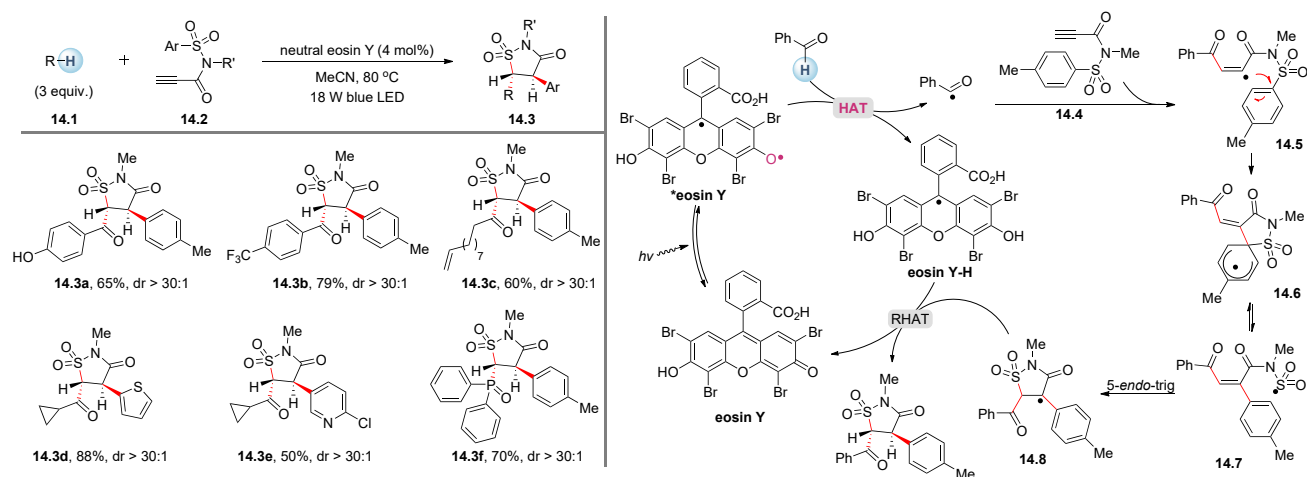
Scheme 12. Equilibration between different forms of eosin Y and their photoreactivities

In 2013, Inoue and co-workers reported C(sp³)-H 4-pyridination using benzophenone and 4-cyanopyridine in aqueous MeCN under UV irradiation.¹⁶ In this reaction, shown in [Scheme 5](#), 2–5 equiv of the C-H substrates was employed. A broad scope of benzylic, allylic, methine, and methylene C-H bonds were found to be competent



Scheme 13. Neutral eosin Y photocatalyzed silane chlorination

BPR, back pressure regulator. Reprinted with permission from Fan et al.²⁹ Copyright 2019 WILEY-VCH.



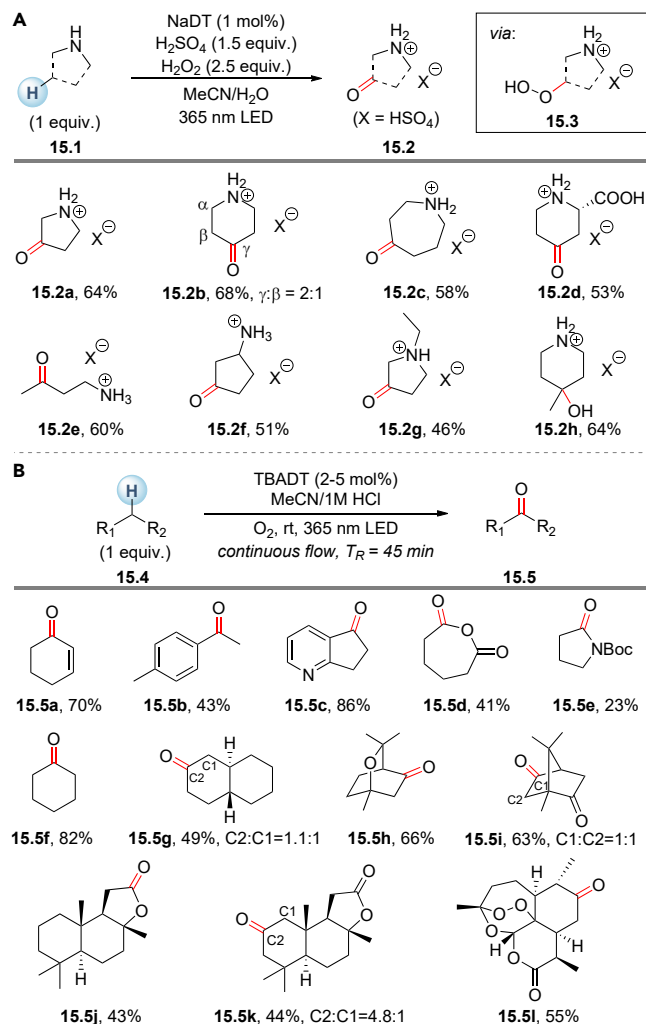
Scheme 14. Photoinduced radical Smiles rearrangement with neutral eosin Y

substrates. The most electron-rich methine C-H bond of a linear alkane (4-methylpentyl acetate) underwent 4-pyridination to give **5.3f**. Notably, *O*-pivaloyl totarol was converted to the pyridine derivative (**5.3c**) with excellent site selectivity. Despite its intrinsically higher reactivity, no pyridination occurred at the isopropyl group, as it is sterically shielded by the nearby pivalic group. Mechanistic investigation suggests that after HAT, the electron-rich ketyl radical (**5.4**) and the electron-deficient 4-cyanopyridine reorganize through a PCET process, resulting in the formation of the carbon radical (**5.5**). The coupling of the transient radical ($R\cdot$) with the persistent radical (**5.5**) gives the final aromatized product after releasing HCN.¹⁷

The choice of SOMOphile could have a dramatic influence on the direct HAT photocatalysis reaction outcome, as demonstrated by Kamijo et al. (Scheme 6). With photoexcited benzophenone, the sulfonation of ethers was achieved using alkyl or aryl sulfonyl chlorides (**6.2**),¹⁸ while efficient chlorination of ethers could be accomplished using *N,N*-dimethylsulfonyl chloride (**6.4**).¹⁹ Control experiments showed that chlorinated ethers and sulfonated ethers could not be interconverted under the reaction conditions, but the exact reason for the dramatically different reactivity of these SOMOphiles is unclear.

Subsequently, in 2015, an interesting enantioselective radical alkynylation reaction was reported by Inoue and co-workers (Scheme 7).²⁰ Using benzophenone and chiral *p*-tolyl *tert*-butyldimethylsilylethynyl sulfoximine (**7.2**) with photoirradiation, $C(\text{sp}^3)\text{-H}$ bonds in carbamates and amides were alkynylated with relatively high enantiomeric excess. The chirality in the sulfoximine was efficiently transmitted to the alkyne products. It was proposed that the hydrogen bonding between $\text{HN}=\text{S}$ and HNBoc was stronger than that between $\text{O}=\text{S}$ and HNBoc , resulting in a favored transition state (**7.5**) and formation of (*S*)-**7.3**. This was evidenced by the reaction using *N-p*-tosyl-substituted sulfoximine (**7.7**). The observed low enantioselectivity of **7.8** was in accord with the decreased basicity of the $\text{N}=\text{S}$ in **7.7** and decreased strength of the hydrogen bonding.

The introduction of a formyl group to $C(\text{sp}^3)\text{-H}$ bonds is synthetically useful because of the dual reactivities of aldehydes as electrophiles and nucleophiles. An aldoxime can be considered to be a masked formyl group, and Kamijo et al. developed arylsulfonyl oxime reagents for substitutive introduction of an aldoxime functional group

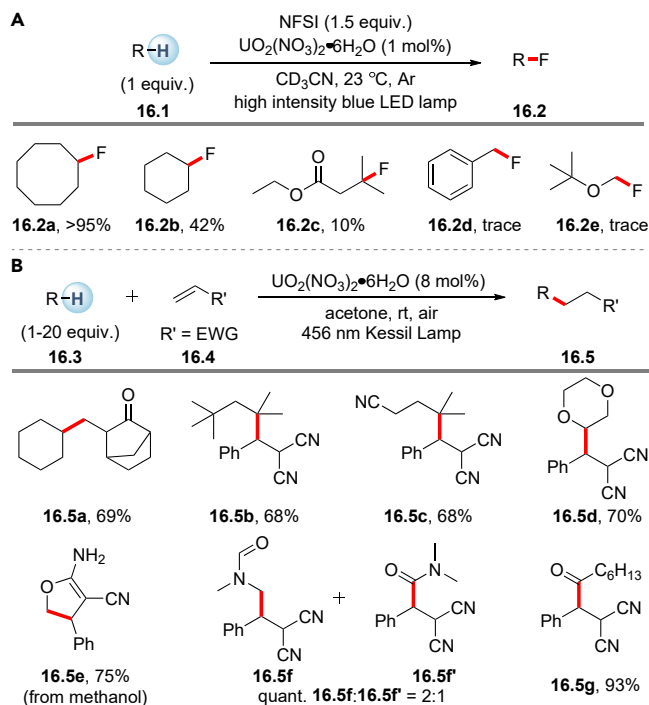


Scheme 15. Photoinduced C(sp³)-H oxidation with decatungstate anion

(A) Photoinduced remote C-H oxidation of aliphatic amines. NaDT, sodium decatungstate.
(B) C(sp³)-H oxidation enabled by decatungstate photocatalysis in flow systems.

(Scheme 8).²¹ The use of electron-deficient 4-benzoylpyridine instead of benzophenone led to higher yields. Transformation of ethers, amides, carbamates, thioethers, methine, and methylene C-H bonds gave aldoxime products, which could be converted to aldehydes by treatment with acid. The reactions of acetals derived from *cis*- and *trans*-cyclohexanediol furnished the same product (8.3b) in 42% (24 h) and 21% (48 h) yields, respectively. The higher reactivity of the *cis*-acetal was attributed to the reduced steric hindrance and higher electron density of the equatorial C-H bond. Based on intramolecular competitive reactions, the reactivity order of C-H bonds in this transformation was classified as α -thioether \geq α -N-Boc $>$ α -ether $>$ methine $>$ methylene C-H bonds. Interestingly, α -N-Boc C-H bonds were selectively functionalized in the presence of α -N-Ts C-H bonds (8.3g). For the RHAT step, it was proposed that the eliminated sulfone radical (8.7) coupled with ketyl radical (8.5) and the ketone was regenerated from the coupled intermediate (8.8).

In addition to functionalization of small molecules, photoexcited aromatic ketones have also been applied to the modification of polymers. An interesting application



Scheme 16. Photoinduced HAT reactions with uranyl cation

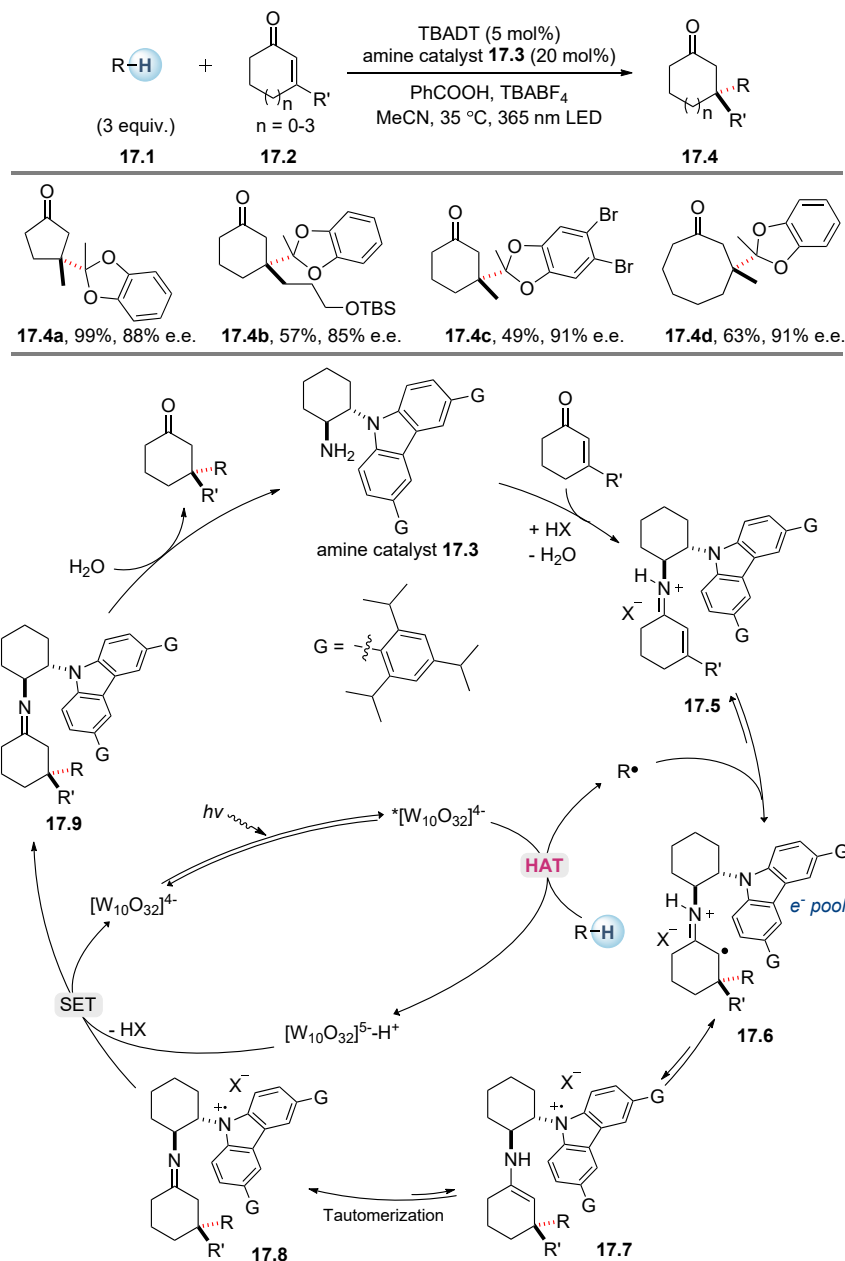
(A) Photoinduced C(sp³)-H fluorination. NFSI, N-fluorobenzenesulfonimide.
 (B) Photoinduced C(sp³)-H alkylation.

is the photoinduced cross-linking of nylon-6,6 (Scheme 9).²² Sixty percent cross-linking was observed when 2 wt % 2-acrylamido anthraquinone was employed under light irradiation. Mechanistic studies showed that triplet anthraquinone could either abstract an H atom or oxidize the terminal amine or amide in the polymer backbone. Both pathways would lead to the generation of macro-alkyl radicals, which then underwent cross-linking.

As C-H bonds are ubiquitous in polymer backbones and functional molecules, polymerization grafting from a C-H bond represents an ideal approach to polymer conjugation as well as introduction of functionality at the end of a polymer chain. In 2020, Fors et al. demonstrated that C-H bonds can serve as radical initiators for controlled radical polymerization through the use of a benzophenone derivative under visible light irradiation (Scheme 10).²³ A variety of ethers, amides, alcohols, and alkanes are suitable initiators for the HAT-RAFT (reversible addition-fragmentation chain transfer) polymerization with generally narrow dispersity (low *D*). Moreover, the α -ether C-H bonds in commercial poly(ethylene glycol) (PEG) polymers could also be activated to obtain graft co-polymers without PEG degradation. In the proposed mechanism, the R \cdot generated from HAT adds to the monomer to form a propagating polymer chain P_n \cdot . Under visible light, two trithiocarbonyl radicals (10.6) are formed after homolysis of the disulfide (10.3). A molecule of 10.6 can combine with the electrophilic chain end, and another molecular of 10.6 is reduced by the ketyl radical (10.7) to turn over the photocatalyst.

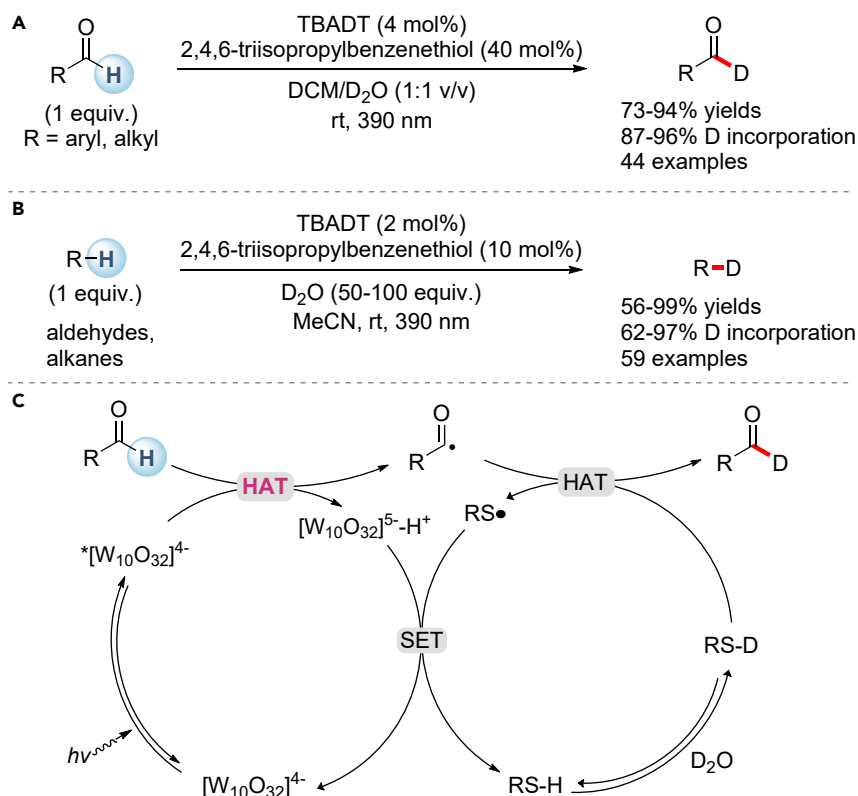
Diacetyl

In theory, almost all carbonyl compounds are photoactive, as their S₁(n,π*) and T₁(π,π*) states are close in energy. In fact the simplest ketone, acetone, is capable



Scheme 17. Photoinduced enantioselective C-C bond formation through decatungstate and iminium catalysis

of abstracting a hydrogen atom when irradiated by short-wavelength UV light (e.g., 254 nm).²⁴ In 2019, Li and co-workers reported that diacetyl, the smallest visible-light-sensitive ketone (absorption up to 460 nm), could act as a direct HAT photosensitizer for metal-free cross-dehydrogenative Minisci coupling reactions (Scheme 11).²⁵ Cyclic and acyclic ethers were successfully coupled with electron-deficient heteroarenes under irradiation from a compact fluorescent lamp (CFL). The selective reaction of 2-methyl tetrahydrofuran at the less hindered α -ether C-H site gave a moderate yield of the desired product (11.3d). A plausible mechanism was proposed in which excited diacetyl abstracts a hydrogen atom from the ether to



Scheme 18. Photoinduced C-H deuteration through decatungstate and thiol catalysis

(A) Formyl C-H deuteration reported by Wang and co-workers.⁴³

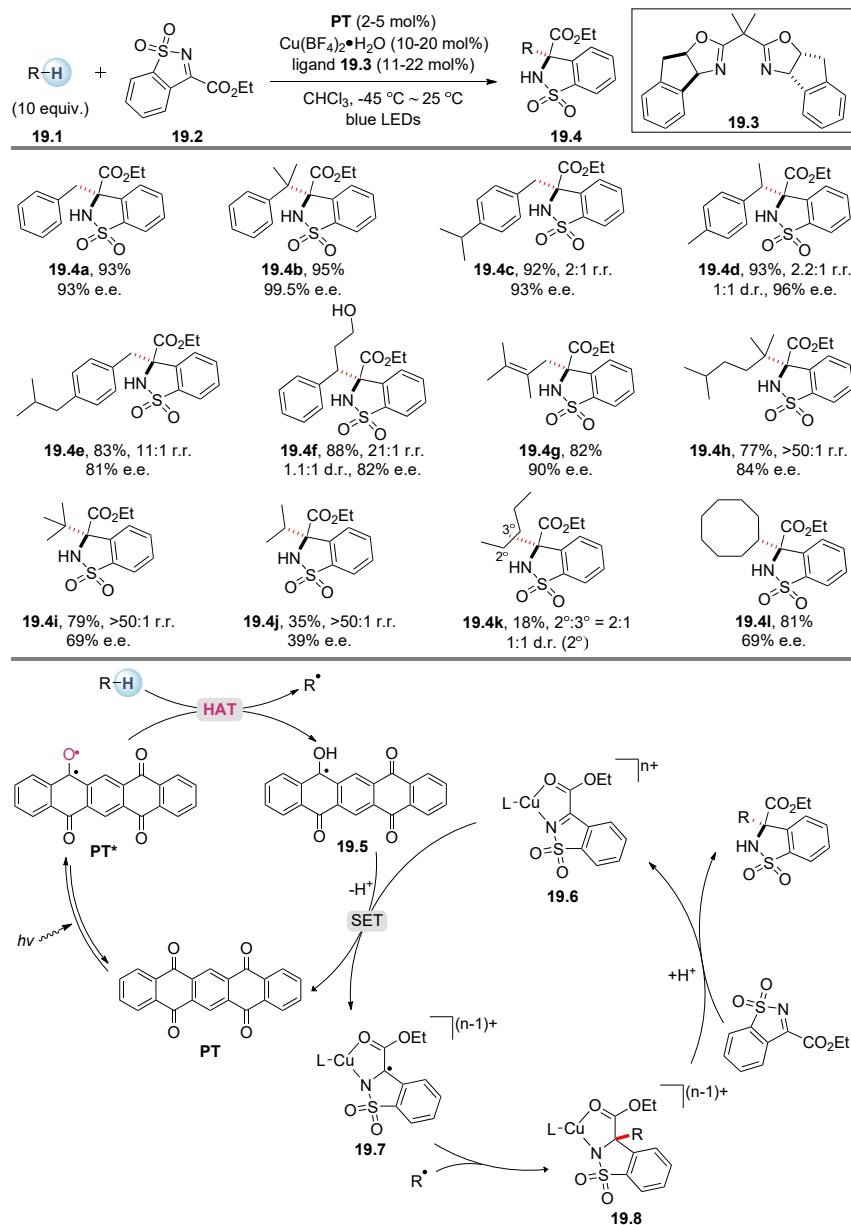
(B) Formyl C-H and hydridic C(sp³)-H deuteration reported by Wu and co-workers.⁴⁴

(C) Proposed mechanism for formyl C-H deuteration.

generate R[•], which couples with the protonated heteroarene to give 11.6. The ketyl radical (11.4) could undergo tautomerization to form an enol radical (11.5), which abstracts a second hydrogen atom from 11.6 to furnish the final product. Both diacetyl and its reduced product, acetoin, could be easily removed by aqueous workup or at reduced pressure.

Neutral eosin Y

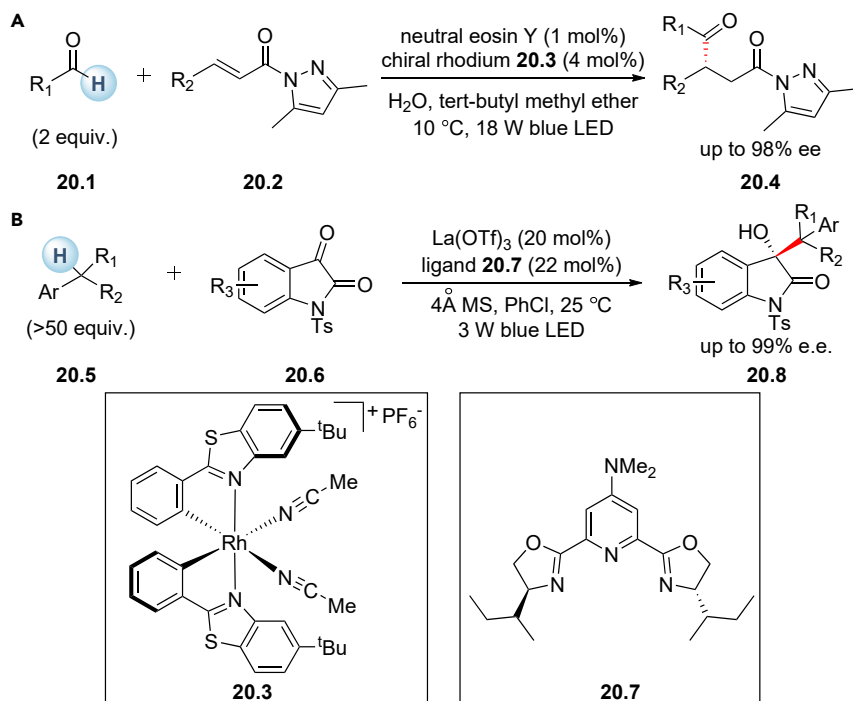
In its anionic form, the organic dye eosin Y is a well-known organic photocatalyst for visible light-driven SET-based transformations.²⁶ However, Wu and co-workers demonstrated that eosin Y, in its neutral form, could behave as an efficient visible light-driven direct HAT photocatalyst.²⁷ In solution, eosin Y can have four different structures: the neutral quinoid form (12.1), the neutral lactone form (12.2), the mono-anionic form (12.3), and the dianionic form (12.4) (Scheme 12).²⁸ Wu and co-workers presented spectroscopic evidence for the neutral quinoid eosin Y (12.1) being the HAT-active species. After the excited neutral eosin Y (12.5) abstracts an H atom, a relatively stable and sterically hindered radical intermediate (12.6) is formed, which is unlikely to participate in dimerization or other side reactions, thus enabling a more effective RHAT process. This feature of neutral eosin Y, along with its inexpensive, readily available, visible-light-active and metal-free character, makes it an appealing direct HAT photocatalyst. To date, neutral eosin Y has been utilized for the alkylation, allylation, alkenylation, arylation, cyanation, oxidation, and chlorination of various C-H, Si-H, and P-H bonds.^{27,29,30}



Scheme 19. Asymmetric C(sp³)-H functionalization through the merger of a ketone photocatalyst with a chiral copper Lewis acid catalyst

In 2019, Fang, Wu, and co-workers disclosed a neutral eosin Y-photocatalyzed silane chlorination using dichloromethane as a chlorinating agent (Scheme 13).²⁹ Gram-scale production of synthetically versatile silyl chlorides proceeded quantitatively in continuous-flow micro-tubing reactors under blue light irradiation (13.1–13.3). Stepwise chlorination of di- and trihydrosilanes was successfully achieved in a highly selective manner (13.4 versus 13.5; 13.6 versus 13.7 versus 13.8). The key to this relied on the excellent mixing efficiency and precise control of reaction temperature and residence time associated with continuous-flow micro-tubing reactors.

A neutral eosin Y-catalyzed radical Smiles rearrangement was recently achieved by Wu et al. (Scheme 14).³⁰ A wide scope of aldehydes and diaryl *H*-phosphine oxides



Scheme 20. Asymmetric transformations through the merger of photoinduced direct HAT with chiral Lewis acid catalysis

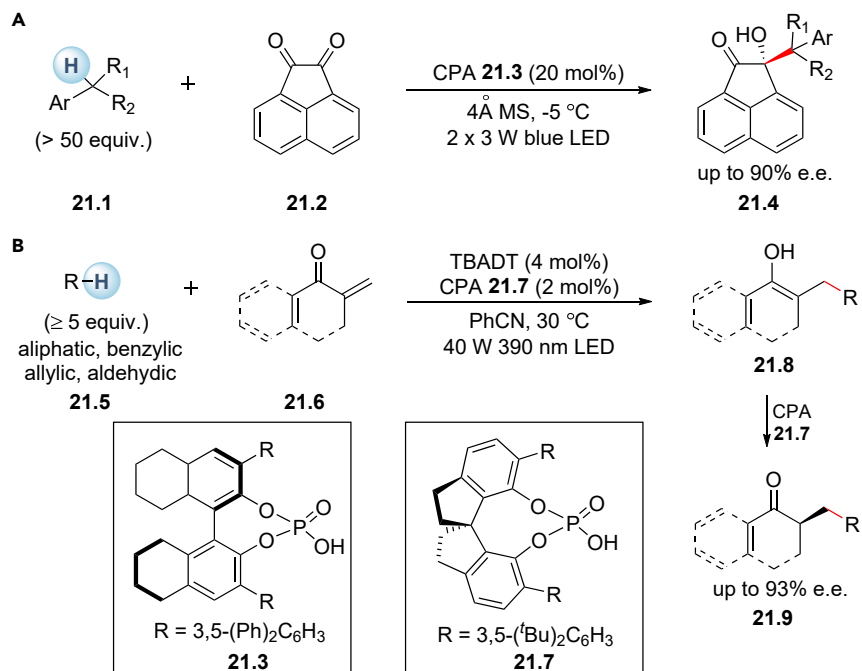
(A) Enantioselective coupling of α,β -unsaturated amide with aldehyde.
(B) Enantioselective coupling of isatin with alkyl benzene.

could be used to form isothiazolidin-3-one 1,1-dioxide heterocycles as single diastereomers under blue light irradiation. Interestingly, the SO_2 moiety was incorporated into the heterocycle product rather than being released in typical radical Smiles rearrangements. The excited *eosin Y could abstract an H atom from the aldehyde to deliver an acyl radical. Upon addition of this nucleophilic acyl radical to an electron-deficient *N*-arylsulfonyl propionamide, a vinyl radical species (**14.5**) is generated and initiates a subsequent Smiles rearrangement to afford a presumed sulfonyl radical (**14.7**). The sulfonyl radical adds to the tethered alkene via 5-endo-trig cyclization to give an electron-deficient benzylic radical (**14.8**), which is capable of regenerating eosin Y via a RHAT process, furnishing the isothiazolidinone product simultaneously.

Decatungstate anion

The decatungstate anion ($[\text{W}_{10}\text{O}_{32}]^{4-}$), a polyoxometalate that possesses high-energy excited states, has been widely used as a direct HAT photocatalyst for the promotion of functionalization of small molecules as well as fullerenes, carbon nanotubes, and PEG polymers.³¹ A unique feature of excited decatungstate anion is its strong hydrogen abstracting power. The rate constant for hydrogen abstraction from cyclohexane with excited tetrabutylammonium decatungstate (TBADT) is 2 orders of magnitude higher than that of excited ketones (ca. 10^7 versus $10^5 \text{ M}^{-1} \text{ s}^{-1}$ in acetonitrile at 298 K).³² This feature was utilized by Noël and co-workers, who demonstrated the functionalization of light hydrocarbons, including isobutane, propane, ethane, and even methane, using decatungstate photocatalysis in flow systems.³³

Schultz et al. developed an oxidation strategy for late-stage synthesis of value-added ketones from amines via decatungstate photocatalysis (Scheme 15A).³⁴



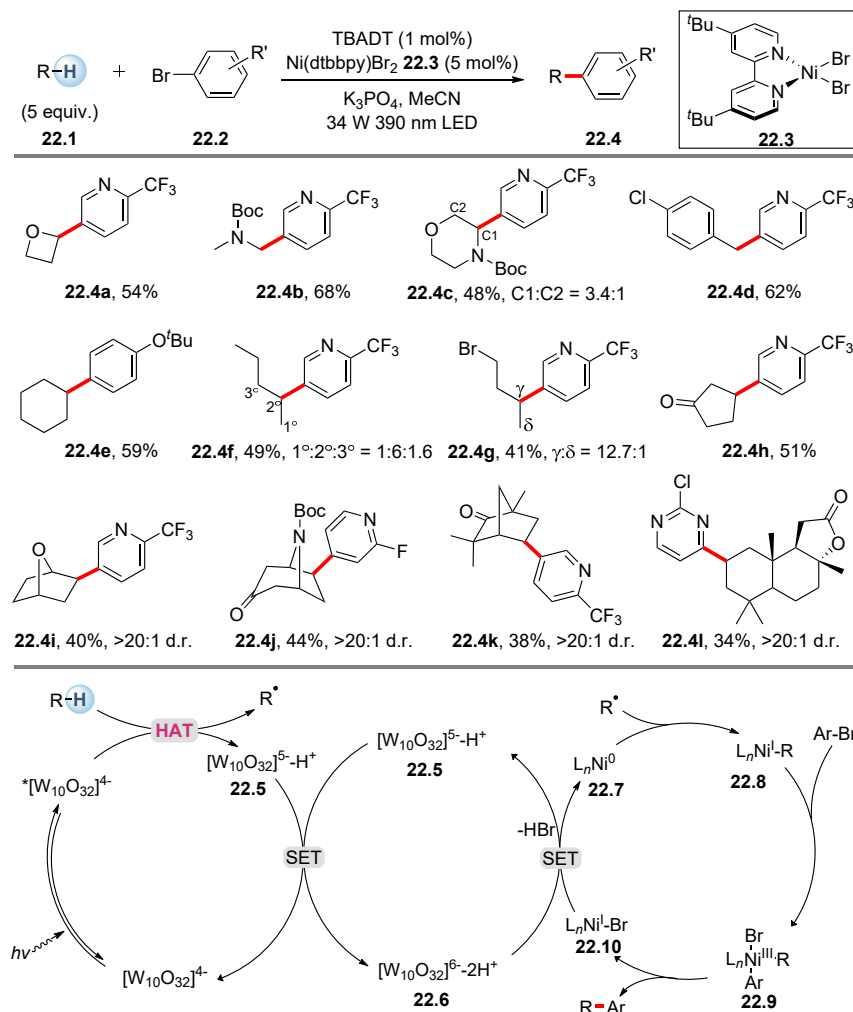
Scheme 21. Asymmetric transformations through the merger of photoinduced direct HAT with chiral Brønsted acid catalysis

(A) Enantioselective coupling of acenaphthoquinone with alkyl benzene.

(B) Enantioselective coupling of enone with hydrocarbon.

Using H₂O₂ as the terminal oxidant, the remote positions of aliphatic amines, the most electron-rich sites under acidic conditions, could be selectively oxidized. Primary, secondary, and tertiary amines are all viable substrates. The oxidation of piperidine gave a 2:1 mixture of γ : β keto products (15.2b), but exclusive oxidation at the most remote C-H site was observed for azepane (15.2c), suggesting that an ion pair comprising the substrate and the catalyst might be involved in the HAT event. Remarkably, the oxidation of butylamine yielded 15.2e as a single regioisomer. The hydroperoxide (15.3) was identified by *in situ* NMR and electrospray ionization mass spectrometry analysis as the intermediate. Finally, a 5 g scale synthesis was demonstrated in a continuous-flow reactor with O₂ gas as the oxidant. Further development in C(sp³)-H oxidation with decatungstate photocatalysis was demonstrated by Noël and co-workers in 2018 (Scheme 15B).³⁵ The addition of hydrochloric acid greatly improved the reaction efficiency, probably due to the improved stability of the decatungstate ion under acidic conditions. The use of a micro-flow reactor enhanced the light penetration and liquid/oxygen mixing. Using 1 equiv of the substrate, both activated and unactivated C-H bonds were efficiently oxidized. As has been showcased in many reports, the regioselectivity in decatungstate catalysts is dictated by dual electronic and steric effects.³⁶ For instance, the more electron-rich benzylic site was preferentially functionalized to give 15.5c, and the less sterically hindered methylene sites in eucalyptol were selectively targeted to afford 15.5h. Site-selective oxidation of natural scaffolds such as (-)-embroider (15.5j), (+)-sclareolide (15.5k), and artemisinin (15.5l) was demonstrated.

The immobilization of direct HAT photocatalysts on solid supports is an attractive pathway toward heterogeneous HAT catalysis and sustainable synthesis. In 2016,

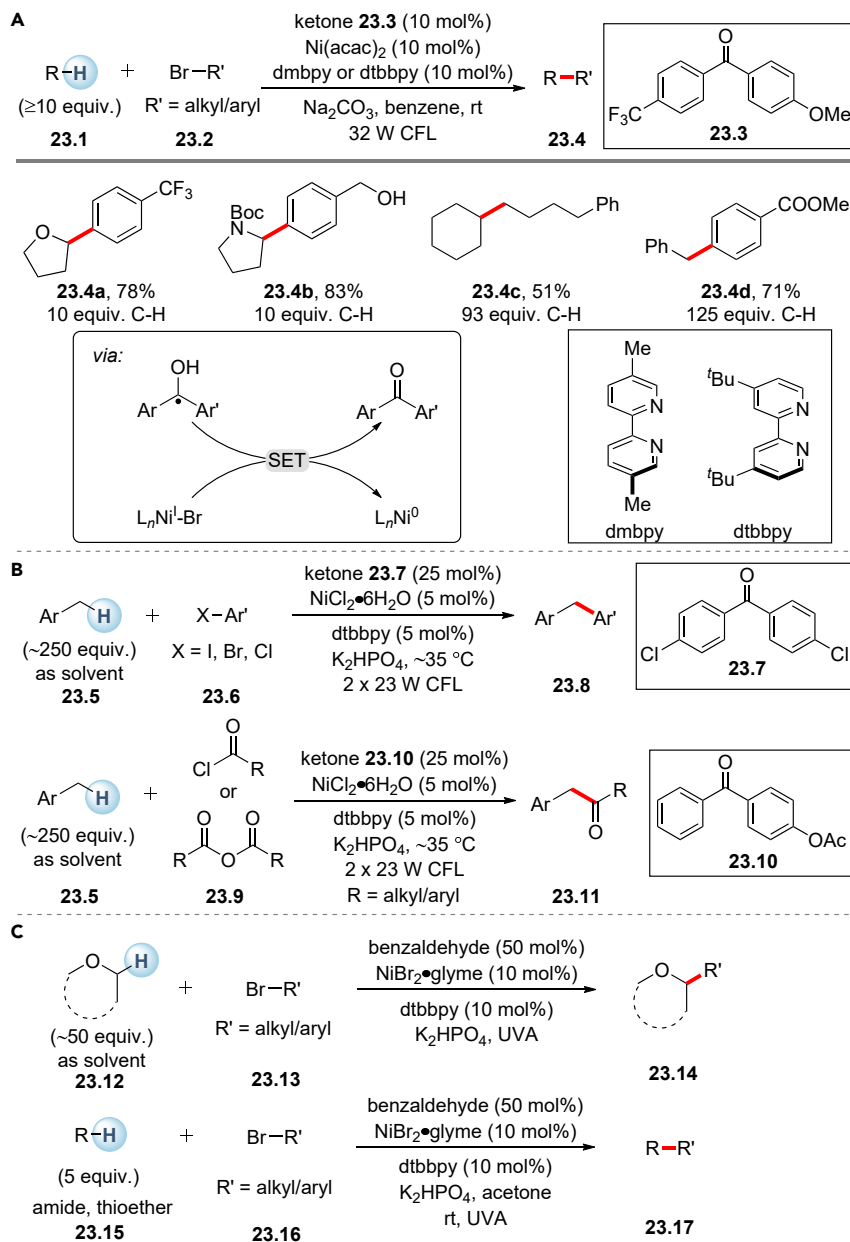


Scheme 22. Photoinduced cross-coupling of C(sp³)-H bonds with aryl halides through decatungstate and nickel catalysis

Duan and co-workers developed a hybrid material, [Cu₄(bpy)₆Cl₂(W₁₀O₃₂)·3H₂O (DT-BPY) for photoinduced alkylation of aliphatic nitriles.³⁷ The DT-BPY was synthesized by a solvothermal reaction of TBADT, Cu(ClO₄)₂·6H₂O, and the ligand 4,4'-bipyridine (BPY) at pH 2.3. Decatungstate anion was embedded in the pores of metal-organic frameworks of Cu-BPY via electrostatic attraction. The efficiency of the heterogeneous catalyst was comparable to that of the homogeneous decatungstate catalyst. It was thought that the one-dimensional hydrophilic/hydrophobic channels facilitated the adsorption of reaction substrates. Through simple filtration, the solid catalyst DT-BPY can be recycled at least three times without significant loss of efficiency.

Uranyl cation

In 2016, Sorenson and co-workers reported the fluorination of unactivated C(sp³)-H bonds with uranyl nitrate hexahydrate, [UO₂(NO₃)₂]·6H₂O, and *N*-fluorobenzenesulfonimide under blue-light irradiation (Scheme 16A).³⁸ The use of uranyl acetate, [UO₂(OAc)₂]·4H₂O, led to much decreased conversion (from 52% to 8%), indicating the importance of the O-ligand. A different study on high-valent metal-oxygen HAT



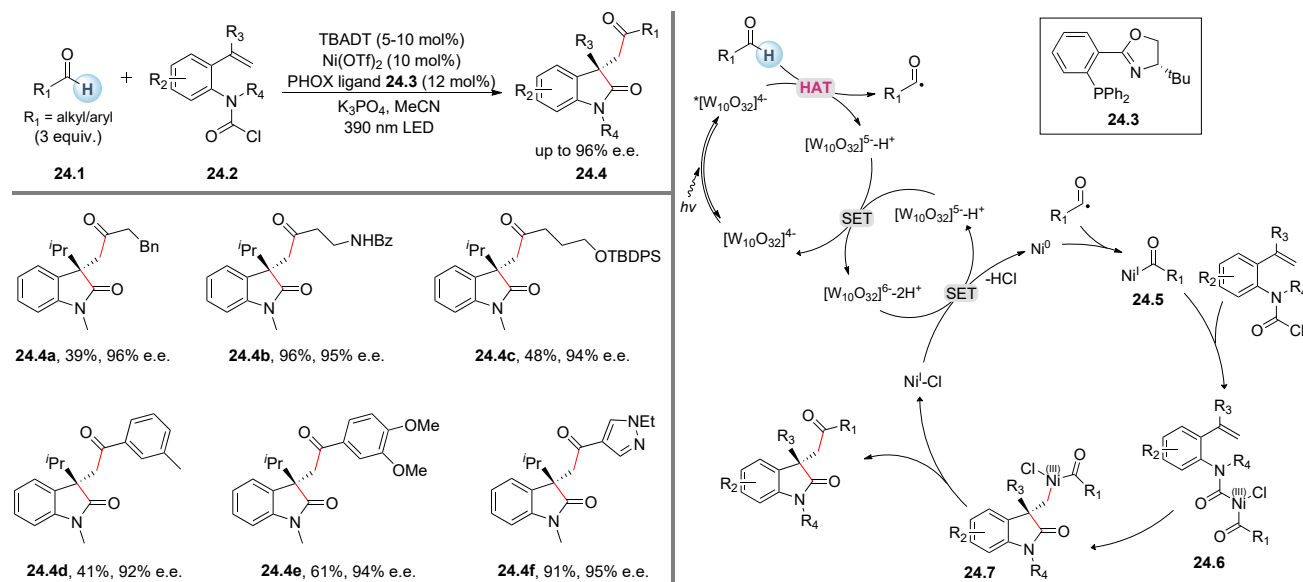
Scheme 23. Photoinduced cross-coupling through ketone and nickel catalysis

(A) Dual aromatic ketone and nickel catalysis reported by Martin and co-workers.⁵² Ni(acac)₂, nickel(II) bis(acetylacetonate).

(B) Dual aromatic ketone and nickel catalysis reported by Rueping and co-workers.⁵³

(C) Dual benzaldehyde and nickel catalysis reported by Hashmi and co-workers.⁵⁴

complexes revealed the reaction rate of Ni^{III}-NO₃ to be 15 times faster than that of Ni^{III}-OAc, indicating the effect of electron deficiency of the O-ligand on HAT power.³⁹ The scope of this catalytic fluorination is limited to several classes of methylene and methine C-H bonds. Benzylic and α-ether C-H bonds were unreactive under the reaction conditions. In 2019, Ravelli and co-workers demonstrated a general C(sp³)-H alkylation strategy with uranyl nitrate hexahydrate as a direct HAT photocatalyst (Scheme 16B).⁴⁰ Various alkanes, ethers, alcohols, amides, and aldehydes



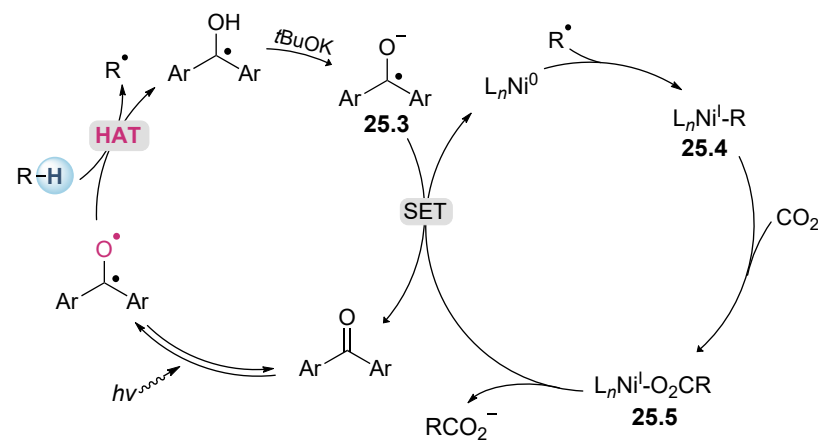
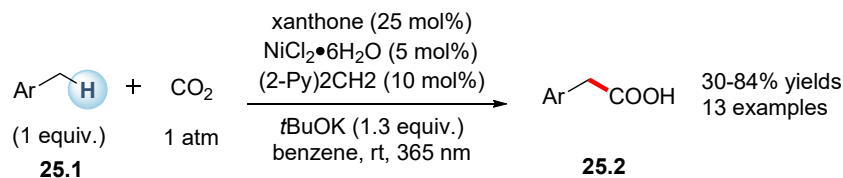
Scheme 24. Photoinduced asymmetric acyl-carbamoylation of alkenes

Bz, benzoyl; TBDPS, *tert*-butyldiphenylsilyl.

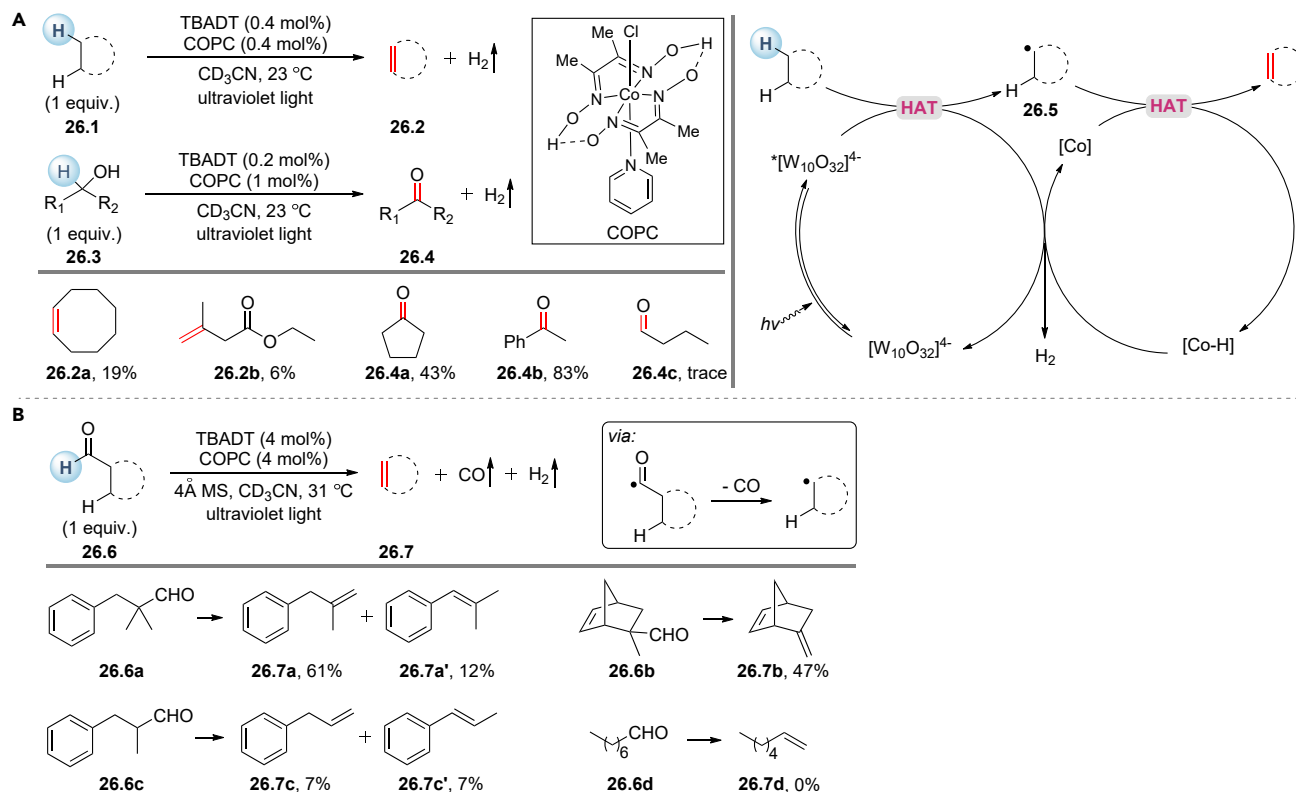
were efficiently alkylated in air under blue-light irradiation. Mechanistic investigations suggested that the uranyl cation photocatalyst, like decatungstate anion, is turned over through sequential ET/PT processes.

Antimony-oxo porphyrin

Recently, Knör, Ravelli, and co-workers reported the use of high-valent antimony-oxo porphyrins as direct HAT photocatalysts in redox-neutral C-H functionalizations.⁴¹ The addition of ethers (10 equiv) or aldehydes (1 equiv) to Michael acceptors



Scheme 25. Photoinduced C(sp³)-H carboxylation with ketone/Ni dual catalysis



Scheme 26. The merger of photoinduced direct HAT with cobalt catalysis

(A) Photoinduced acceptor-less dehydrogenation.

(B) Photoinduced acceptor-less dehydroformylation.

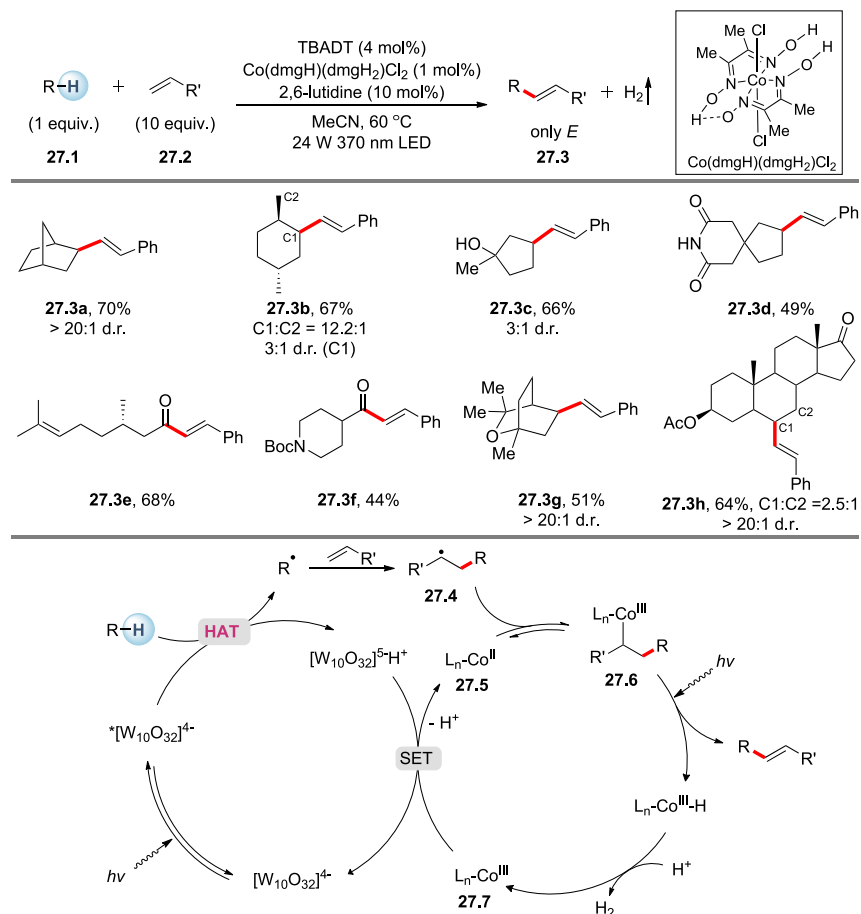
was accomplished in the presence of an antimony-porphyrin catalyst (**2.15**, [Scheme 2](#)) under blue-light irradiation in 10%–47% yield. According to computational analysis, the Sb^V center remains in the high-valent oxidation state during reaction, which suggests that other high-valent porphyrin complexes featuring an oxo ligand could also potentially serve as direct HAT photocatalysts.

The merger of photoinduced direct HAT with other catalysis

Direct HAT photocatalysis offers straightforward approaches for R-H bond activation under mild conditions, often in a regioselective manner. Despite these advantages, the reported reaction patterns are limited, and the established strategies to tune regioselectivity and enantioselectivity remain scarce. The merger of direct HAT with other catalysis such as transition-metal catalysis could significantly expand the reaction patterns and offer new handles for the control of regio- and stereoselectivity. After abstracting an H atom, the direct HAT photocatalyst could engage in an SET process with another catalyst, which lays the foundation for synergistic catalysis. Significant developments have been made in this area recently, enabling previously inaccessible transformations.

The merger of photoinduced direct HAT with iminium catalysis

In 2016, Melchiorre and co-workers reported a photocatalytic strategy for enantioselective C-C bond formation through the merger of decatungstate and iminium catalysis ([Scheme 17](#)).⁴² Various benzodioxoles (**17.1**) and β,β -disubstituted cyclic enones (**17.2**) could be coupled to afford quaternary carbon stereocenters. Notably,

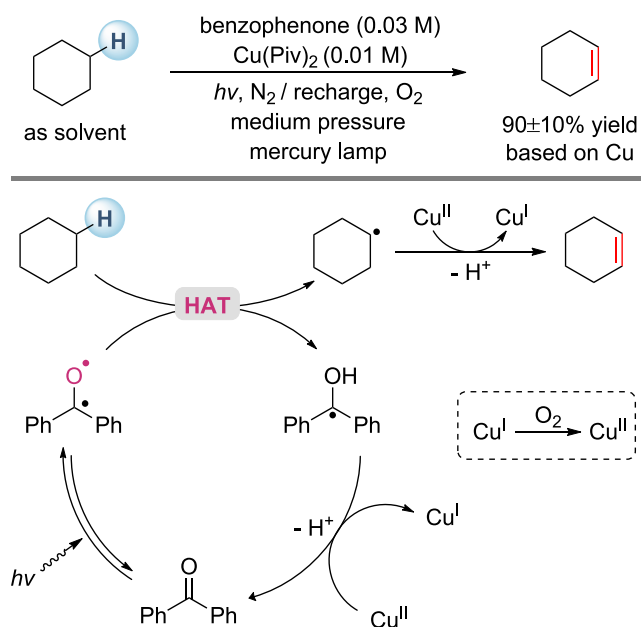


Scheme 27. Photoinduced dehydrogenative alkenylation through decatungstate and cobaloxime catalysis

racemic background reactions were negligible in the absence of a chiral amine catalyst, enabling a highly stereoselective transformation. In the proposed mechanism, an iminium ion (17.5) is formed by the reaction of a chiral amine (17.3) with the enone. Subsequently, enantioselective addition of $R\cdot$ to the iminium ion (17.5) furnishes an unstable radical cation 17.6, which is immediately reduced by the adjacent electron-rich carbazole moiety, which serves as an “ e^- pool.” The back ET in 17.7 is prevented by tautomerization to the corresponding imine (17.8). The carbazole moiety is essential for this electron-relay process thanks to its excellent electron-donating capabilities and the long lifetime of carbazole radical cations. Regeneration of the photocatalyst is achieved by reduction of the carbazoliumyl radical cation in 17.8, and the amine catalyst (17.3) is liberated upon hydrolysis of the imine (17.9).

The merger of photoinduced direct HAT with thiol catalysis

Deuterium labeling is useful in the investigation of reaction mechanisms, optimization of drug candidates, and spectroscopic studies. In 2020, the groups of Wang and Wu independently disclosed photoinduced methods for deuterium labeling of formyl C-H and hydridic $C(sp^3)$ -H bonds with D_2O as an inexpensive deuterium source (Scheme 18).^{43,44} The transformation was achieved via a synergistic combination of decatungstate and thiol catalysis. In the proposed mechanism for deuteration of aldehydes, selective abstraction of H from the aldehyde by excited decatungstate affords a nucleophilic formyl radical. Meanwhile, the thiol catalyst exchanges

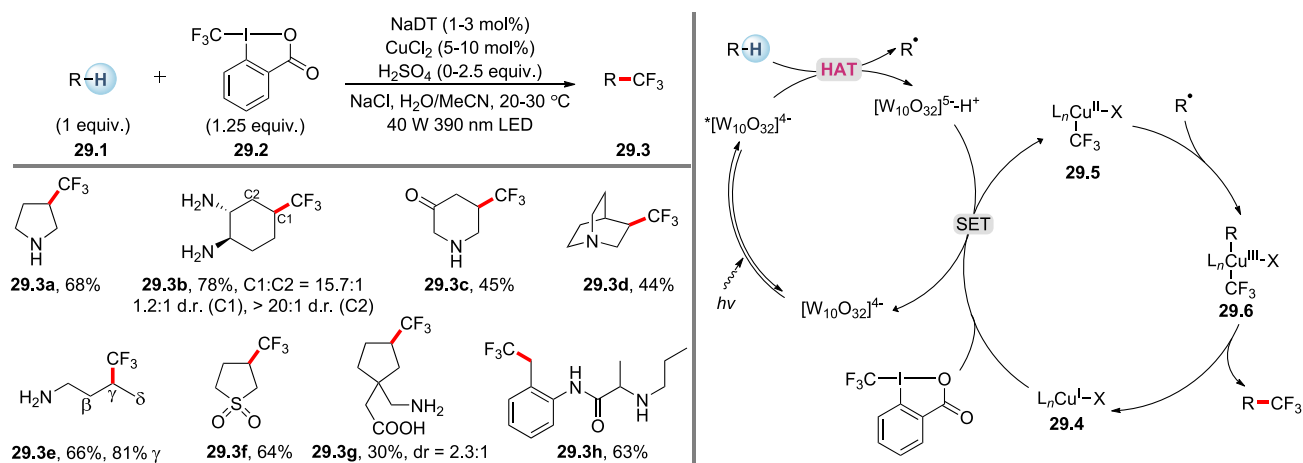


Scheme 28. Photoinduced dehydrogenation of cyclohexane through the merger of benzophenone with copper catalysis

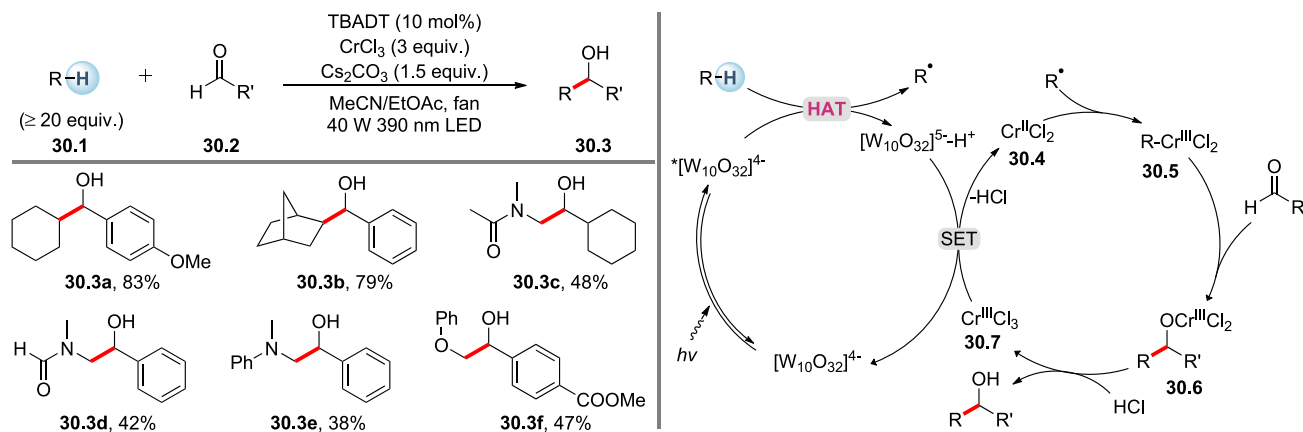
with D₂O to give deuterated thiol. A polarity-matched HAT between a formyl radical and a deuterated thiol then furnishes the deuterated aldehyde and an electrophilic thiol radical.⁴⁵ Finally, an SET event between the thiol radical and reduced decatungstate closes both catalytic cycles.

The merger of photoinduced direct HAT with chiral Lewis/Brønsted acid catalysis

Asymmetric synthesis using chiral Lewis acids or Brønsted acids is a general strategy in organic chemistry, and photoinduced HAT is no exception. In 2019, Gong and co-workers demonstrated a photoinduced asymmetric C(sp³)-H functionalization of benzylic, allylic hydrocarbons and unactivated alkanes (Scheme 19).⁴⁶ Through synergistic catalysis consisting of a direct HAT photocatalyst (5,7,12,14-pentacenetetrone,

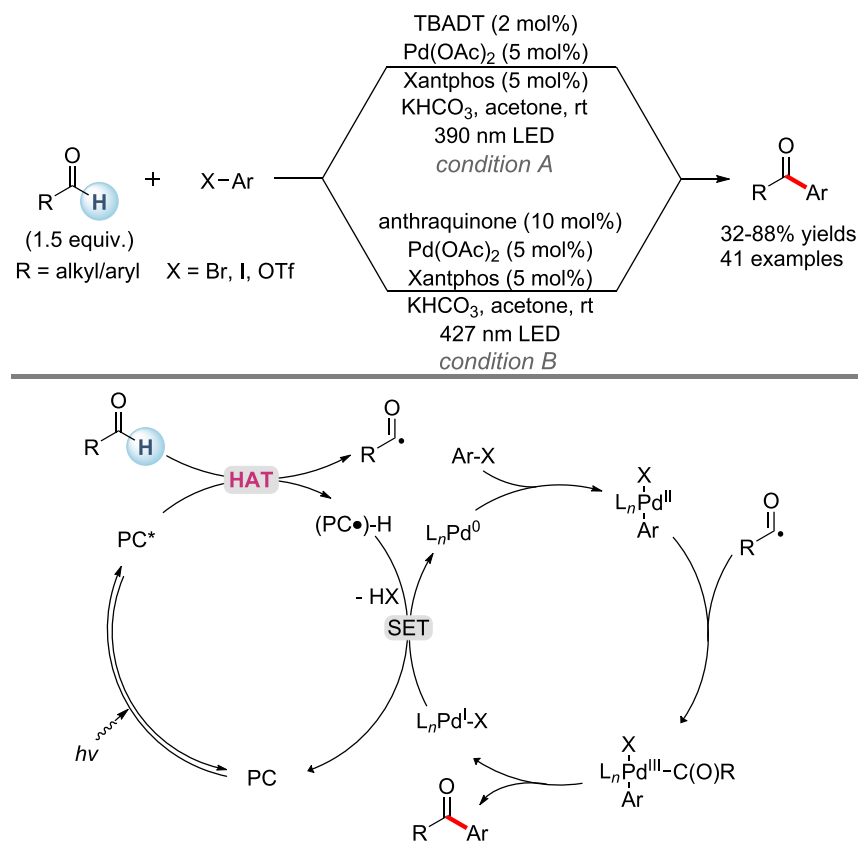


Scheme 29. Photoinduced C(sp³)-H trifluoromethylation through the merger of decatungstate with copper catalysis

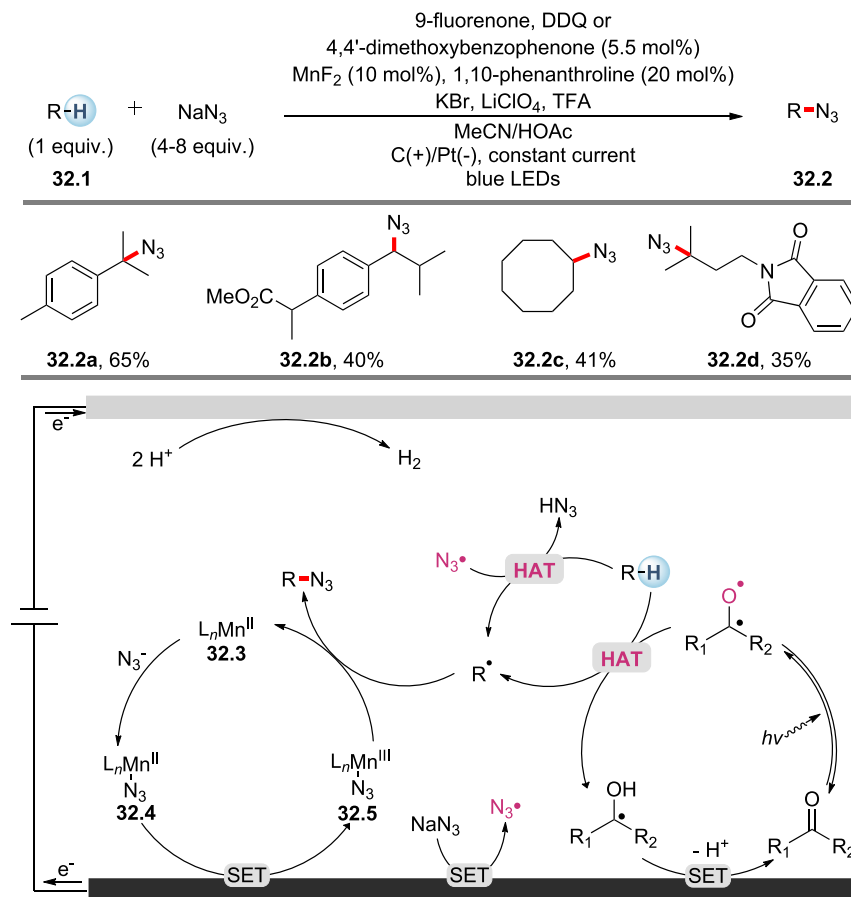


Scheme 30. Photoinduced aldehyde alkylation through decatungstate and chromium catalysis

PT) and a chiral Cu-isooxazoline (Cu-BOX) Lewis acid catalyst, α -amino acid derivatives were obtained in high enantioselectivity under blue-light irradiation. The observed regioselectivity is generally in accordance with the electron density of C-H bonds except in **19.4c** and **19.4e**, where steric hinderance plays an important role. A higher regioselectivity of **19.4c** from 2:1 to 4:1 was obtained when a bulkier bisoxazoline ligand was used, suggesting that the regioselectivity is also governed by the copper catalyst. A hypothetical mechanism was proposed in which the excited PT abstracts an H atom from



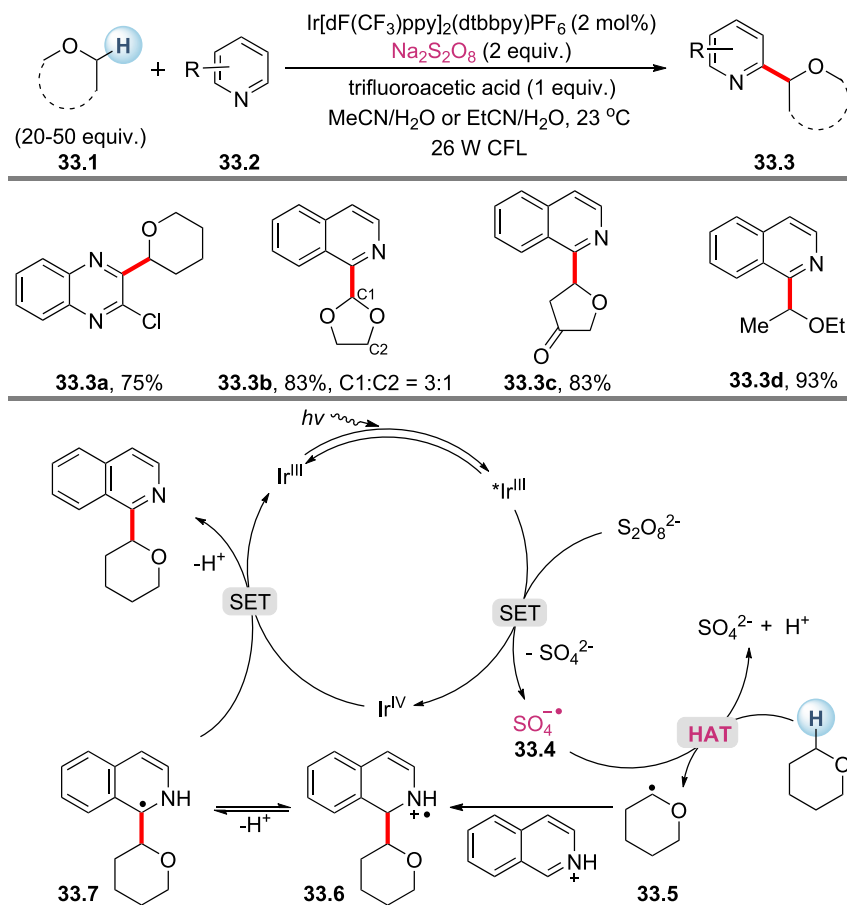
Scheme 31. Photoinduced aldehyde C-H arylation through HAT and palladium catalysis



Scheme 32. Electrocatalytic C(sp³)-H azidation

the R-H bond, furnishing R[•] and a semiquinone-type intermediate (19.5). Meanwhile the imine substrate coordinates with the chiral copper catalyst to give 19.6, which undergoes an SET with 19.5 to close the photocatalytic cycle affording the metal-stabilized carbon radical (19.7). The cross-coupling between the persistent radical (19.7) and the transient radical R[•] delivers the complex (19.8).¹⁷ The stereoselectivity in 19.8 is governed by the chiral ligand-copper moiety. Finally, a ligand substitution and protonation yields the product and regenerates 19.6.

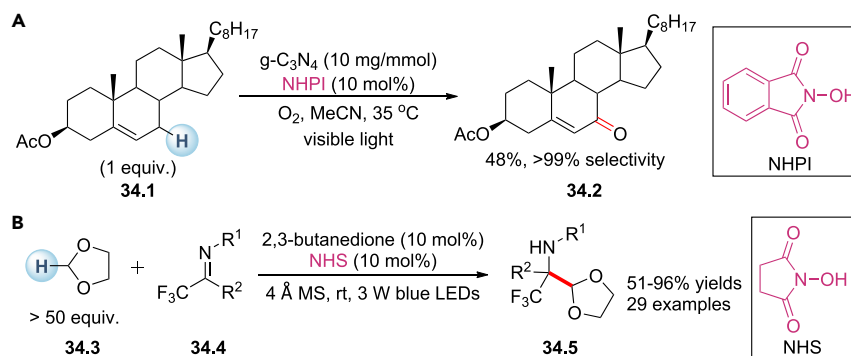
The next contribution to the merger of direct HAT with chiral Lewis acid catalysis was from Wu and co-workers in 2019 (Scheme 20A).⁴⁷ Chiral 1,4-dicarbonyl compounds can be efficiently synthesized directly from aldehydes and α,β -unsaturated amides through synergistic cooperation of neutral eosin Y with a chiral rhodium Lewis acid catalyst (20.3). The reaction proceeds via the addition of an acyl radical to the *N,O*-rhodium-coordinated unsaturated amide. A subsequent RHAT process with eosin Y-H turns over the HAT catalytic cycle, which differs from an SET pathway. In the same year, Jiang et al. reported a photoinduced asymmetric benzylic functionalization with a La(OTf)₃/pybox (OTf, trifluoromethanesulfonate) Lewis acid catalyst (Scheme 20B).⁴⁸ The substrate isatin (20.6) can be excited by blue light and then interact with alkyl arenes via a HAT or oxidation/deprotonation pathway to generate benzylic radicals and dioxindolyl radicals. Control experiments showed that both



Scheme 33. Photoinduced arylation of ethers using persulfate as an indirect HAT reagent

pathways exist. The chiral lanthanum catalyst provides stereo control for the radical cross-coupling by interacting with the merostabilized dioxindolyl radical.

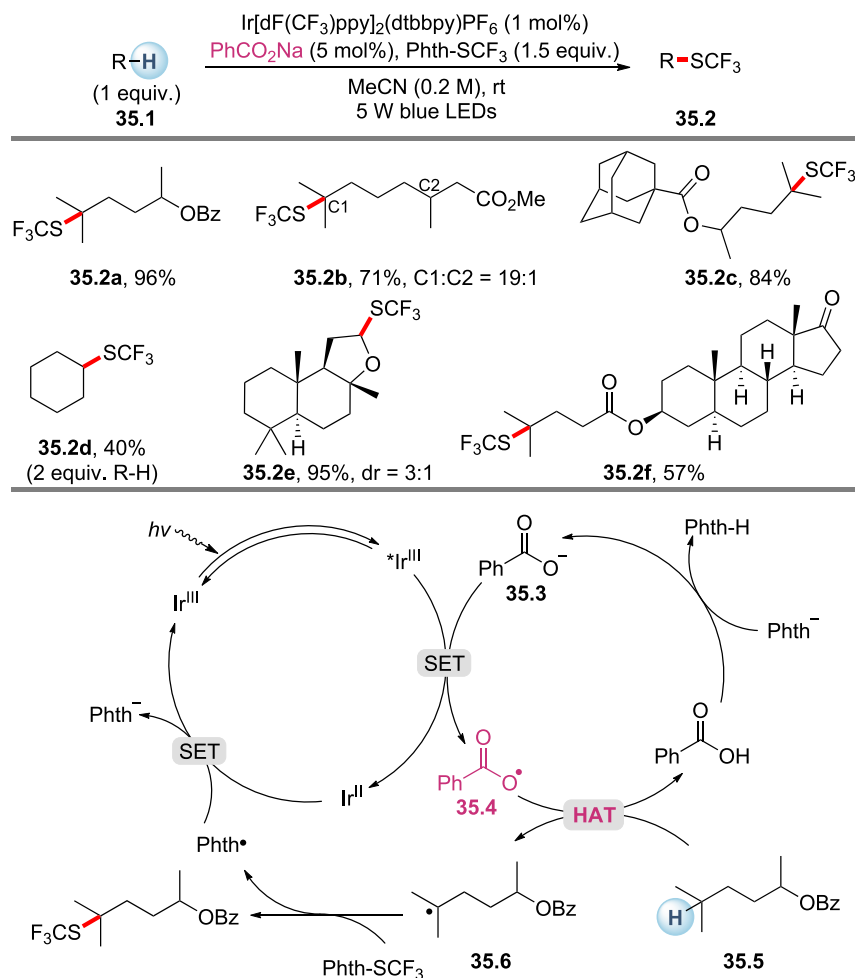
Similar to the coordination of chiral Lewis acid, the protonation of organic functional groups with chiral Brønsted acids can also be used to control the enantioselectivity.



Scheme 34. Photoinduced C-H functionalizations using N-hydroxyl compounds as indirect HAT catalysts

(A) Oxidation of cholesteryl acetate. NHPI, N-hydroxyphthalimide.

(B) Synthesis of masked fluoroalkyl amino aldehydes. NHS, N-hydroxysuccinimide.

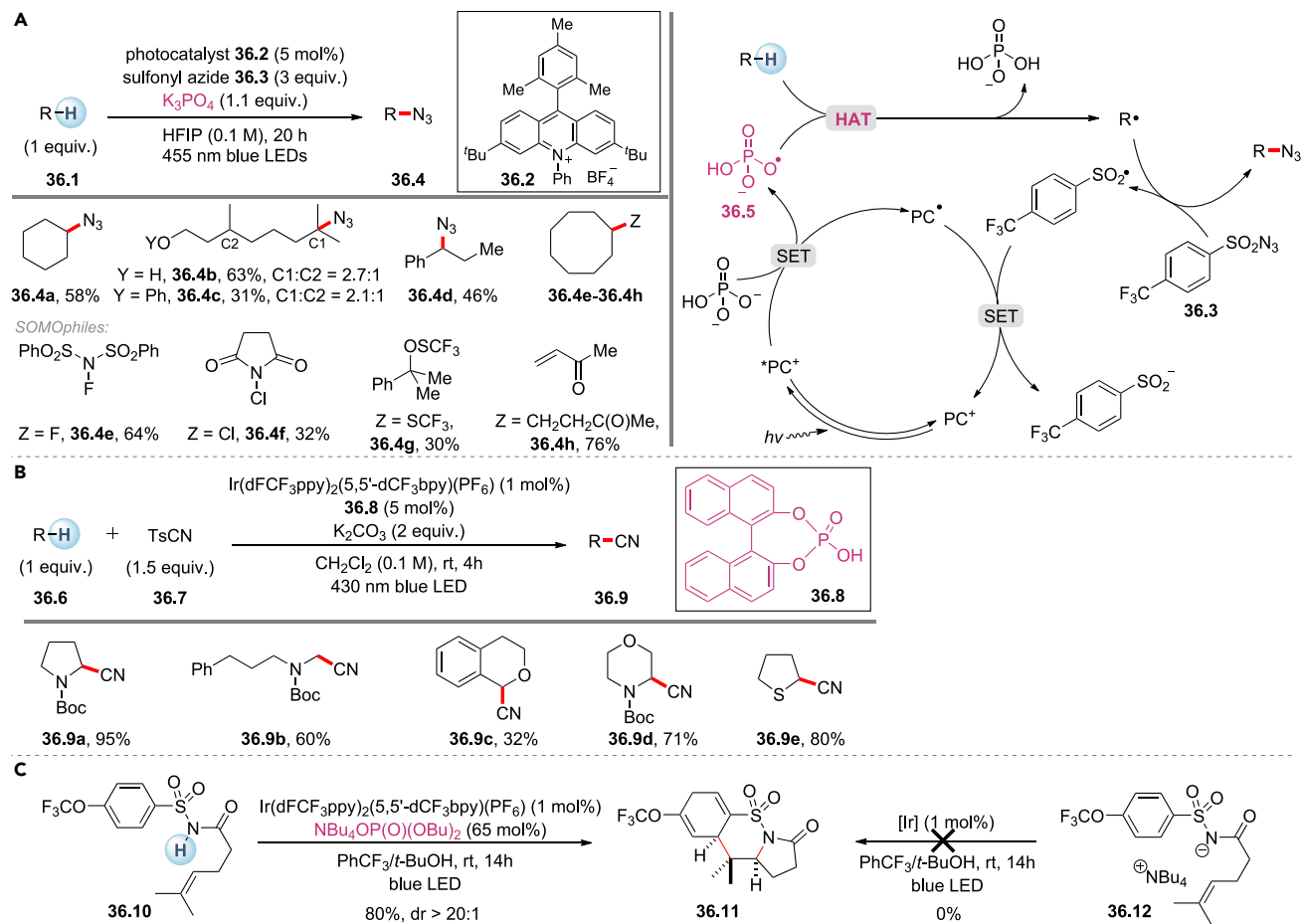


Scheme 35. Photoinduced C(sp³)-H trifluoromethylthiolation using benzoate salt as an indirect HAT catalyst

The merger of photoinduced direct HAT with chiral phosphoric acid (CPA) was reported by Jiang and co-workers for enantioselective coupling of the acenaphthoquinone (21.2) with benzylic C-H bonds (Scheme 21A).⁴⁸ The transformation was proposed to occur through photoexcitation of the substrate 21.2, followed by HAT and CPA-assisted radical coupling. In 2020, Wang and co-workers demonstrated a photoinduced asymmetric coupling of C-H bonds with exocyclic enones in the presence of TBADT and chiral spiro phosphoric acid (21.7) (Scheme 21B).⁴⁹ A wide range of cycloalkanes, aldehydes, and benzylic and allylic hydrocarbons are tolerated. Sequential HAT, radical addition, and RHAT afford the enolic species (21.8), which undergoes enantioselective protonation to give the chiral ketone product (21.9).

The merger of photoinduced direct HAT with nickel catalysis

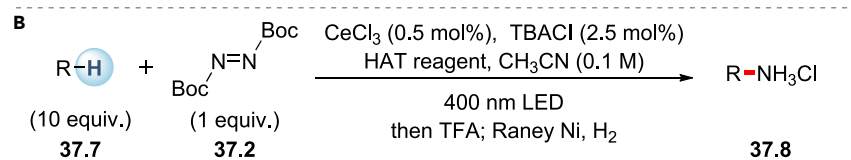
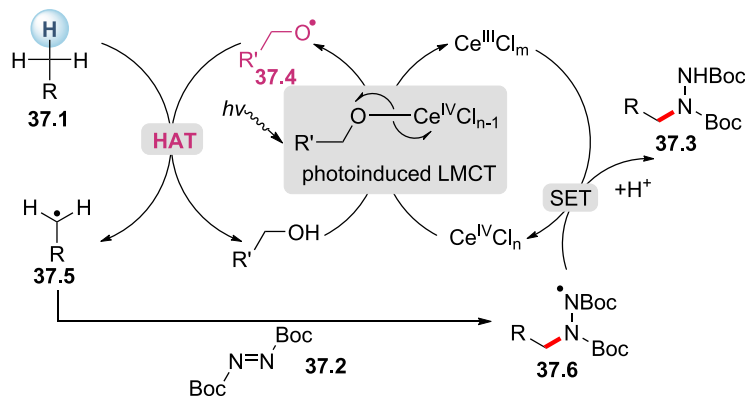
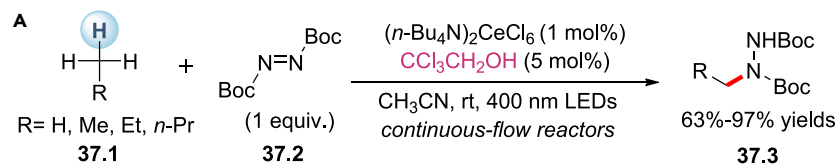
Cooperative photoredox and nickel catalysis has emerged as a versatile synthetic platform for coupling reactions, partly owing to the ability of nickel complexes to undergo facile oxidative addition and ET to give multiple oxidation states.⁵⁰ In 2018, MacMillan and co-workers first demonstrated the merger of direct HAT photocatalysis with nickel-catalyzed cross-coupling (Scheme 22).⁵¹ With aryl bromide as the aryl coupling partner, direct arylation of C(sp³)-H bonds was achieved with TBADT and



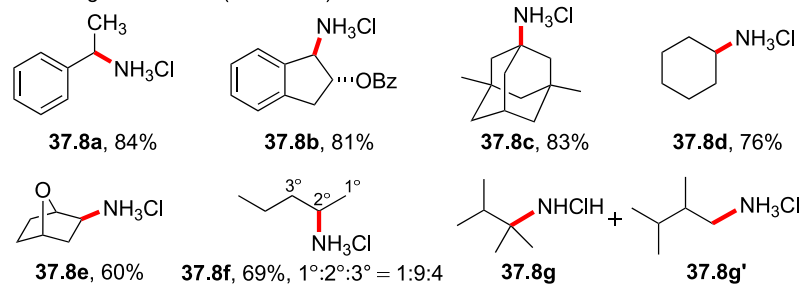
Scheme 36. Photoinduced C-H functionalizations using phosphate salts as indirect HAT reagents

Ni(dtbbpy)Br₂ (dtbbpy = 4,4'-di-*tert*-butyl-2,2'-bipyridine) under 390 nm light irradiation. Activated (22.4a–22.4d) and unactivated (22.4e–22.4l) C(sp³)-H bonds could both be arylated smoothly. The most hydridic and sterically accessible C-H sites were selectively functionalized (e.g., 22.4k from fenchone, 22.4l from sclareolide). In this catalytic system, a HAT event produces R· and singly reduced decatungstate (22.5). Disproportionation of 22.5 regenerates the HAT photocatalyst and gives the doubly reduced decatungstate (22.6). On the other hand, the Ni⁰ species (22.7) formed from the reduction of Ni^{II} precatalyst could capture R· to furnish the Ni^I species (22.8). Subsequent oxidative addition of aryl bromide would afford Ni^{III} species (22.9), which provides the cross-coupled product after reductive elimination. The newly generated Ni^I species 22.10 ($E^{\text{red}}[\text{Ni}^{\text{I}}/\text{Ni}^{\text{0}}] \approx -1.13$ V versus Ag/Ag⁺ in dimethylformamide [DMF]) undergoes single electron reduction by the doubly reduced decatungstate 22.6 ($E_{1/2}^{\text{red}}[\text{W}_{10}\text{O}_{32}]^{5-}/[\text{W}_{10}\text{O}_{32}]^{6-} = -1.52$ V versus Ag/Ag⁺ in MeCN), closing both catalytic cycles.

After HAT is performed, the ketyl radical intermediate generated from a photoexcited aromatic ketone is a strong reductant ($E_{1/2}^{\text{red}}[\text{Ph}_2\text{CO}] = -2.20$ V versus Ag/Ag⁺ in MeCN) and can engage in an SET process with Ni^I species. In 2018, Martin and co-workers reported the cross-coupling of C(sp³)-H bonds with aryl or alkyl bromides using nickel and diaryl ketone (23.3) under CFL irradiation (Scheme 23A).⁵²



HAT reagent = MeOH (200 mol%)

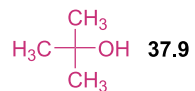


HAT reagent (50 mol%) Yield(**37.8g**+**37.8g'**) Selectivity (**37.8g** : **37.8g'**)

CH₃OH

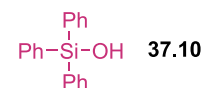
81%

97 : 3



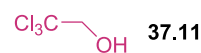
49%

64 : 36



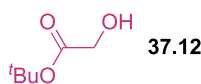
60%

53 : 47



82%

44 : 56



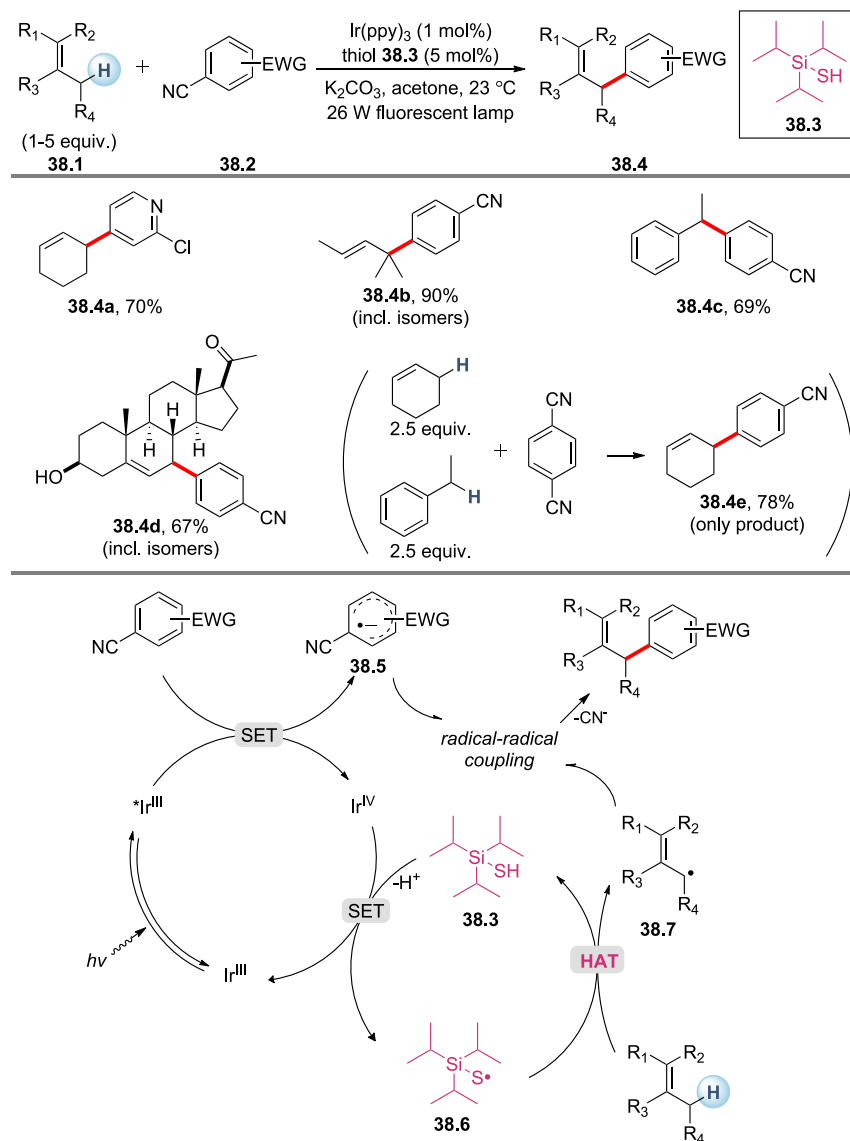
61%

46 : 54

Scheme 37. Photoinduced C(sp³)-H amination using alcohols as indirect HAT catalysts

(A) C(sp³)-H amination of light alkanes.

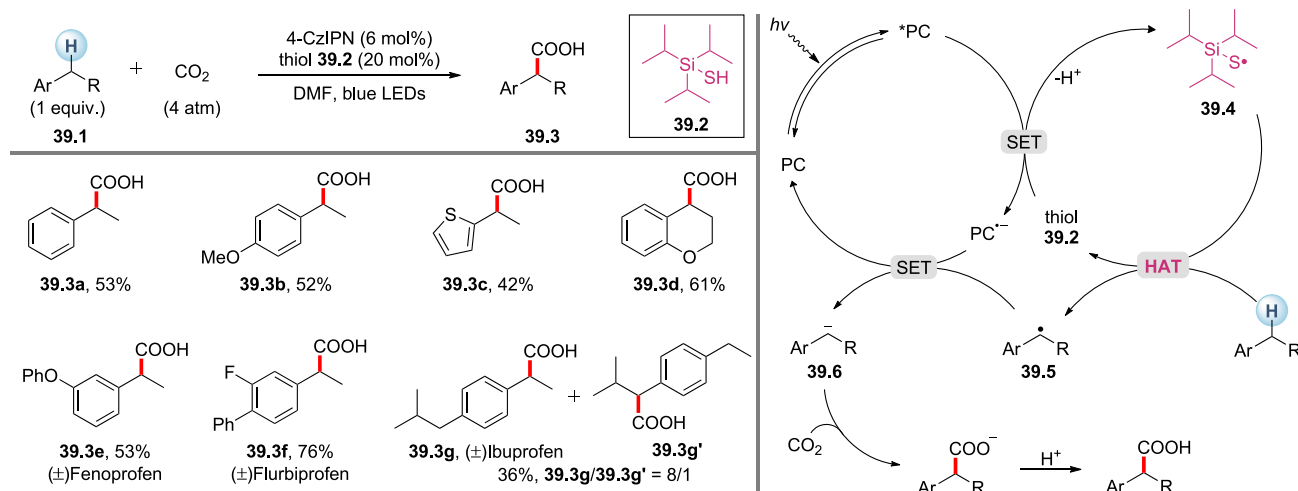
(B) C(sp³)-H amination of alkanes with different alcohols.



Scheme 38. Photoinduced allylic arylation with trisopropylsilanethiol as an indirect HAT catalyst

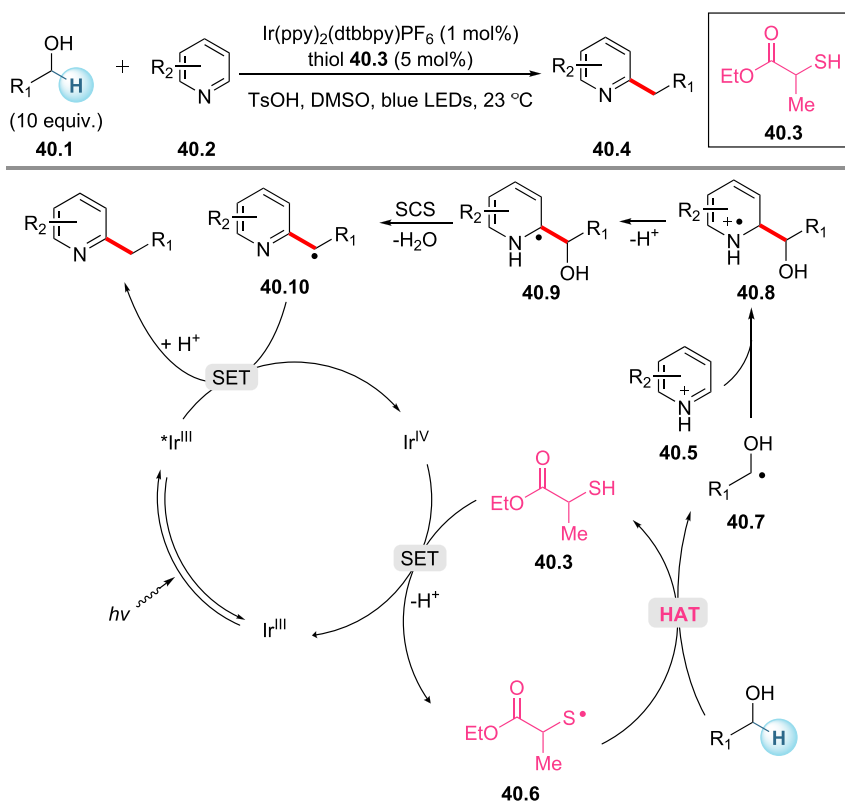
Subsequently, Rueping and co-workers realized the cross-coupling of benzylic C-H bonds with aryl halides, acid chlorides, and anhydrides using nickel and substituted benzophenone (Scheme 23B).⁵³ In 2019, Hashmi and co-workers developed synergistic nickel and benzaldehyde catalysis for alkylation and arylation of ethers, amides, and thioethers under UVA irradiation (Scheme 23C).⁵⁴ However, compared with the dual TBADT/Ni catalytic system, a larger amount of C-H substrate was usually required for aromatic ketone (derivative) photocatalysts, presumably due to their weaker hydrogen abstraction ability.

In 2020, Wang and co-workers developed an asymmetric acyl-carbamoylation of alkenes to access chiral oxindole scaffolds by the cooperative catalysis of TBADT and a nickel-phosphinoxazoline complex (Scheme 24).⁵⁵ Various aliphatic and aromatic aldehydes were incorporated as acyl radical precursors even in the presence of other active C-H bonds such as benzylic, α -ether, or α -amide bonds. The preference of

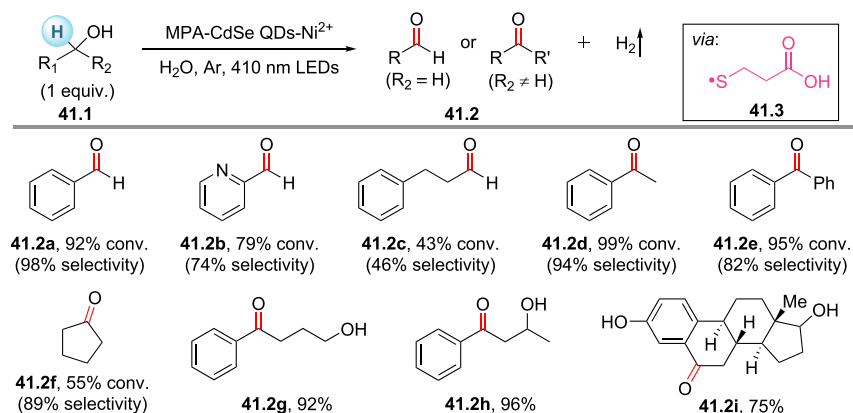


Scheme 39. Photoinduced carboxylation of benzylic C-H bonds

formyl C-H abstraction can be explained by the polar transition state due to the partial positive charge on the carbonyl carbon. The plausible mechanism is similar to the one in [Scheme 22](#) except the Ni⁰ species captures the acyl radical and furnishes the Ni^I species (**24.5**). Subsequent oxidative addition of carbamoyl chloride affords the Ni^{III} species (**24.6**). Intermediate **24.7** is formed after a Ni^{III}-mediated migratory insertion, which might be the enantio-determining step in the catalytic cycle. Reductive elimination of **24.7** gives the chiral oxindole product.



Scheme 40. Photoinduced C-H alkylation of heteroarenes with alcohols as the alkylating reagents



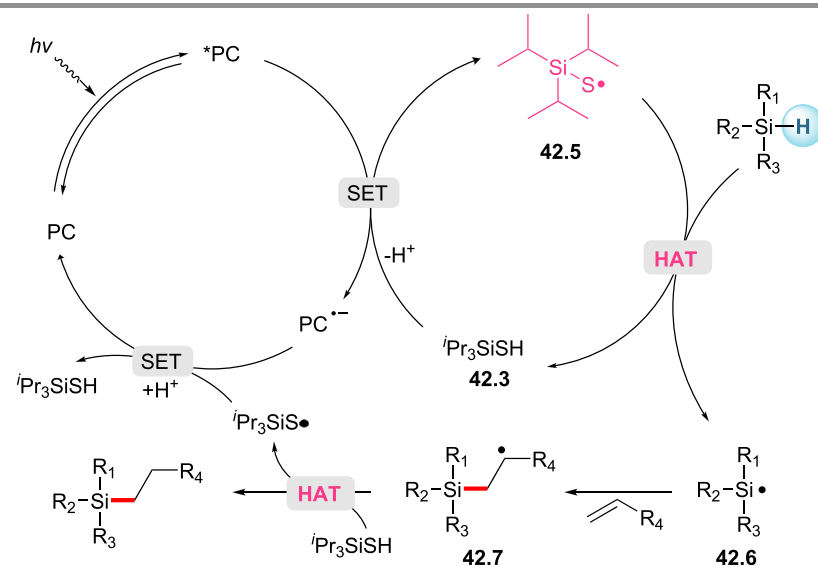
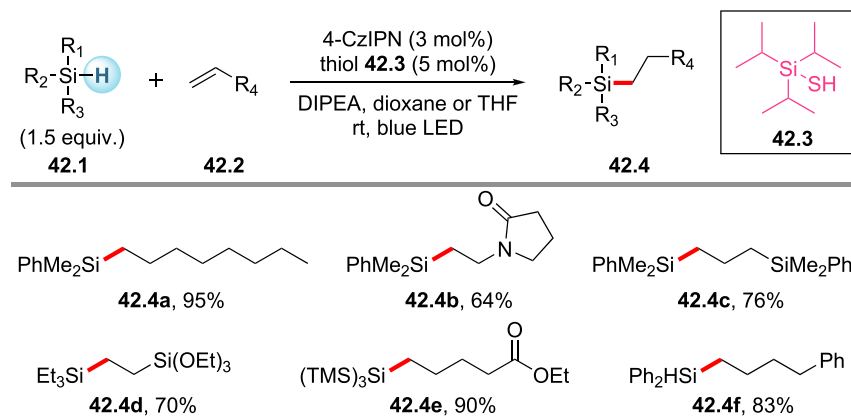
Scheme 41. Photoinduced oxidation of alcohols with mercaptopropionic acid (MPA)-capped CdSe quantum dots and nickel(II) chloride in water

The merger of direct HAT with nickel catalysis was also employed in the photoinduced carboxylation of benzylic and aliphatic C-H bonds by Ishida, Murakami, and co-workers (Scheme 25).⁵⁶ With an aromatic ketone, a nickel complex, and potassium *tert*-butoxide, alkyl benzenes were effectively carboxylated at the benzylic position under CO₂ at atmospheric pressure and UV-light irradiation. The carboxylation of saturated hydrocarbons such as cyclohexane proceeded in low yields (8–32 turnover numbers based on Ni). It was proposed that carbon dioxide inserts into the C-Ni(I) bond to give a nickel(I) carboxylate (25.5), which accepts a single electron from the ketyl radical anion (25.3) to release the carboxylate anion with regeneration of the Ni(0) species.

The merger of photoinduced direct HAT with cobalt catalysis

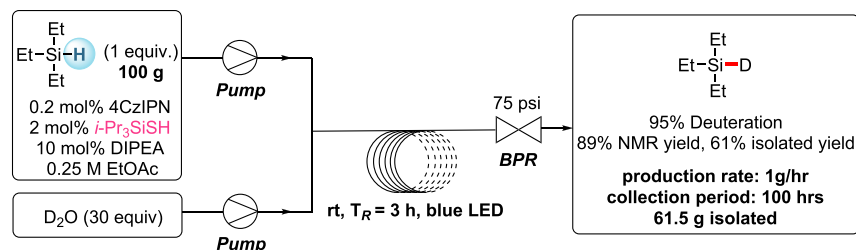
Cobaloximes are an interesting family of cobalt complexes with a rich radical chemistry and excellent proton reduction reactivity.⁵⁷ In 2015, Sorenson and co-workers developed an acceptor-free dehydrogenation strategy for small molecules through cooperative decatungstate and cobaloxime catalysis (Scheme 26A).⁵⁸ Under near-UV irradiation, dehydrogenation of unactivated alkanes and secondary alcohols proceeded at room temperature with hydrogen as the sole by-product. Notably, the non-thermodynamic product (26.2b) was obtained exclusively from ethyl isovalerate, which differs from organometallic dehydrogenations. A mechanism involving two successive HAT processes was proposed. Excited decatungstate could activate a strong C-H bond (~100 kcal mol⁻¹) and give the alkyl radical (26.5) (“hard” HAT). Subsequently, the C-H bond β to the radical in 26.5 is weakened (<50 kcal mol⁻¹) and could be abstracted by Co (“easy” HAT). Finally, each catalyst could donate a hydrogen atom equivalent to liberate H₂ and turn over the system. Later, the same group extended this catalytic system to DE hydroformylation, the reverse reaction of hydroformylation (Scheme 26B).⁵⁹ Tertiary aliphatic aldehydes generally gave good conversions, since their corresponding acyl radicals are prone to decarbonylation. Primary aliphatic aldehydes and aromatic aldehydes were not reactive on account of their slow decarbonylation.

The dehydrogenative alkenylation of C-H bonds represents an atom- and step-economical approach for olefin synthesis. In 2020, Wu and co-workers reported a photocatalytic method for site-selective alkenylation of alkanes and aldehydes through synergistic decatungstate and cobaloxime catalysis (Scheme 27).⁶⁰ With C-H partner as the limiting reagent, commodity feedstocks and pharmaceutical

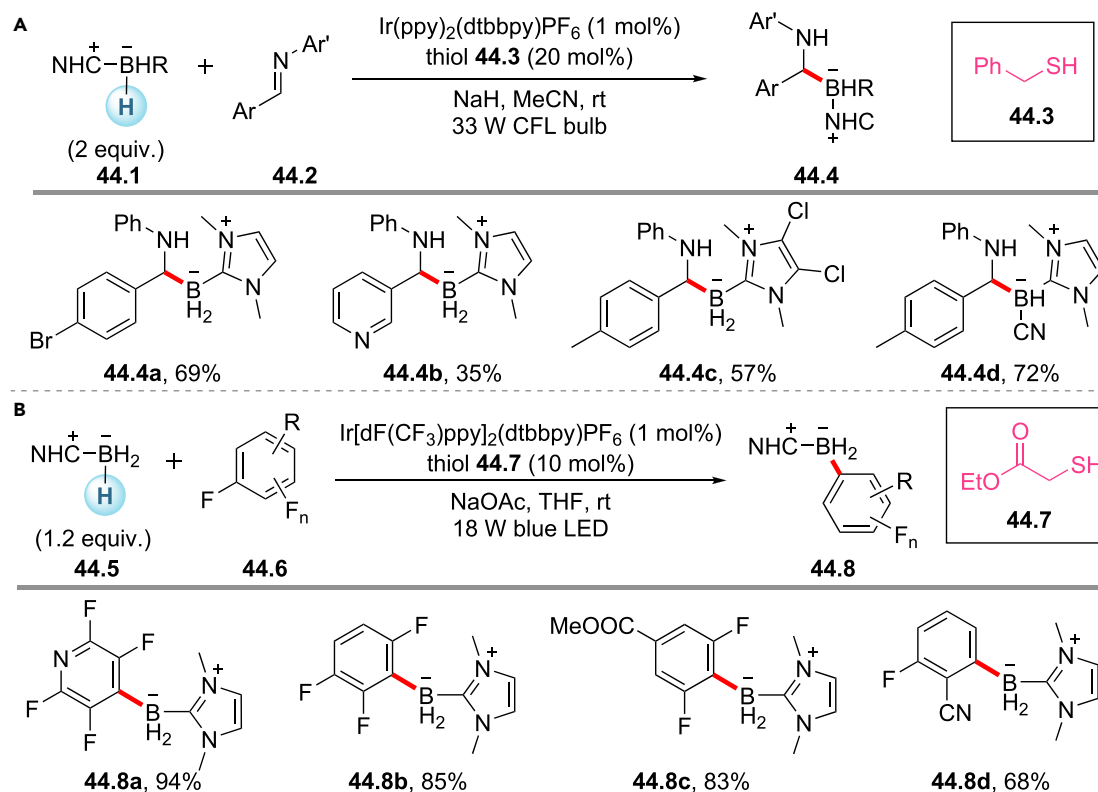


Scheme 42. Photoinduced hydrosilylation of electron-rich alkenes
TMS, trimethylsilyl.

compounds were successfully alkenylated exclusively in the *E* form. High levels of site selectivity were observed for sterically accessible and electron-rich C-H bonds, as shown in 27.3b, 27.3c, 27.3d, 27.3g, and 27.3h. Control experiments suggested that the bulk ligands on the cobalt catalyst also contributed to the high regioselectivity. A hypothesized catalytic cycle was proposed. Carbon-centered radical $R\cdot$ and reduced decatungstate are generated after a HAT event. Subsequent radical addition of $R\cdot$ to an alkene furnishes a radical intermediate (27.4), which can be reversibly



Scheme 43. Photoinduced deuteration of silanes in a continuous flow reactor



Scheme 44. Photoinduced functionalization of NHC-boranes through cooperative photoredox and thiol catalysis

(A) Hydroboration of imines reported by Xie, Zhu, and co-workers.⁸⁷

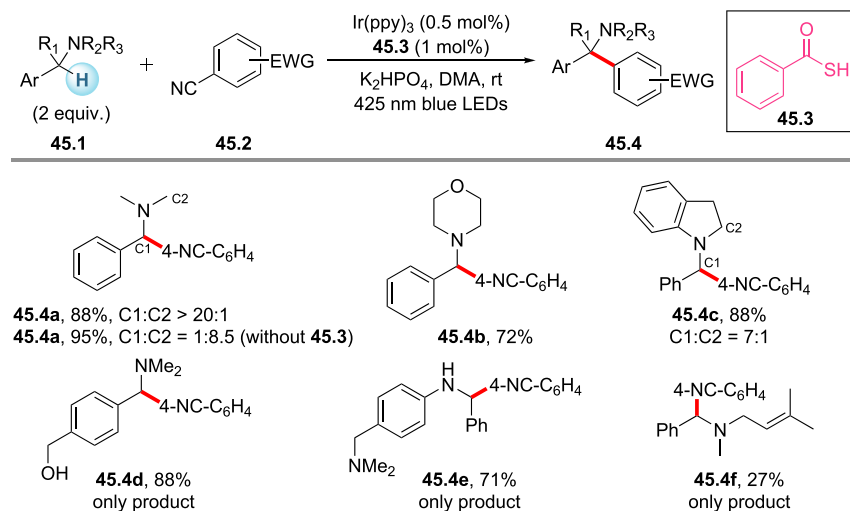
(B) Defluoroborylation reported by Wu and co-workers.⁸⁸

captured by Co^{II} (27.5) to form a Co^{III} intermediate (27.6). Photoirradiation of 27.6 delivers the alkene product along with a $\text{Co}^{\text{III}}\text{-H}$ intermediate via a formal $\beta\text{-H}$ elimination process. $\text{Co}^{\text{III}}\text{-H}$ could react with another proton to release H_2 and deliver a Co^{III} complex (27.7). Finally, an SET between 27.7 ($E_{1/2} \text{Co}^{\text{III}}/\text{Co}^{\text{II}} = -0.68 \text{ V}$ versus Ag/Ag^+ in MeCN) and the reduced decatungstate ($E_{1/2} [\text{W}_{10}\text{O}_{32}]^{4-}/[\text{W}_{10}\text{O}_{32}]^{5-} = -0.96 \text{ V}$ versus Ag/Ag^+ in MeCN) regenerates both catalysts.

The merger of photoinduced direct HAT with copper catalysis

Jones and co-workers studied the dehydrogenation of cyclohexane using benzophenone in conjunction with Cu^{II} pivalate (Scheme 28).⁶¹ The reaction mixture was irradiated under N_2 until the blue color disappeared, indicating the reduction of Cu^{II} to colorless Cu^{I} . The solution was then exposed to air to regenerate Cu^{II} before being again subjected to irradiation under N_2 . This two-step process was repeated 10 times and a $90\% \pm 10\%$ yield of cyclohexene (based on the Cu^{II} consumed) was observed. The authors proposed a mechanism in which photoexcited benzophenone abstracts an H atom from cyclohexane to generate cyclohexyl radical. Cu^{II} subsequently serves to both oxidize this radical and regenerate the photocatalyst. Finally, Cu^{I} can be reoxidized by oxygen.

The introduction of a trifluoromethyl group can dramatically improve the biological properties of organic molecules. In 2020, MacMillan and co-workers disclosed the merger of decatungstate with copper catalysis for photoinduced aliphatic $\text{C}(\text{sp}^3)\text{-H}$ trifluoromethylation (Scheme 29).⁶² Primary, secondary, and tertiary amines and



Scheme 45. Photoinduced arylation of benzylamines with thiocarboxylate as an indirect HAT catalyst

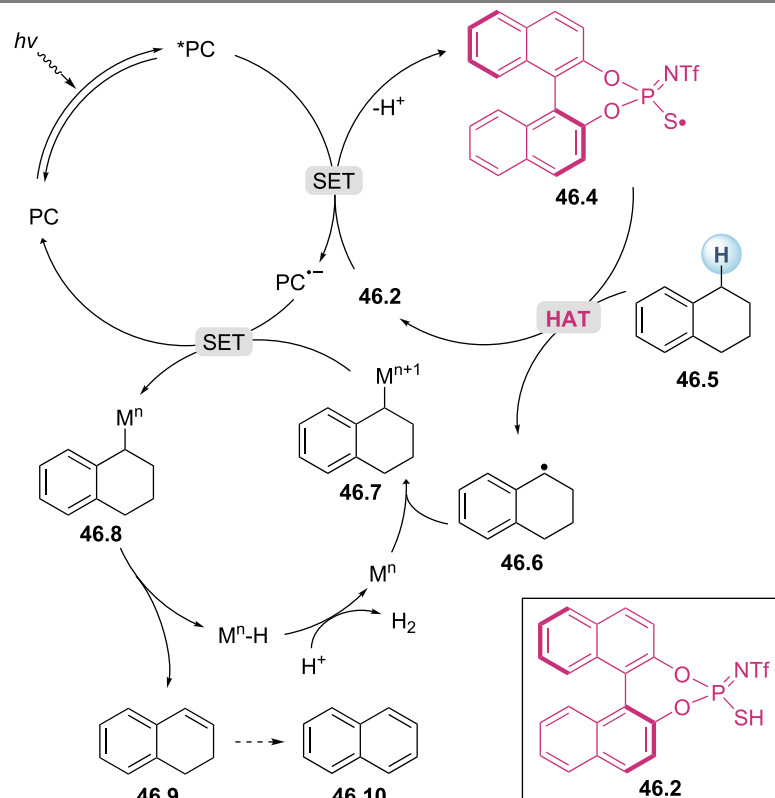
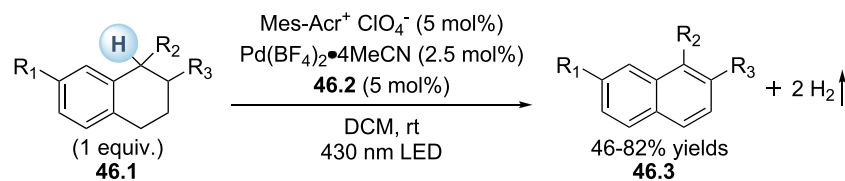
alkanes as well as benzylic C-H bonds were selectively trifluoromethylated using just 1 equiv of a C-H substrate. The regioselectivity was guided by electronic and steric effects as described above. In the proposed mechanism, formal reduction of the electrophilic CF_3 reagent (**29.2**) by reduced decatungstate in the presence of the Cu^{I} catalyst (**29.4**) affords a $\text{Cu}^{\text{II}}\text{-CF}_3$ intermediate (**29.5**). Compound **29.5** could readily capture R^\cdot to produce the Cu^{III} complex (**29.6**), which delivers the product upon reductive elimination.

The merger of photoinduced direct HAT with chromium-mediated reactions

In 2020, Yahata and co-workers described the generation of an organochromium carbanion species from $\text{C}(\text{sp}^3)\text{-H}$ bonds and its nucleophilic addition to aldehydes (Scheme 30).⁶³ Using a decatungstate photocatalyst and chromium(III) trichloride salt under 390 nm light irradiation, both aliphatic and aromatic aldehydes could be reacted with cyclic alkanes, amides, amines, or ethers to generate secondary alcohols. It was proposed that the organochromium complex (**30.5**) is formed after CrCl_2 captures the alkyl radical. This complex (**30.5**) then reacts with aldehydes with high chemoselectivity to give the final product and CrCl_3 . A single electron reduction of CrCl_3 ($E_{1/2} \text{Cr}^{\text{III}}/\text{Cr}^{\text{II}} = -0.65 \text{ V}$ versus Ag/Ag^+ in H_2O) by reduced decatungstate ($E_{1/2} [\text{W}_{10}\text{O}_{32}]^{4-}/[\text{W}_{10}\text{O}_{32}]^{5-} = -0.96 \text{ V}$ versus Ag/Ag^+ in MeCN) could close both catalytic cycles.

The merger of photoinduced direct HAT with palladium catalysis

Transition-metal-catalyzed coupling of aldehydes with carbon electrophiles is an ideal pathway with which to synthesize ketones. However, the insertion of a transition metal such as palladium into the aldehyde C-H bond is challenging because of the high bond dissociation energies and low acidities. In 2020, Zheng and co-workers realized direct arylation of aldehydes by combining palladium catalysis with photoinduced HAT catalysis (Scheme 31).⁶⁴ Both TBADT and anthraquinone are effective HAT catalysts. Density functional theory calculations suggested that the reaction proceeds through a $\text{Pd}^0\text{-Pd}^{\text{II}}\text{-Pd}^{\text{III}}\text{-Pd}^{\text{I}}\text{-Pd}^0$ pathway involving sequential oxidative addition, radical combination, reductive elimination, and catalyst regeneration with an overall energy barrier of only 12.1 kcal/mol.



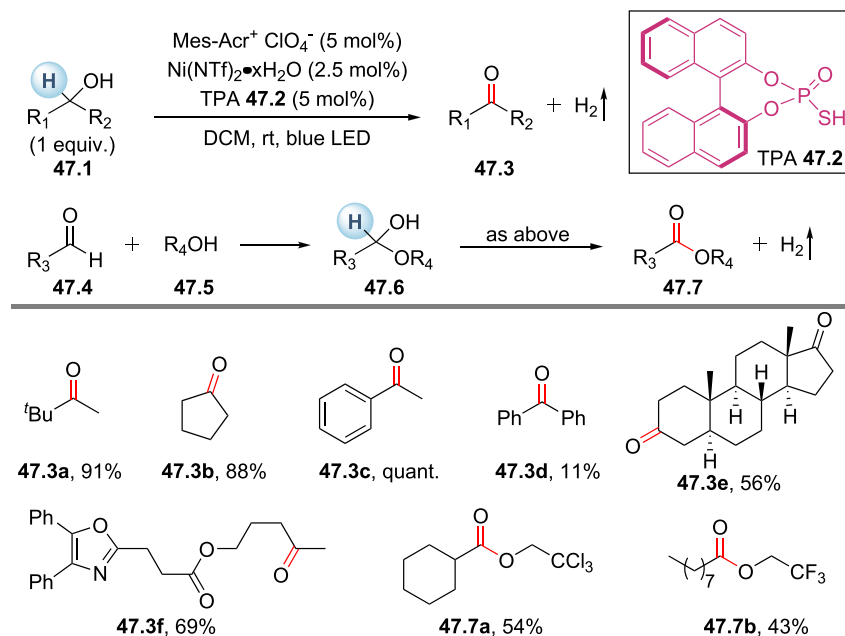
Scheme 46. Photoinduced acceptor-less dehydrogenation of tetrahydronaphthalenes

Miscellaneous examples

In 2020, Lei and co-workers demonstrated a manganese-catalyzed C(sp³)-H azidation under electrophotocatalytic conditions with nucleophilic sodium azide as the azidation reagent (Scheme 32).⁶⁵ The use of excess substrate or stoichiometric chemical oxidant was avoided by merging the C(sp³)-H abstracting ability of ketone photocatalysts with sustainable electrochemical oxidation and manganese-assisted radical azidation. Benzylic, methine, and methylene C(sp³)-H bonds in hydrocarbons as well as in bioactive molecules could be effectively functionalized in moderate to high yields. In this catalytic system, photoexcitation of ketones promotes the hydrogen abstraction and provides the alkyl radical R[•]. Regeneration of the ketone catalyst could be accomplished by anodic oxidation. In the manganese catalytic cycle, Mn(II) coordinated by N₃⁻ and ligands (32.4) undergoes anodic oxidation to deliver the Mn(III)-N₃ intermediate (32.5), which transfers azide to R[•], furnishing the product. Since NaN₃ could be directly oxidized to an azide radical on the anodic surface, the azide radical might also contribute to the C(sp³)-H abstraction.

PHOTOINDUCED INDIRECT HAT REACTIONS

Despite the enormous progress in photoinduced direct HAT reactions, the choice of competent catalyst is limited to several families of oxo complexes. To fully exploit



Scheme 47. Photoinduced acceptor-less dehydrogenation of aliphatic secondary alcohols and hemiacetals

TPA, thiophosphoric acid.

the reactivity of different hydrogen atom abstractors, photoinduced indirect HAT becomes a promising strategy for the functionalization of R-H (R = C, Si, etc.) bonds. As described in [Scheme 1](#), the indirect HAT catalyst could be activated through SET, EnT, or direct photoexcitation. The following section summarizes representative examples in this rapidly developing area.

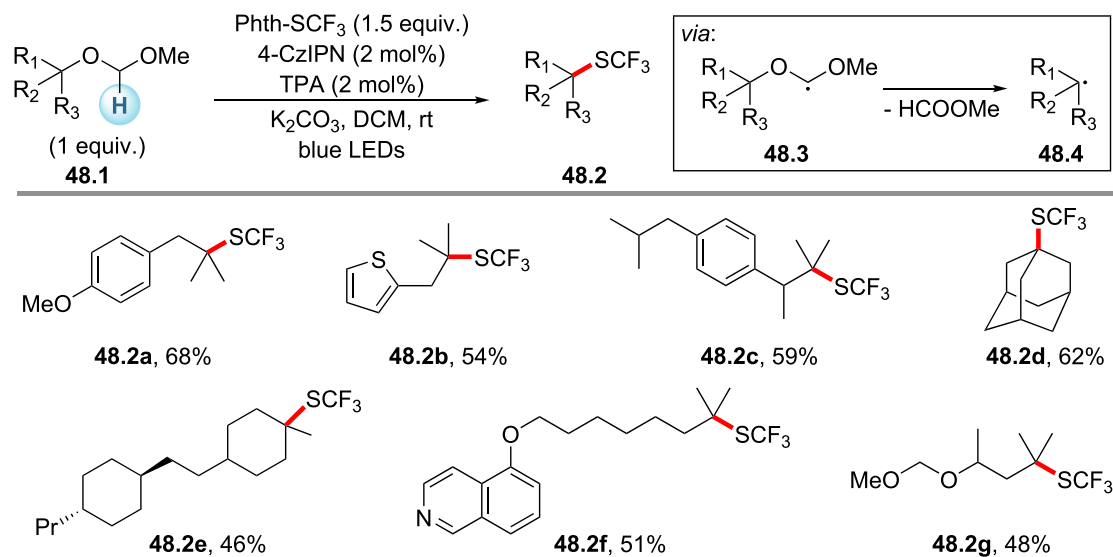
O-centered abstractors

From peroxides

It has been well established that O-centered radicals can be generated from peroxides through heating, UV irradiation, or transition-metal catalysis. Recently, facile generation of O-centered radicals from peroxides via photoinduced single electron reduction or EnT has been developed, and this features mild conditions, a metal-free character, and the use of inexpensive organic dyes as photocatalysts. Stoichiometric amounts of *tert*-butyl hydroperoxide, di-*tert*-butyl peroxide, or benzoyl peroxide are commonly employed as precursors to *tert*-butoxy radical (^tBuO·) or benzoyloxyl radical (PhCOO·), which can abstract an H atom from α -ether, α -alcohol, and formyl and methylene C-H bonds.⁵

From persulfates

The single electron reduction of persulfate (S₂O₈²⁻) could generate a sulfate radical anion (SO₄^{·-}), whose HAT reactivity was illustrated by MacMillan and co-workers in photoinduced Minisci-type arylation of ethers ([Scheme 33](#)).⁶⁶ Using excess amounts of C-H substrates, various cyclic and acyclic ethers were smoothly coupled with electron-deficient arenes. The authors proposed that the excited iridium photocatalyst could reduce the persulfate anion to give SO₄^{·-} (**33.4**), which abstracts an H atom from ether to generate nucleophilic radical (**33.5**). Subsequent addition of **33.5** to protonated heteroarene furnishes **33.6**. Upon loss of a proton, **33.6** gives the α -amino radical species (**33.7**). An SET between **33.7** and Ir^{III} closes the photocatalytic cycle and releases the product after deprotonation. In addition to



Scheme 48. Photoinduced trifluoromethylthiolation of tertiary alkyl ethers

functionalization of ethers, photogenerated sulfate radical anions have also been used in the activation of α -amides and formyl and methylene C-H bonds.

From N-alkoxyl compounds

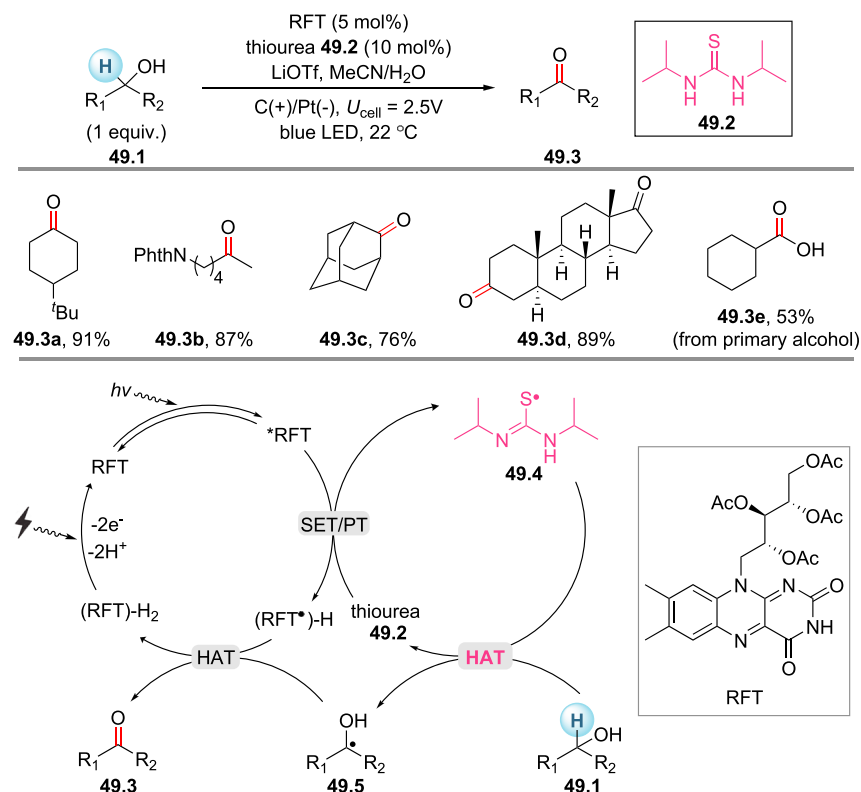
In 2016, Lakhdar and co-workers reported a visible light-photocatalyzed synthesis of benzo[*b*]phosphole oxides from arylphosphine oxides and alkynes.⁶⁷ Single electron reduction of *N*-ethoxy-2-methylpyridinium tetrafluoroborate by a photocatalyst produces the key ethoxy radical, which abstracts hydrogen from the relatively weak P-H bond of phosphine oxides (bond dissociation energy [BDE] = 75.8 kcal/mol for diphenylphosphine oxide). The study used 1.5 equiv of the *N*-alkoxide as it cannot be regenerated.

From N-hydroxyl compounds

Photoinduced single electron oxidation of *N*-hydroxyl compounds can generate nitroxyl radicals capable of activating C-H bonds. With oxygen as a green oxidant and heterogeneous graphitic carbon nitride as a reusable organic photocatalyst, Li and co-workers developed selective allylic and benzylic C-H oxidation using a catalytic amount of *N*-hydroxyphthalimide under visible light irradiation (Scheme 34A).⁶⁸ In 2019, Gong and co-workers demonstrated that *N*-hydroxysuccinimide could be used as an indirect HAT catalyst in the activation of 1,3-dioxolane to synthesize masked fluorinated α -amino aldehydes (Scheme 34B).⁶⁹

From benzoate salts

In 2016, Glorius and co-workers explored the generation of benzoyloxy radicals (PhCOO \cdot) from benzoate salts for the installation of trifluoromethylthio (SCF₃) groups into C(sp³)-H bonds (Scheme 35).⁷⁰ Using 1 equiv of C-H substrate, a range of functionalized hydrocarbons were efficiently trifluoromethylthiolated with high selectivity for the electron-rich tertiary C-H bonds. Cycloalkanes and ethers were also viable substrates, but the reaction of benzylic C-H bonds was messy, possibly due to their relatively low oxidation potentials. Stern-Volmer quenching studies revealed an efficient oxidation of the benzoate (35.3) by excited iridium photocatalyst. The benzoyloxy radical that formed (35.4) (BDE_{O-H} for PhCOOH = 111 kcal/mol) was highly electrophilic and could abstract H from the tertiary C-H bond in



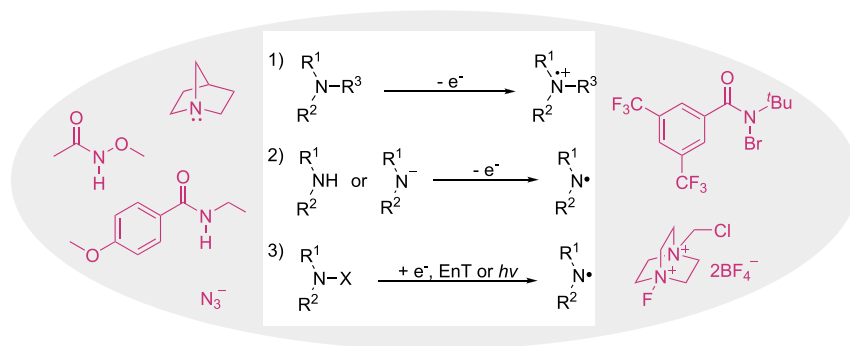
Scheme 49. Photoelectrocatalytic oxidation of alcohols

35.5 (BDE for (CH₃)₃C-H = 96.5 kcal/mol). The generated nucleophilic alkyl radical (35.6) subsequently reacts with Phth-SCF₃ to form the product along with the phthalimide radical Phth·. Single electron oxidation of the reduced photocatalyst by Phth· would regenerate the photocatalyst and Phth⁻. Finally, Phth⁻ deprotonates benzoic acid to regenerate the benzoate salt. In the follow-up efforts, the same group successfully utilized this strategy in photoinduced alkylation⁷¹ and trifluoromethylthiolation⁷² of aldehydes. In addition to aliphatic and aryl aldehydes, the less-explored formamide and formic ester derivatives could also participate in alkylation smoothly.

From phosphate salts

In 2018, Nicewicz, Alexanian, and co-workers demonstrated a general approach to the functionalization of aliphatic C-H bonds using an acridinium photoredox catalyst and a phosphate salt (Scheme 36A).⁷³ It was hypothesized that the highly oxidizing acridinium photoredox catalyst (36.2) ($E_{1/2}(\text{cat}^*/\text{cat}\cdot) = +2.08$ V versus Ag/Ag⁺) could oxidatively generate oxygen-centered radicals from anionic inorganic bases. A survey of various bases, including phosphate, carbonate, and benzoate salts, revealed potassium phosphate to be most efficient in the azidation of tertiary C-H bonds. With the C-H substrate as limiting reagent, cyclic and acyclic alkanes as well as benzylic C-H bonds successfully reacted at the most electron-rich C-H sites. Importantly, a diverse array of C-H functionalizations could be accomplished using different SOMOphiles as trapping reagents (36.4e–36.4h). The reaction mechanism resembles the one in Scheme 35.

In the same year, Kanai and co-workers disclosed an aliphatic C-H cyanation strategy using an iridium photoredox catalyst and an organic phosphate (36.8) (Scheme



Scheme 50. Generation of N-centered abstractors and representative precursors

36B).⁷⁴ Various activated C(sp³)-H bonds were cyanated in good yields. Similarly, a phosphate radical species generated from the single electron oxidation of **36.8** was responsible for HAT. In 2020, Stephenson and co-workers reported a radical cascade arene dearomatization in which a phosphate radical was responsible for abstracting an H atom from the N-H bond in N-sulfonyl amide and generating an N-centered radical (Scheme 36C).⁷⁵ Control experiments supported a HAT process instead of a PCET pathway (no product formation from **36.12**).

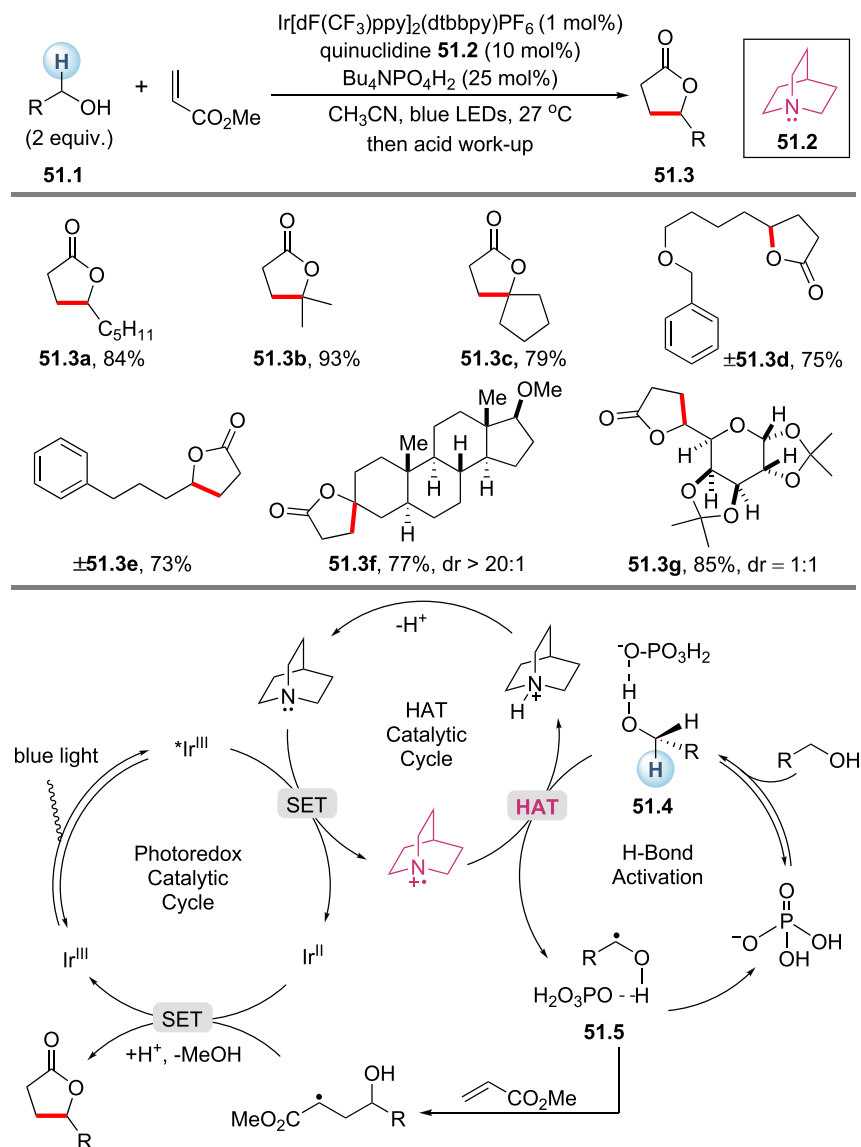
From nitrate salts

Traditionally, the nitrate radical NO₃• can be generated from the reaction of nitrogen dioxide with ozone or the photolysis of (NH₄)₂Ce(NO₃)₆ under UV light. In 2015, Wille, König, and co-workers demonstrated that NO₃• could be easily accessed from nitrate anion (E_{1/2p}^{ox} = +1.97 V) with an acridinium photoredox catalyst, which was applied to the aerobic oxidation of alcohols.⁷⁶ Nicewicz and co-workers recently reported a homobenzylic oxygenation strategy through the combination of photoredox, HAT, and cobalt catalysis.⁷⁷ Lithium nitrate was employed as the precursor of nitrate radical, which could activate the benzylic C-H bond.

From alcohols

Abundant free alcohols are ideal precursors to alkoxy radicals, but direct generation of alkoxy radicals from alcohols is a formidable challenge due to the high oxidation potential of alkoxides and the strong O-H bond of alcohols. In 2018, Zuo and co-workers exploited the ligand-to-metal charge-transfer (LMCT) photoreactivity of Ce^{IV}-alkoxide complexes for the functionalization of methane, ethane, and higher alkanes (Scheme 37A).⁷⁸ In the proposed mechanism, a Ce^{IV}-alkoxy complex, generated *in situ* from alcohol and a Ce^{IV} salt, undergoes photoinduced LMCT to generate the electrophilic alkoxy radical (**37.4**) and a reduced Ce^{III} species. The alkoxy radical (**37.4**) then abstracts an H atom from the alkane to generate the radical (**37.5**), which readily couples with the electron-deficient azo compound (**37.2**) to give **37.6**. Single electron reduction of **37.6** by reduced Ce^{III} regenerates Ce^{IV} and furnishes the desired product after protonation.

The use of alcohols as HAT catalysts could allow facile access to alkoxy radicals with varied electronic and steric properties, as demonstrated by Liu, Zuo, and co-workers in 2020 (Scheme 37B).⁷⁹ In the process of exploring cerium-catalyzed C(sp³)-H amination of alkanes under photoirradiation, it was found that good reactivity and regioselectivity could be obtained by using methanol as a HAT reagent. The reaction of 2,3-dimethylbutane furnished two products (**37.8g**, **37.8g'**) (97:3) preferentially involving the tertiary C-H site. Interestingly, when sterically bulkier alcohols, such



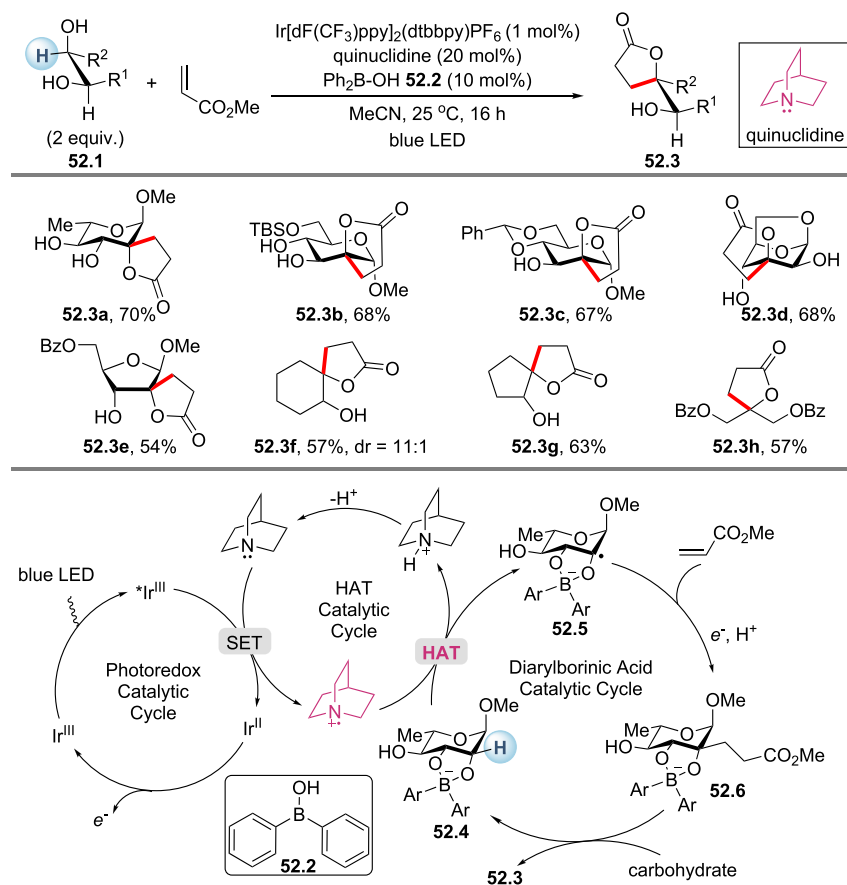
Scheme 51. Photoinduced C-H alkylation of alcohols

as *tert*-butanol (**37.9**) and triphenylsilanol (**37.10**), were utilized under the same conditions, the proportion of **37.8g'** increased substantially, since primary C-H sites are less sterically hindered. Introduction of electron-withdrawing groups to the alcohols (**37.11**, **37.12**) also resulted in lower selectivity, probably due to the stronger O-H bond and the more electrophilic alkoxy radical.

S-centered abstractors

From thiol and disulfide

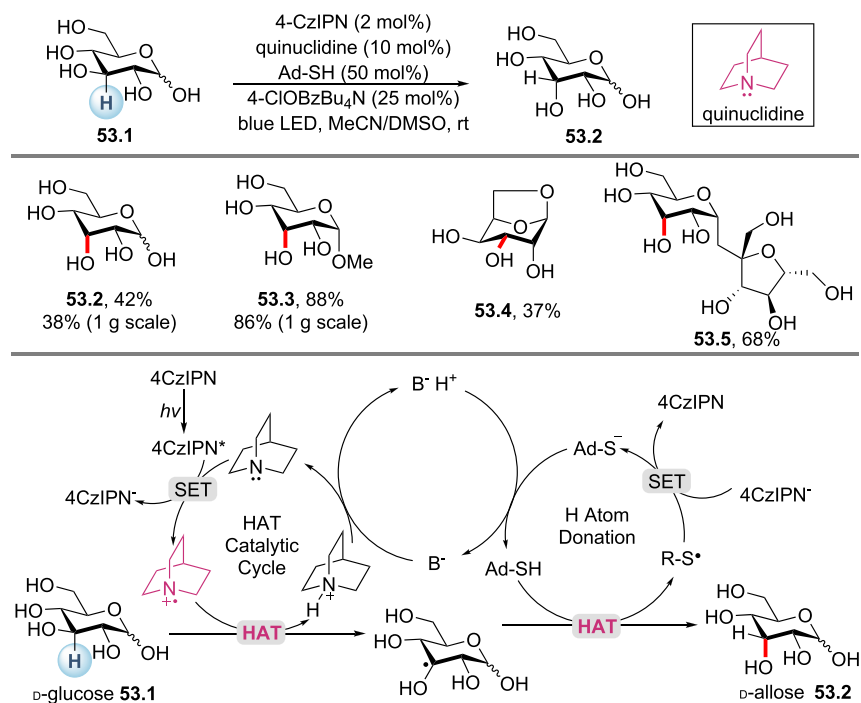
The hydrogen atom abstracting reactivity of thiyl radicals has been known for decades.⁸⁰ Recently, the synergistic merger of photocatalysis with thiol catalysis has enabled efficient generation of thiyl radicals and has offered new and green pathways for the concise assembly of complex molecular structures. A pioneering report was published by MacMillan and co-workers in 2015.⁸¹ Visible-light-driven cross-coupling of allylic/benzylic $\text{C}(\text{sp}^3)\text{-H}$ bonds with electron-deficient aryl nitriles facilitated by 1 mol % of $\text{Ir}(\text{ppy})_3$ and 5 mol % of $^i\text{Pr}_3\text{SiSH}$ delivered products in yields of



Scheme 52. Photoinduced C-H alkylation of carbohydrates

50%–95% (Scheme 38). The method proved robust in terms of functional group tolerance and regioselectivity (e.g., **38.4d**). Interestingly, competitive experiments between cyclohexene and ethylbenzene, two competent C-H substrates, afforded allylic-functionalized **38.4e** as the sole product. In the proposed reaction mechanism, the excited Ir(ppy)₃ undergoes an SET process with the electron-deficient arene (**38.2**) to generate a persistent arene radical anion (**38.5**) along with the oxidized photocatalyst Ir^{IV}. The weakly acidic thiol ($E_{1/2}^{\text{red}} = +1.12$ V versus Ag/Ag⁺ for butanethiol in MeCN) is deprotonated to yield the thiolate anion ($E_{1/2}^{\text{red}} = -0.85$ V versus Ag/Ag⁺ for butanethiolate in MeCN). The latter species is subsequently oxidized by Ir^{IV} ($E_{1/2}^{\text{red}} = +0.77$ V versus Ag/Ag⁺ in MeCN) to regenerate the photocatalyst and form a thiyl radical (**38.6**), which, with a BDE for S-H of 87 kcal/mol, could abstract an H atom from allylic C-H bonds (BDE 81–83 kcal/mol) and give the allylic radical (**38.7**). Finally, an intermolecular radical-radical coupling furnishes the C-C coupled product after rearomatization.

The HAT reactivity of thiyl radicals toward benzylic C-H bonds was used by König and co-workers for photocarboxylation (Scheme 39).⁸² With the C-H substrate as the limiting reagent, carboxylation with CO₂ proceeded in the presence of 2,4,5,6-tetra(carbazol-9-yl)isophthalonitrile (4CzIPN) and triisopropylsilanethiol under irradiation with blue light. A broad range of benzylic C-H bonds were transformed to 2-arylpropionic acids in moderate to good yields, and the synthesis of several drugs was reported. The benzylic radical intermediate (**39.5**) produced by HAT could accept an electron from the reduced photocatalyst. The resulting



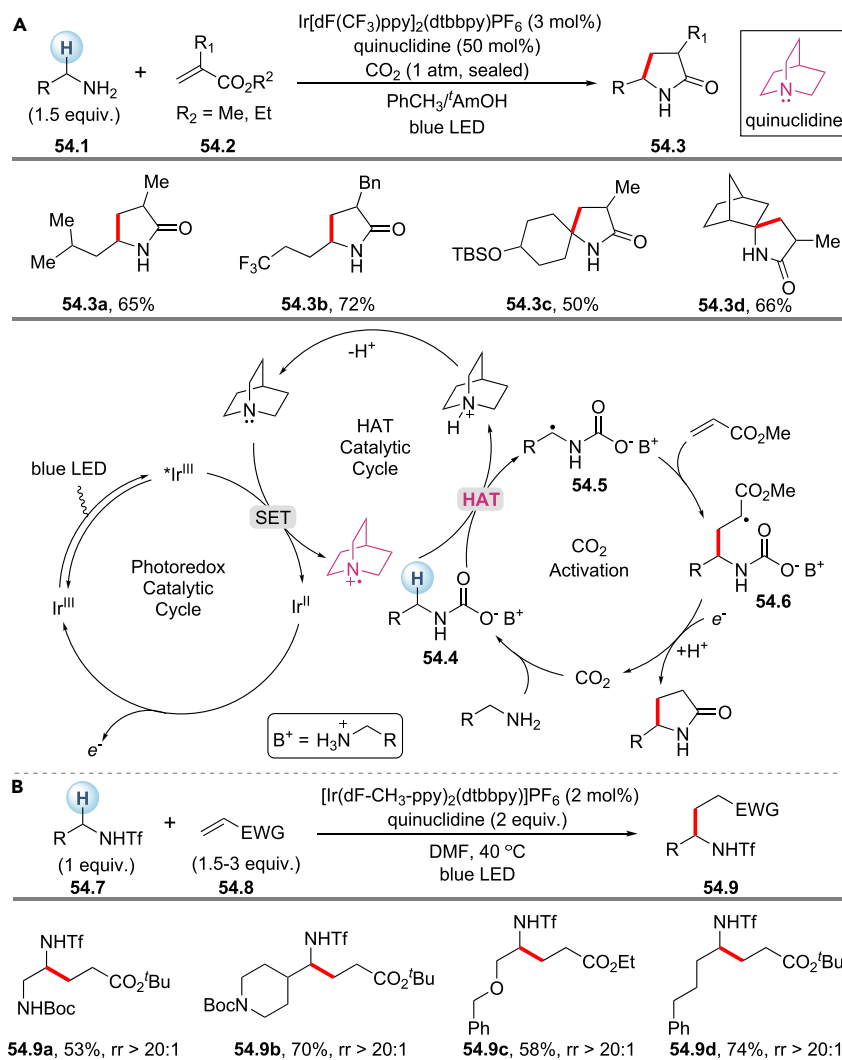
Scheme 53. Photoinduced epimerization of carbohydrates

Ad, adamantyl; B, base.

benzylic anion (39.6) reacts with CO₂ to afford the corresponding carboxylic acid after protonation. It was found that one of the cyano groups in 4CzIPN was substituted by a benzyl moiety, generating a stronger reducing photocatalyst, which was proposed as the main active catalyst for carbanion generation.

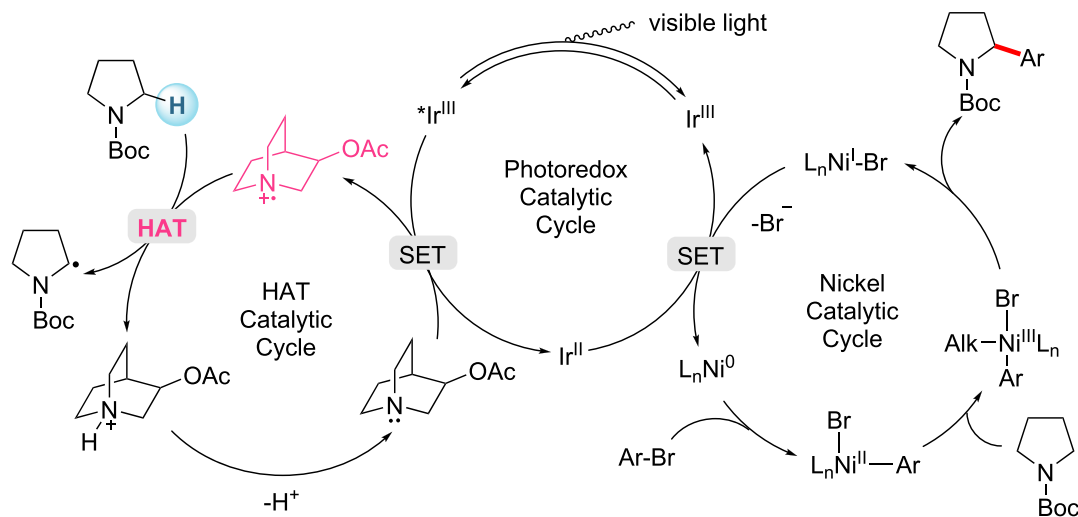
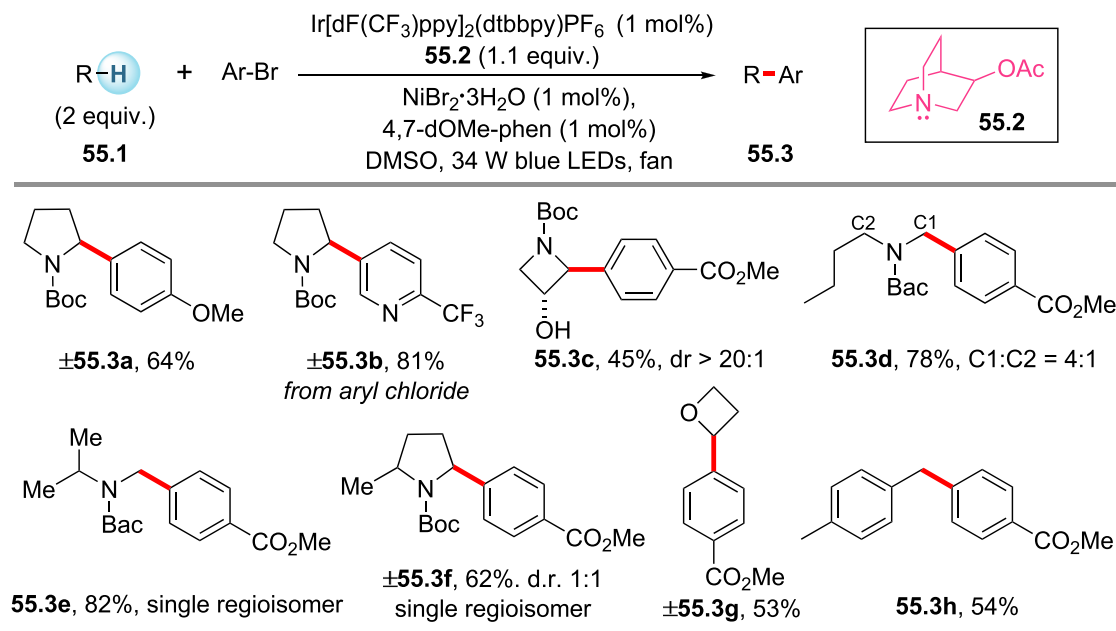
In 2015, MacMillan et al. developed a heteroarene alkylation strategy with alcohols as alkylating reagents via the combination of photoredox and thiol catalysis (Scheme 40).⁸³ A broad range of heteroarenes and alcohols were efficiently coupled to produce alkylated heterocycles in 43%–98% yields. Ethers were also amenable substrates, affording the corresponding ring-opened alcohol products. The authors proposed that the excited Ir photocatalyst is initially oxidatively quenched by a sacrificial amount of protonated heteroarene (40.5) to form Ir^{IV}. Given the relatively high oxidation potential of Ir^{IV} ($E_{1/2}^{\text{red}} = +1.21$ V versus Ag/Ag⁺ in MeCN), an SET from the thiol catalyst (40.3) ($E_{1/2}^{\text{red}} = +0.85$ V versus Ag/Ag⁺ for cysteine) to Ir^{IV} would furnish the thiyl radical (40.6) after deprotonation. A HAT from the alcohol (40.1) (BDE for methanol α -C-H 96 kcal/mol) to 40.6 (BDE for methyl 2-mercaptoacetate S-H 87 kcal/mol) is driven by the polar effect in the transition state. The generated nucleophilic radical (40.7) would then add to the protonated heteroarene to afford the aminyl radical cation (40.8), which forms the α -amino radical (40.9) after deprotonation. Intermediate 40.9 is primed to undergo a spin-center shift to eliminate one molecule of H₂O and generate the benzylic radical (40.10). The resulting open-shell species is protonated and then reduced by the excited photocatalyst to provide the alkylation product.

Thiyl radicals also played a key role in the photoinduced acceptor-less dehydrogenation of alcohols reported by Wu and co-workers in 2017 (Scheme 41).⁸⁴ Heterogeneous CdSe quantum dots were employed as photocatalysts in conjunction with



adsorbed 3-mercaptopropionic acid and NiCl₂, which served as a HAT catalyst and proton reduction catalyst, respectively. After light absorption, hole transfer from the valence band to the surface-adsorbed thiolate anion generates the thiyl radical (41.3). Disproportionation of two ketyl radicals generated by the HAT process affords the starting alcohol and a carbonyl product. A broad set of alcohols could be converted into aldehydes or ketones in aqueous media with concomitant H₂ formation. Non-benzylic alcohols (41.2c, 41.2f) underwent dehydrogenation, albeit with lower conversion and selectivity. The authors exploited this reactivity difference in the chemoselective dehydrogenation of the polyhydroxy compounds (41.2g–41.2i).

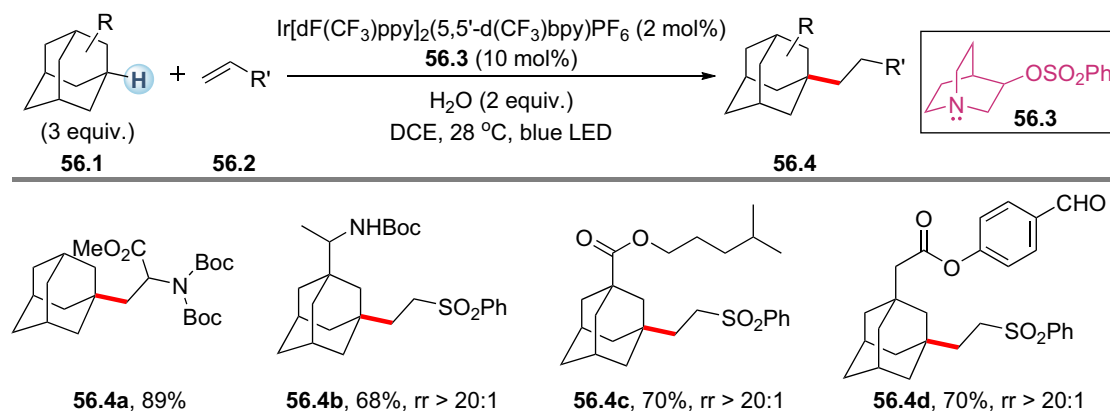
The polar effect is a remarkable property that enables considerably endergonic R-H abstractions by thiyl radicals,⁴⁵ as demonstrated by the activation of alcohols in Schemes 40 and 41. Moreover, thiols can rapidly transfer hydrogen atoms to carbon radicals ($K_{\text{HAT}} = 2 \times 10^7 \text{ M}^{-1} \text{ s}^{-1}$ from alkyl thiol to primary carbon radical at 298 K).⁸⁰ These features of thiol catalysis were employed by Wu and co-workers in 2017 for photoinduced hydrosilylation of electron-rich alkenes (Scheme 42).⁸⁵ Various silanes



Scheme 55. Photoinduced C-H arylation through photoredox, quinuclidine, and nickel catalysis
Ac, acetyl; Bac, *tert*-butylaminocarbonyl.

and alkenes were successfully coupled, generally in high yields via synergistic use of 4CzIPN and triisopropylsilanethiol. Mechanistically, the electrophilic thiyl radical (42.5) could selectively abstract the H atom from the more hydridic Si-H (compared with C-H) bond to deliver the silyl radical (42.6). Regioselective addition of the silyl radical (42.6) to the electron-rich alkene affords the radical adduct (42.7). The nucleophilic radical (42.7) then undergoes another polarity-matched HAT process with triisopropylsilanethiol to generate the hydrosilylation product,⁴⁵ along with the formation of thiyl radical (42.5). The reduced photocatalyst is finally oxidized by 42.5 back to its ground state.

In 2019, Wu and co-workers reported a 100 g scale synthesis of deuterated silanes in continuous-flow micro-tubing reactors through cooperative photoredox catalysis



Scheme 56. Photoinduced C-H alkylation of adamantanes

and thiol-mediated polarity-reversal catalysis (Scheme 43).⁸⁶ Using a combination catalyst of 0.2 mol % 4CzIPN and 2 mol % triisopropylsilanethiol, deuterated triethylsilanes were obtained with excellent D incorporation (95%) and good crude yield (89%) at a production rate of 1 g/h.

Recently, the concept of cooperative photoredox and thiol catalysis has also been applied by Xie, Zhu, and co-workers⁸⁷ and by Wu and co-workers⁸⁸ in the functionalization of N-heterocyclic carbene (NHC) boranes (Scheme 44). A kinetically favored and polarity-matched HAT between electrophilic thiyl radical and NHC-borane (BDE of B-H 73–80 kcal/mol) furnishes an NHC-boryl radical, which can couple with another reductively generated persistent radical to deliver the desired product.¹⁷

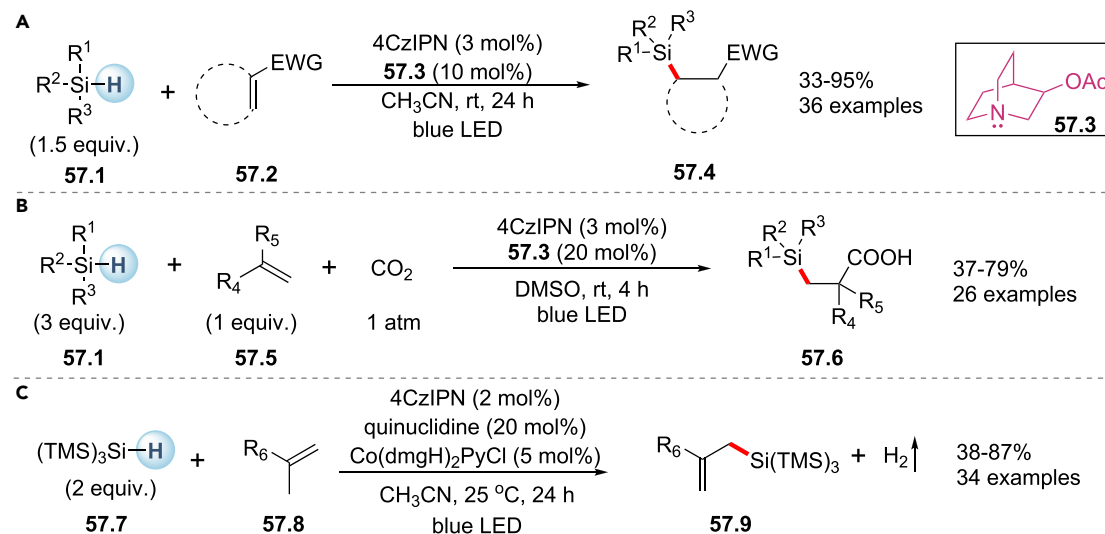
The HAT-active thiyl radicals can also be generated from disulfides via single electron reduction or direct photolysis, as demonstrated by the groups of Hong⁸⁹ and Dilman⁹⁰ in the thiolation of allylic and unactivated C(sp³)-H bonds, respectively. In Dalman's study, the use of electron-deficient tetrafluoropyridinyl disulfide greatly lowered the energy barrier of the thiyl group transfer step and overcame the unproductive H-donor activity of thiol.⁸⁰

From thiocarboxylate salts

In 2018, Hamashima et al. disclosed a highly regio- and chemoselective C-H arylation of benzylamines with thiobenzoic acid (45.3) as the indirect HAT catalyst (Scheme 45).⁹¹ When the arylation reaction of *N,N*-dimethylbenzylamine (45.4a) proceeded under purely photoredox conditions via the deprotonation of aminium radical cation, the *N*-methyl C-H site was selectively targeted (benzyl:Me = 1:8.5). In contrast, addition of 1 mol % of 45.3 completely switched the regioselectivity to the slightly more hydridic *N*-benzylic C-H position (benzyl:Me > 20:1). Measurement of oxidation potentials supported a HAT process, as the oxidation potential of the thiocarboxylate potassium salt ($E_p^{ox} = +0.8$ V versus Ag/Ag⁺ in DMF) is lower than that of the substrate amine ($E_p^{ox} = +0.97$ V versus Ag/Ag⁺ in DMF for *N*-benzyl tetrahydroquinoline). The ability of the S-centered abstractor to selectively target the most electron-rich *N*-benzylic C-H bond among various activated C-H bonds is remarkable and is especially evidenced by the products 45.4d–45.4f.

From thiophosphoric acids and thiophosphoric imides

Catalytic acceptor-less dehydrogenation from saturated organic compounds to produce unsaturated molecules and hydrogen gas is a difficult but important chemical



Scheme 57. Photoinduced Si-H functionalizations with quinuclidines as indirect HAT catalysts

(A) Hydrosilylation of alkenes.

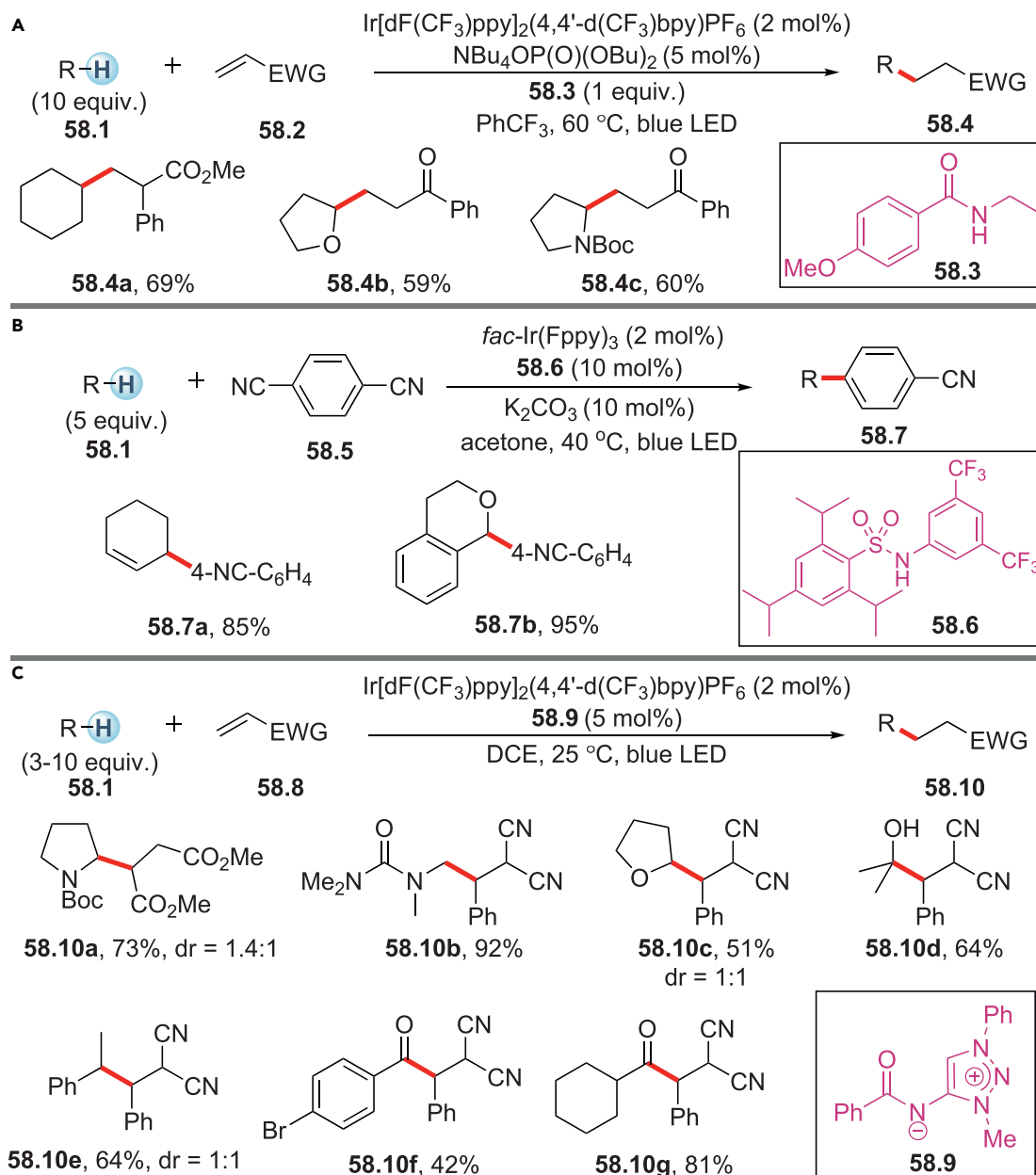
(B) Silacarboxylation of alkenes.

(C) Dehydrogenative silylation of alkenes. TMS, trimethylsilyl.

process. In 2017, Kanai and co-workers reported a photoinduced acceptor-less dehydrogenation of tetrahydronaphthalenes through ternary hybrid catalysis, including an acridinium photoredox catalyst, a Pd metal catalyst, and the thiophosphoric imide organocatalyst (**46.2**) (Scheme 46).⁹² The combined use of three different catalysts was essential for the catalytic activity and led to naphthalene products in yields of 46%–82%. In pursuing a suitable S-centered radical as HAT catalyst, thiophosphoric imide exhibited good reactivity, whereas aliphatic and aryl thiols and thiocarboxylate were found to be unreactive. The authors attributed the observed reactivity to the higher H atom abstraction ability of the electron-deficient sulfur-centered radical (**46.4**) generated from **46.2**. In the proposed mechanism, **46.4** could abstract an H atom from tetrahydronaphthalene (**46.5**) to give a benzylic radical (**46.6**). The radical (**46.6**) would combine with a metal catalyst (M^n) to generate an organometallic species (**46.7**), which in turn would accept an electron from the reduced photocatalyst, affording the organometallic species (**46.8**). β -hydride elimination from **46.8** would produce a dihydronaphthalene (**46.9**) and a metal hydride species M^n-H , which reacts with a proton to evolve hydrogen gas. Repeating the catalytic cycle would finally produce naphthalene, **46.10**.

In a subsequent effort, Mitsunuma, Kanai, and co-workers achieved acceptor-less dehydrogenation of aliphatic secondary alcohols using a mechanistically similar ternary hybrid catalyst system (Scheme 47).⁹³ A broad scope of alcohols afforded ketone products in high yields under visible light irradiation at room temperature, including sterically hindered alcohols such as **47.3a**. Alcohols such as benzhydrol (**47.3d**) that do not contain a β -C-H bond reacted poorly, which is consistent with a β -hydride elimination process. Hemiacetals (**47.6**) derived from aldehydes and alcohols also underwent acceptor-less dehydrogenation smoothly to furnish ester products (e.g., **47.7a**, **47.7b**).

Recently, Mitsunuma, Kanai, and co-workers disclosed photocatalytic allylation of aldehydes with unactivated alkenes based on another ternary hybrid catalyst system



Scheme 58. Photoinduced C-H functionalization with amides or sulfonamides as indirect HAT catalysts

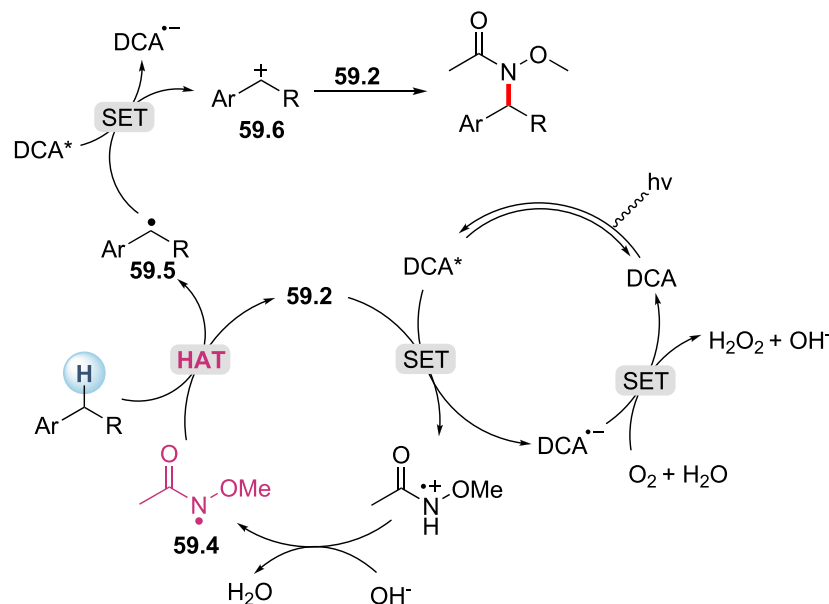
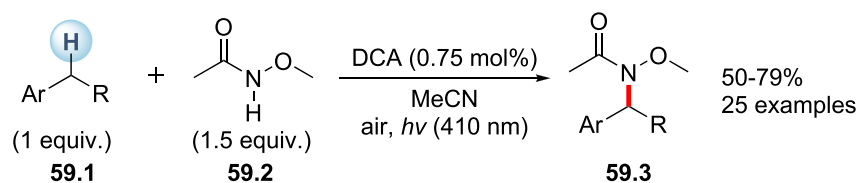
(A) An amide HAT catalyst reported by Knowles and co-workers.¹¹²

(B) A sulfonamide HAT catalyst reported by Oisaki, Kanai, and co-workers.¹¹³

(C) An amidate HAT catalyst reported by Ooi and co-workers.¹¹⁴

comprising an acridinium photoredox, a thiophosphoric imide HAT catalyst, and a chromium catalyst.⁹⁴ Activation of the allylic C-H bond by a sulfur-centered radical produces an allyl radical intermediate, which could be intercepted by chromium(II) to give a key allyl chromium(III) species that readily reacts with the aldehyde. This method could be applied to catalytic asymmetric allylation of aldehydes using a chiral indane-BOX ligand (up to 88% enantiomeric excess [ee]).

In 2018, Xie, Zhu, and co-workers developed an umpolung trifluoromethylthiolation of tertiary alkyl ethers with 4-CzIPN as a photoredox catalyst and thiophosphoric

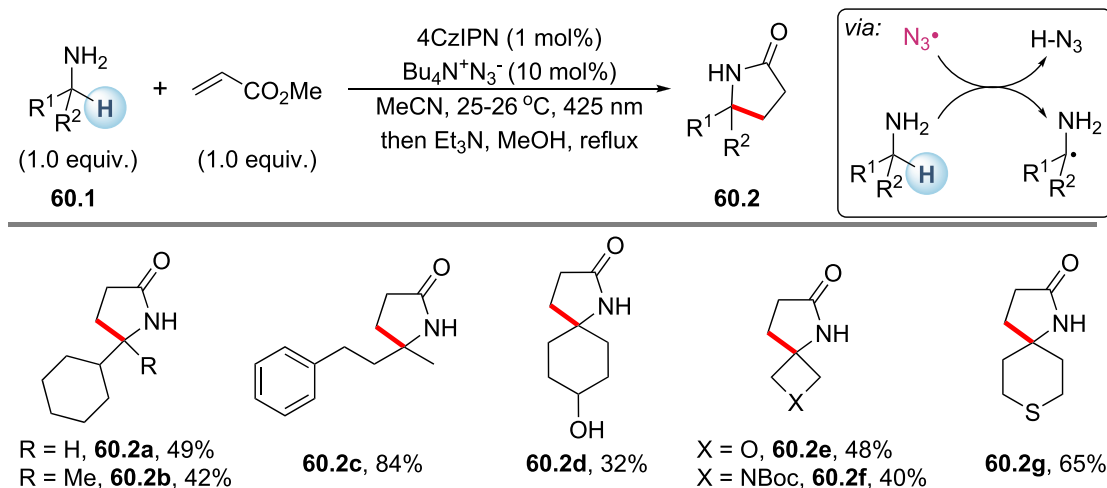


Scheme 59. Photoinduced benzylic C(sp³)-H amination via cross-dehydrogenative coupling
DCA, 9,10-dicyanoanthracene.

acid as an indirect HAT catalyst (Scheme 48).⁹⁵ Hydrogen atom abstraction from methoxymethyl (MOM)-type tertiary alkyl ether (48.1) generates a radical intermediate (48.3), which could undergo fragmentation to form a tertiary alkyl radical (48.4). This polarity-matched HAT was found to be highly site selective in the presence of multiple α -ether, methine, and benzylic C-H bonds. Interestingly, when the substrate contains both secondary and tertiary MOM-ether units, the tertiary MOM-ether moiety was preferentially trifluoromethylthiolated (48.2g).

From thiourea

In 2020, Lin and co-workers demonstrated a photoelectrocatalytic approach to the oxidation of unactivated alcohols using a flavin photocatalyst and an allylthiourea HAT catalyst (Scheme 49).⁹⁶ The electrochemistry was essential, as it avoided the use of O₂ and the generation of the H₂O₂ by-product, both of which could oxidatively degrade thiourea. In the presence of 5 mol % riboflavin tetraacetate (RFT) and 10 mol % thiourea (49.2) under blue light, various secondary alcohols provided the desired ketones in satisfactory yields (66%–91%) in an electrolysis cell (cell voltage 2.5 V) using carbon foam as the anode, Pt coil as the cathode, LiOTf in MeCN as the electrolyte solution, and H₂O as the proton source. Primary alcohols were also found to be compatible, affording the carboxylic acid (49.3e) in 53% yield. A plausible mechanism was subsequently proposed. Upon light irradiation, ET followed by PT between excited RFT* ($E_{1/2}^{\text{red}} = +1.67$ V versus Ag/Ag⁺) and thiourea 49.2 ($E^{\text{ox}} = \sim 0.9$ V versus Ag/Ag⁺) generates an S-centered radical (49.4) and semiquinone form (RFT[•]-H). The radical (49.4) then abstracts an H atom from the alcohol (49.1) to produce the C-centered radical (49.5), which could further react with (RFT[•]-)



Scheme 60. Photoinduced α -alkylation of primary aliphatic amines

H through another HAT process to afford the ketone product (**49.3**). Finally, the dihydroquinone form of (RFT)-H₂ is oxidized at the anode surface, regenerating the RFT catalyst.

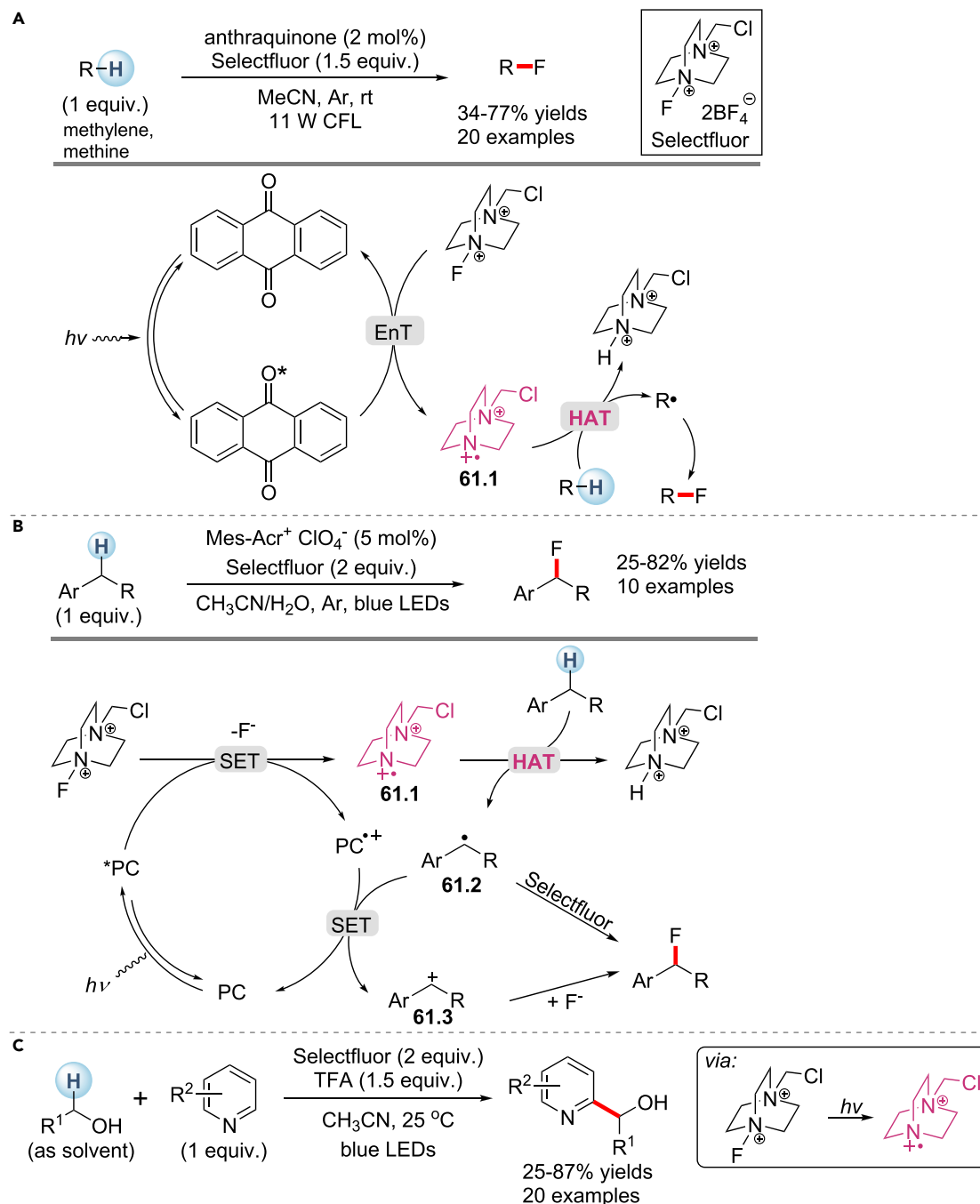
N-centered abstractors

In addition to O- and S-based abstractors, N-centered radicals have also found wide applications in photoinduced intermolecular HAT. In general, there are three ways to generate N-centered abstractors from their precursors: (1) single electron oxidation of tertiary amine to furnish the amine radical cation; (2) single electron oxidation of an N-H bond or an N-centered anion to furnish the N radical; (3) single electron reduction, EnT, or photolysis of N-X bonds to furnish the N radical (Scheme 50). It is known that tertiary amine radical cations could undergo α deprotonation to form α -amino carbon radicals. However, this process is not favored for some tertiary amines (e.g., quinuclidine) due to the poor H-C-N orbital overlap in the rigid bicyclic structure.

From tertiary amine

Single electron oxidation of quinuclidine forms the highly electrophilic nitrogen radical cation (BDE for H-N⁺ bond 100 kcal/mol in quinuclidinium cation), whose HAT ability was utilized by Macmillan and co-workers for C-H alkylation of alcohols in 2015 (Scheme 51).⁹⁷ Both primary and secondary alcohols reacted well, with yields ranging from 61% to 93%. This protocol was further applied to the post-modification of complex molecules exclusively targeting α -alcohol C-H sites (e.g., **51.3f**, **51.3g**). The key to the efficient and selective alkylation is the hydrogen bonding between the hydroxy group of alcohol and tetra-*n*-butylammonium phosphate. This non-covalent interaction in **51.4** greatly increases the n- σ^* delocalization of the oxygen lone pair, making the α -alcohol C-H more hydridic. It was proposed that a polarity-matched HAT between this C-H bond and the quinuclidine radical cation furnishes a C radical (**51.5**). Subsequent radical addition, single electron reduction, and cyclization afford the lactone product.

Apart from non-covalent interactions, the use of covalent bonding to weaken an α -alcohol C-H bond has also been reported. In 2019, Mark and co-workers disclosed a site-selective and stereoselective C-H alkylation of carbohydrates via cooperative



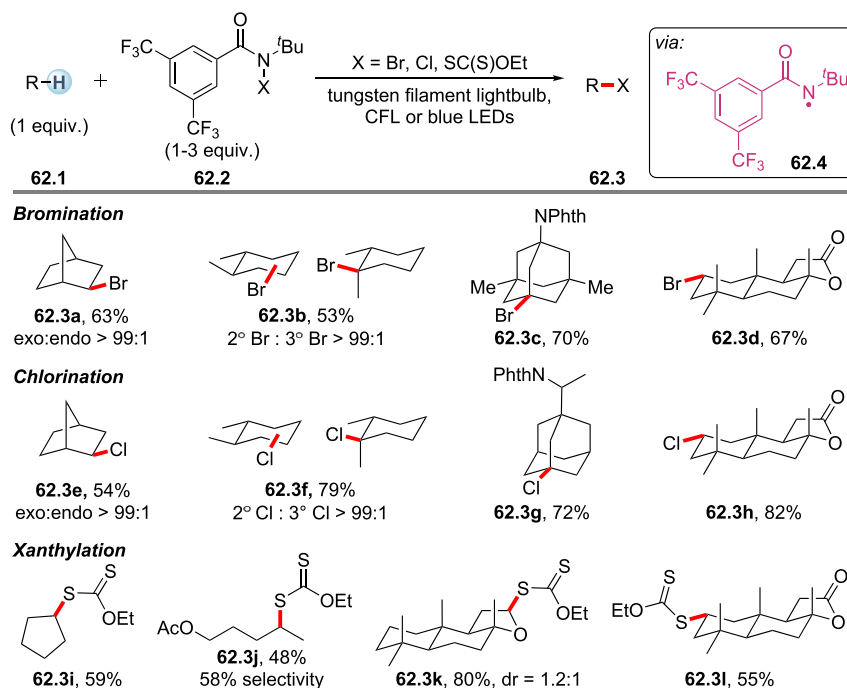
Scheme 61. C-H functionalizations with Selectfluor as the indirect HAT reagent

(A) C-H fluorination via energy transfer to Selectfluor reported by Tan and co-workers.¹¹⁷

(B) Benzylic C-H fluorination via single electron reduction of Selectfluor reported by Wu and co-workers.¹¹⁸

(C) α -arylation of alcohols via homolysis of Selectfluor reported by Lei and co-workers.¹¹⁹

photoredox, quinuclidine, and diarylborinic acid catalysis (Scheme 52).⁹⁸ Alkylation proceeded exclusively at the equatorial C-H sites of *cis*-1,2-diols giving products in good yields (54%–70%). The use of Ph₂BOH (52.2) consistently provided an enhancement in reaction efficiency. Computational modeling suggested that the 1,2-diol moieties of carbohydrates first react with diarylborinic acid (52.2), delivering

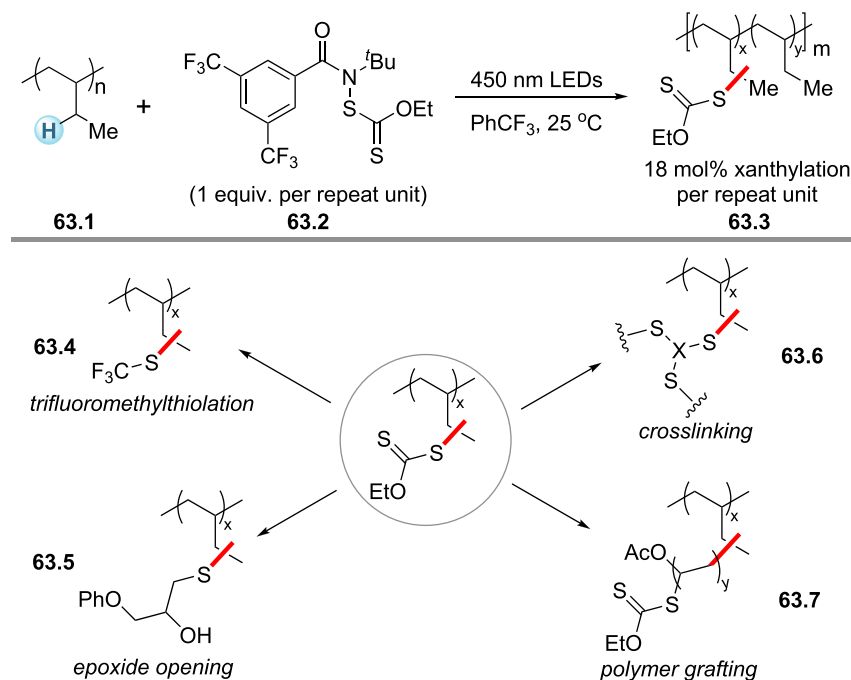


Scheme 62. Photoinduced C-H functionalizations with *N*-bromoamide, *N*-chloroamide, and *N*-xanthylamide

the tetracoordinate borinic ester (**52.4**). A HAT event between **52.4** and the quinuclidine radical cation, which is accelerated by polarity match and ion pair effects, affords the C radical (**52.5**). The observed retention of configuration in the product is probably due to the association with the borinic acid. In 2020, Oisaki, Kanai, and co-workers discovered that the use of a spiroilane catalyst could lower the BDEs of α -hydroxy C-H bonds by 2–3 kcal/mol via covalent interactions.⁹⁹

In 2020, a site-selective epimerization of carbohydrates was developed by Wendlandt and co-workers for the synthesis of rare sugar isomers, which had previously been prepared only through multistep chemical or enzymatic syntheses (Scheme 53).¹⁰⁰ With 2 mol % 4-CzIPN, 10 mol % quinuclidine, 50 mol % adamantane thiol, and 25 mol % tetrabutylammonium *p*-chlorobenzoate, various saccharides and glycans afforded selectively epimerized products under blue-light irradiation. Little or no epimerization was observed in the absence of photocatalyst, quinuclidine, thiol, or light. Mechanistic data supported an irreversible HAT between the quinuclidine radical cation and the α -hydroxy C-H bond in the sugar molecule, followed by a thiol-mediated diastereoselective hydrogen atom donation process.

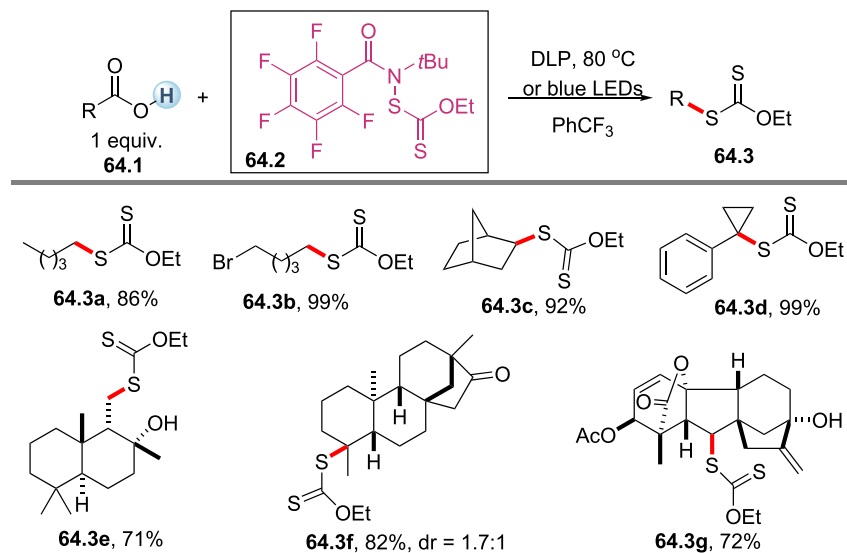
Analogous to α -hydroxy C-H bonds, α -amino C-H bonds (BDE 89–94 kcal/mol) are hydridic and are widely present in functional molecules. In 2018, Rovis, Schoenebeck, and co-workers proposed a CO₂-activation strategy for the direct transformation of primary aliphatic amines to γ -lactams (Scheme 54A).¹⁰¹ Control experiments revealed that the iridium photocatalyst, visible light, quinuclidine, and CO₂ were all necessary for an efficient transformation. A diverse array of primary amines, including sterically hindered amines (e.g., **54.3c**), are viable in this transformation, which provides γ -lactams in moderate to good yields. Mechanistically, primary amine reacts first with CO₂ to deliver the carbamate (**54.4**), which then undergoes HAT with an electrophilic quinuclidine radical cation to form the C radical (**54.5**).



Scheme 63. Photoinduced C-H functionalization of polyolefins

The electrostatic interaction between the carbamate (54.4) and the quinuclidine radical cation is important in the HAT process, and this is evidenced by experimental and computational studies. The nucleophilic radical formed (54.5) is subsequently trapped by electron-deficient acrylate before being reduced and protonated to furnish, after cyclization, the γ -lactam product. In a subsequent effort, Rovis and co-workers demonstrated a triflate-protecting strategy for photoinduced α -alkylation of primary amines (Scheme 54B).¹⁰² Site-selective α -C-H activation of trifluoromethanesulfonamide was achieved in the presence of competitive hydridic C-H bonds (54.9a–54.9d). Deprotonation of the N-H bond in triflimide ($\text{p}K_{\text{a}(\text{N-H})} \sim 7.6$) furnishes a more hydridic α -amino C-H bond, which is more susceptible to H atom abstraction.

The photoinduced quinuclidine-mediated HAT process could also be merged with nickel-catalyzed cross-coupling reactions, enabling the use of $\text{C}(\text{sp}^3)\text{-H}$ bonds as latent nucleophiles. In 2016, Macmillan and co-workers realized the coupling of α -amino, α -ether, and benzylic C-H bonds with aryl electrophiles using a combination of an Ir photocatalyst, a HAT catalyst (55.2), and a nickel catalyst (Scheme 55).¹⁰³ Electron-deficient and electron-rich aryl bromides, and even aryl chlorides, are compatible electrophiles. In some cases, N-Bac-substituted amines delivered the arylated products in higher yields than N-Boc-substituted amines, and this was attributed to the diminished electron-withdrawing nature of the Bac group. Interesting regioselectivity patterns were observed in unsymmetrical amine substrates (55.3d–55.3f) and the reactivity order was found to be least-hindered methyl > methylene > most-hindered methine α -amino C-H bonds. In this catalytic system, the nickel catalytic cycle starts with the oxidative addition of Ni^0 species to the aryl bromide, furnishing a Ni^{II} species. Subsequent radical addition and reductive elimination provide the cross-coupled product. A final SET between Ni^{I} and reduced photocatalyst closes these two catalytic cycles.



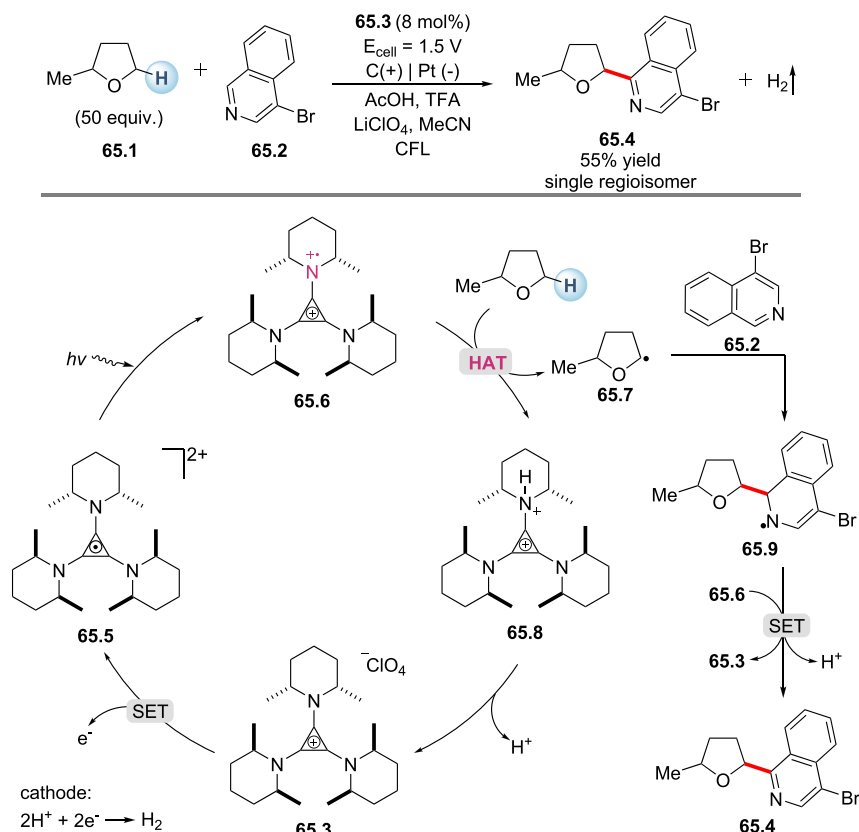
Scheme 64. Decarboxylative xanthylation via HAT from acidic O-H bonds

DLP, dilauroyl peroxide.

In 2017, Macmillan and co-workers demonstrated a conceptually similar coupling of α -hetero C-H bonds with alkyl bromides.¹⁰⁴ Various alkyl groups were successfully incorporated into the α -amino, α -ether, and α -thioether C-H positions with 41%–83% yields. Later, the triple catalytic system consisting of a photoredox catalyst, a quinuclidine HAT catalyst, and a nickel catalyst was utilized by the same group in the arylation and alkylation of α -hydroxy¹⁰⁵ and aldehydic¹⁰⁶ C-H bonds. Zinc chloride (ZnCl_2) served as an important additive in the α -arylation of alcohols. As a Lewis acid, ZnCl_2 activates α -hydroxy C-H bonds via alcohol deprotonation while deactivating other hydridic bonds such as α -amino and α -oxy C-H bonds. Moreover, the C-O bond formation was simultaneously suppressed due to inhibited formation of nickel alkoxide species in the presence of zinc salts.

The target of quinuclidine-mediated HAT is not limited to α -heteroatom C-H bonds. In 2019, Martin et al. reported a highly selective tertiary $\text{C}(\text{sp}^3)$ -H alkylation of adamantanes using an iridium photoredox catalyst and a quinuclidine derivative catalyst (Scheme 56).¹⁰⁷ Comparison between quinuclidine, 3-acetoxyquinuclidine, and quinuclidin-3-yl benzenesulfonate (56.3) revealed that the most electron-deficient 56.3 led to the highest reaction rate and yield, especially with electron-poor adamantanes. This effect was attributed to the increased strength of the H-N⁺ bond in the corresponding ammonium cation. Interestingly, the tertiary $\text{C}(\text{sp}^3)$ -H sites of adamantanes were exclusively alkylated in the presence of weaker bonds such as α -amino methine (56.4b), aldehydic (56.4d), and other tertiary (56.4c) C-H bonds. Due to the high stability of the 1-adamantyl carbocation, the transition state of 1-adamantyl C-H abstraction by the quinuclidine radical cation could be stabilized by a favorable positive charge on 1-adamantyl carbon. This beneficial polar effect is further enhanced by the electron-withdrawing substituent in 56.3.

Although similar in terms of their BDE, Si-H bonds are more hydridic than C-H bonds (electronegativity of Si is 1.90 versus that of C, which is 2.55 on the Pauling scale) and could thus be selectively targeted by a quinuclidine radical cation. In 2017 and 2018, Wu and co-workers reported the hydrosilylation⁸⁵ and silacarboxylation¹⁰⁸ of alkenes by using 4CzIPN as a photocatalyst and 3-acetoxyquinuclidine as a HAT



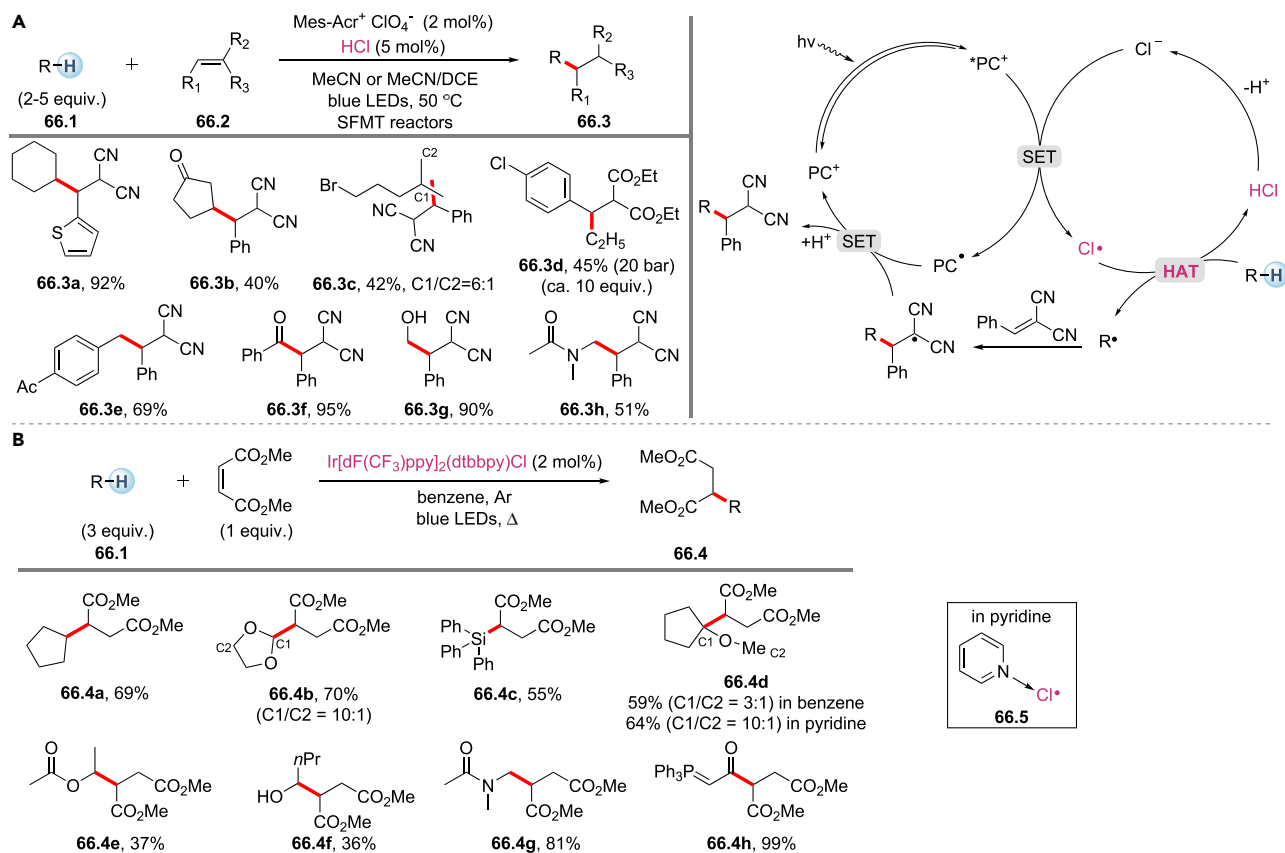
Scheme 65. Electrophotocatalytic arylation of ether

catalyst (Scheme 57). In 2019, Xu and co-workers demonstrated an efficient dehydrogenative silylation of alkenes through the combined use of 4CzIPN, quinuclidine, and a proton-reduction cobaloxime catalyst (Scheme 57C).¹⁰⁹

1,4-Diazabicyclo[2.2.2]octane, a structural analog of quinuclidine, has recently been reported as an indirect HAT catalyst in photocatalysis by Li and co-workers¹¹⁰ and by Alemán and co-workers.¹¹¹

From N-H compounds and N-centered anions

Nitrogen radicals can be generated from the N-H bonds in amides and sulfonamides through photoinduced PCET or stepwise PT/ET. In an early study by Knowles and co-workers, *N*-ethyl-4-methoxybenzamide (58.3) was used as the HAT catalyst in combination with a photoredox catalyst and a phosphate base for the alkylation of cyclohexane, tetrahydrofuran, and *N*-Boc pyrrolidine (Scheme 58A).¹¹² Experimental data, including Stern-Volmer quenching and kinetic analysis, suggested a concerted PCET mechanism for N-radical generation. In 2018, Oisaki et al. demonstrated that catalytic amounts of sulfonamide and base could promote allylic and benzylic C-H arylation in cooperation with an iridium photoredox catalyst (Scheme 58B).¹¹³ A survey of sulfonamides revealed that diarylsulfonamide (58.6), which comprises a sterically hindered electron-donating aryl sulfone moiety and a strongly electron-withdrawing aniline moiety, is optimal. The deprotonated sulfonamide ($E^{\text{ox}} = 0.47 \text{ V}$ versus Ag/Ag^+) could be readily oxidized by the excited photocatalyst to afford the HAT-active sulfonamidyl radical (BDE for N-H 95 kcal/mol). Very recently, Ooi et al. reported that the bench-stable zwitterionic 1,2,3-triazolium amidate (58.9) is



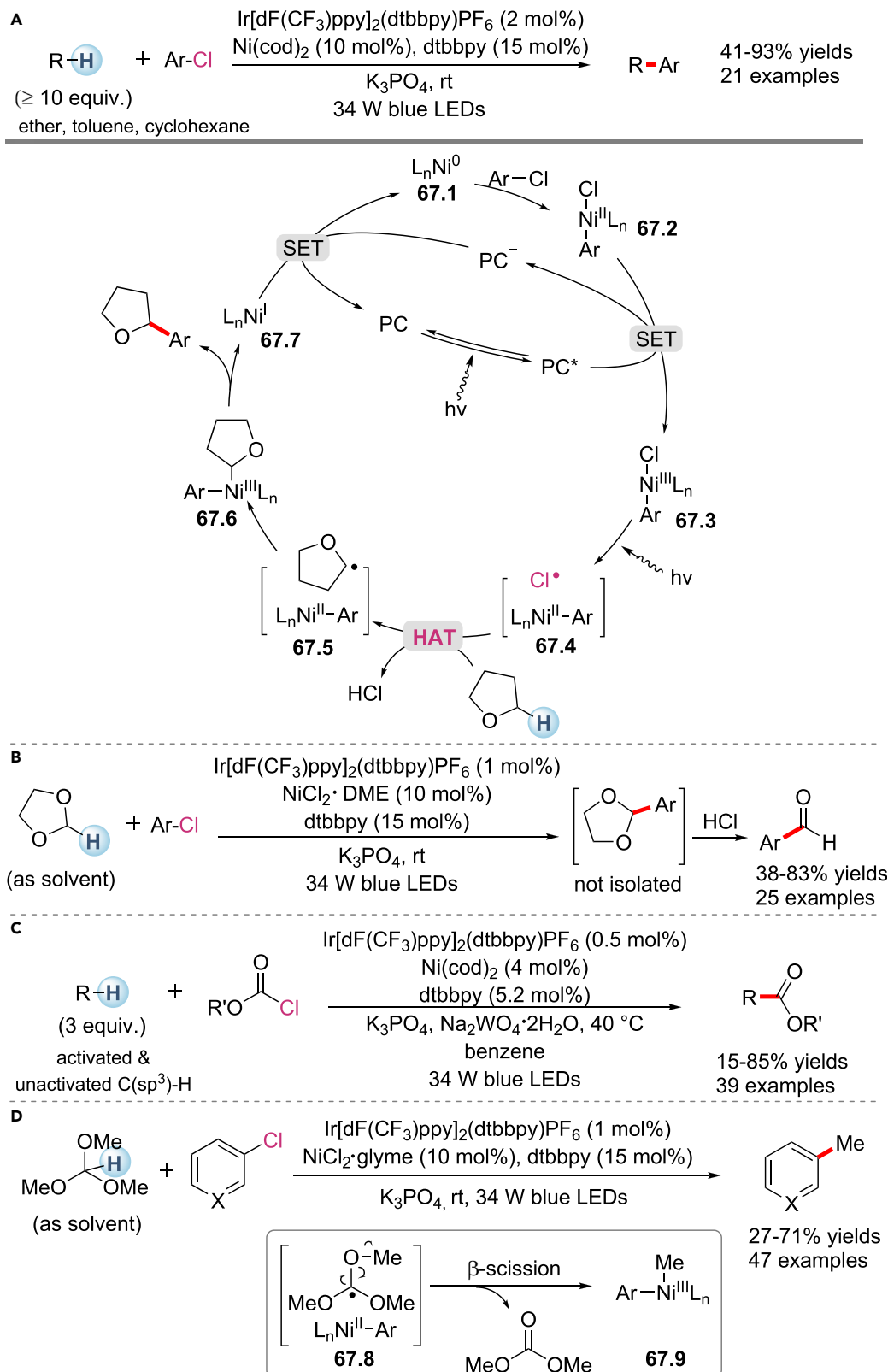
Scheme 66. Photoinduced C-H functionalizations via chlorine radicals

(A) An acridinium complex combined with hydrogen chloride used by Wu and co-workers.¹²⁸ SFMT, stop-flow micro-tubing reactor. (B) An iridium complex, [Ir(dF(CF₃)ppy)₂(dtbbpy)]Cl, used by Barriault and co-workers.¹²⁹

an effective HAT catalyst for photoredox C-H functionalization (Scheme 58C).¹¹⁴ In combination with an Ir photoredox catalyst, a broad range of carbamates, amides, ethers, alcohols, alkyl benzenes, and aldehydes were alkylated in 42%–99% yields. Similarly, **58.9** ($E^{\text{ox}} = 1.28$ V versus Ag/Ag⁺) could be single electron oxidized by photoexcited *Ir ($E_{1/2}^{\text{red}} = 1.65$ V versus Ag/Ag⁺) to furnish a highly reactive amidyl radical (calculated BDE for N-H 100.2 kcal/mol for **58.9**·H).

In 2015, Pandey et al. reported a photoinduced aerobic benzylic C(sp³)-H amination reaction in which an amide served as both HAT and amination reagent (Scheme 59).¹¹⁵ With 9,10-dicyanoanthracene as the photoredox catalyst, various alkyl arenes were monoaminated in yields ranging from 50% to 79% using 1 equiv of a benzylic substrate. It was proposed that the captodative aminyl radical (**59.4**) is generated by single electron oxidation and deprotonation. The benzylic radical (**59.5**) formed after the HAT process can be further oxidized to a benzylic carbocation species (**59.6**), which is then trapped by **59.2** to furnish the final product.

Primary alkyl amines are prevalent in pharmaceutical compound libraries, and methods for the α -C-H alkylation of primary amines hold significant synthetic value. Cresswell and co-workers recently reported the direct α -alkylation of unprotected primary aliphatic amines using 4CzIPN as an organic photocatalyst in combination with tetrabutylammonium azide as a HAT catalyst (Scheme 60).¹¹⁶ Single electron



Scheme 67. Nickel/photoredox-catalyzed C(sp³)-H cross-coupling via chlorine radicals

- (A) C(sp³)-H arylation with aryl chlorides.¹³²
(B) Formylation of aryl chlorides.¹³⁴
(C) C(sp³)-H esterification with chloroformate derivatives.¹³³
(D) Methylation of (hetero)aryl chlorides via β scission of trimethyl orthoformate radical.¹³⁵

oxidation of the azide ion ($E_{p/2}^{ox}$ of $N_3^- = +0.87$ V versus Ag/Ag⁺ in MeCN) by the photoexcited 4CzIPN ($E_{1/2}(PC^*/PC^{\bullet-}) = +1.35$ V versus Ag/Ag⁺) generates the electrophilic azidyl radical, which participates in a polarity matched HAT with the relatively weak α -C-H bond of the primary amine (BDE = $89-91 \pm 2$ kcal/mol). Although primary amines are also easily oxidizable, Stern-Volmer luminescence quenching experiments suggested the quenching rate of excited photocatalyst with azide ion to be >200 times faster than that with cyclohexylamine. This protocol was found to be highly selective for α -amine sites. The presence of other hydridic C-H bonds, such as benzylic, α -hydroxy, α -ether, α -carbamate, and α -thioether bonds, gave negligible (<5%) amounts of the regioisomers (**60.2c–60.2g**). This α -amino C-H alkylation process could be performed on a 10 g scale in a continuous flow reactor with a production rate of 1.9 g/h.

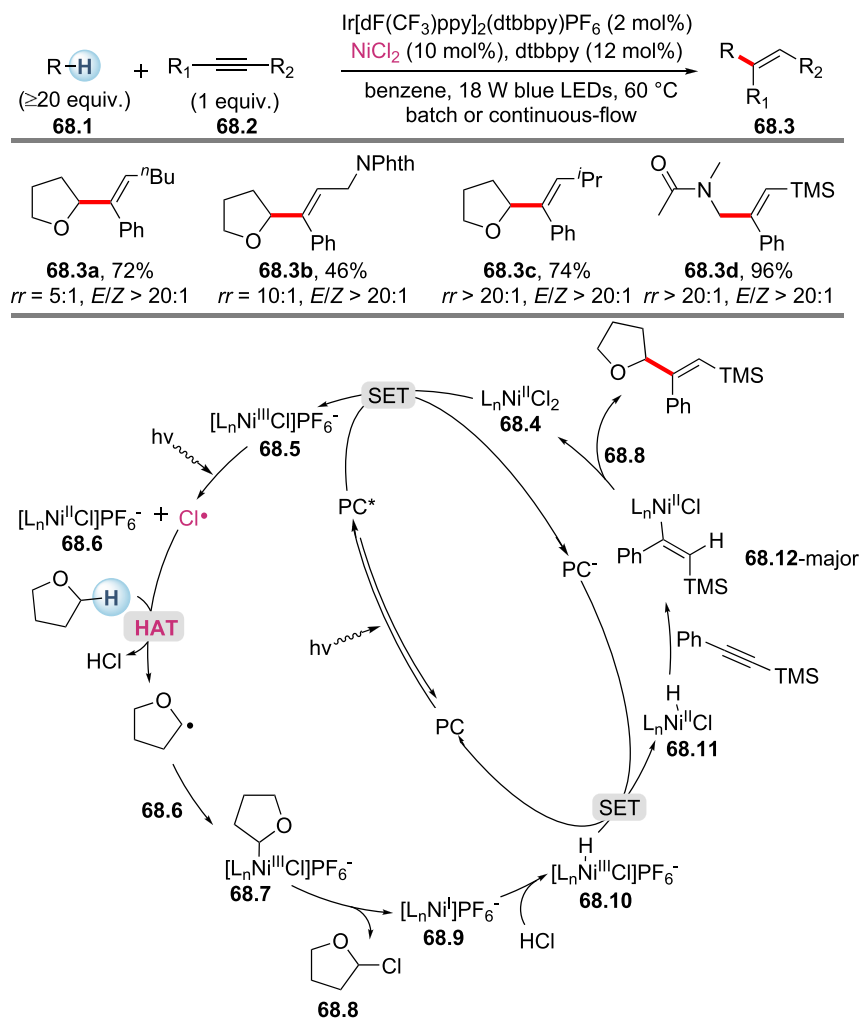
From N-X compounds

The electrophilic fluorination reagent Selectfluor can be utilized in radical fluorination, as demonstrated by Chen and co-workers in aryl ketone catalyzed benzylic C-H fluorination (Scheme 4). While Chen and co-workers presented evidence for C-H activation by excited ketones, Tan and co-workers studied anthraquinone-catalyzed C(sp³)-H fluorination with Selectfluor and proposed a different pathway involving an N-centered abstractor (Scheme 61A).¹¹⁷ After comparing several photocatalysts with various triplet energies, they proposed that an EnT event from triplet anthraquinone to singlet Selectfluor generates the triplet Selectfluor. This results in a significant lengthening of the N-F bond and subsequent formation of an N-radical dication (**61.1**), which performs the H abstraction.

The single electron reduction of Selectfluor could also produce the corresponding N-radical dication, as was reported by Wu and co-workers in 2017 (Scheme 61B).¹¹⁸ With an acridinium photoredox catalyst, benzylic C-H fluorination could be achieved using Selectfluor under visible light irradiation. Mechanistically, an SET reduction of Selectfluor ($E^{red} = -0.04$ V versus Ag/Ag⁺ in MeCN) by the excited photocatalyst ($E^{ox} = -0.57$ V versus Ag/Ag⁺ in MeCN) would afford the radical dication (**61.1**), which abstracts an H atom from the benzylic C-H bond. The benzylic radical (**61.2**) formed in this way could directly react with Selectfluor to afford the benzylic fluoride. Alternatively, **61.2** could be oxidized by PC^{•+} to generate the benzylic carbocation (**61.3**), followed by nucleophilic addition by F⁻.

In 2019, Lei and co-workers showed that under blue-light irradiation, Selectfluor can effectively promote oxidative cross-coupling between alcohols and heteroarenes (Scheme 61C).¹¹⁹ Electron paramagnetic resonance experiments suggested that visible light irradiation induces the direct N-F activation of Selectfluor (BDE for N-F 63.5 kcal/mol) to yield the corresponding N-radical dication.

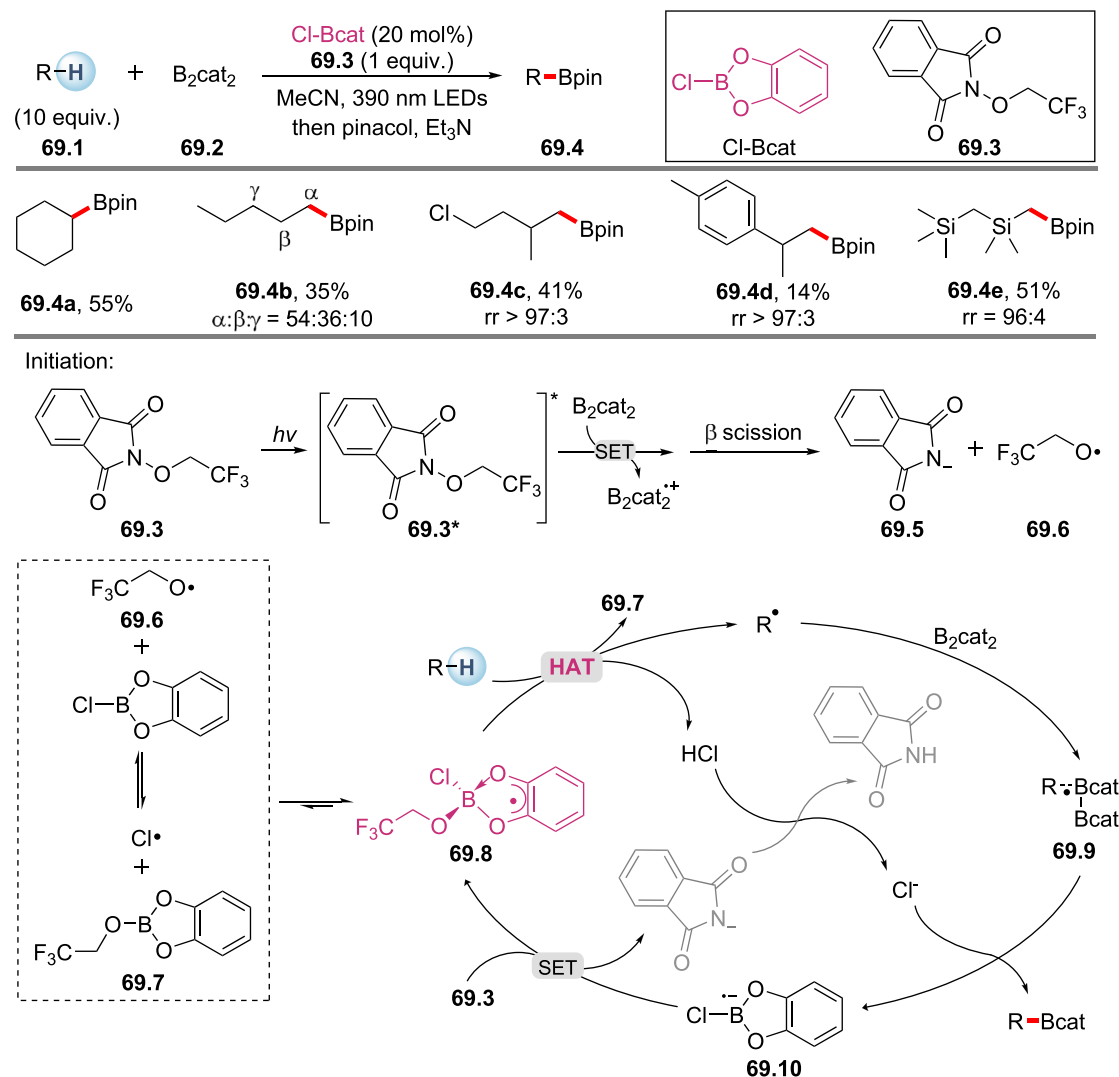
Since 2014, Alexanian and co-workers have developed a series of bench-stable N-functionalized amides (**62.2**) to achieve intermolecular C-H functionalization (Scheme 62).^{120–122} Upon photoirradiation, the amidyl radical formed (**62.4**) could undergo a HAT with a diverse array of organic substrates. Using the substrate as the limiting reagent, C-H functionalizations proceeded in generally good yields



Scheme 68. Nickel/photoredox-catalyzed hydroalkylation of internal alkynes via chlorine radicals

with high regioselectivity for sterically accessible and electron-rich C-H sites. For instance, the bromination of *trans*-1,2-dimethylcyclohexane proceeded only at the less-hindered methylene sites (**62.3b**). This is different from traditional radical bromination in which weaker tertiary C-H bonds are favored. The site-selective chlorination of (+)-sclareolide (**62.3h**) was applied to the synthesis of chlorolissoclamide, a potentially cytotoxic labdane diterpenoid. The xanthylation products can undergo a broad range of radical-mediated as well as polar bond-forming reactions, providing access to an array of C-H functionalizations such as deuteration, hydroxylation, and amination.

Post-polymerization modification without chain scission is an ideal method for the incorporation of polar groups into polyolefins. In 2018, Alexanian, Leibfarth, and co-worker demonstrated that N-xanthylamide could be applied in the metal-free C-H functionalization of branched polyolefins (Scheme 63).¹²³ Under blue-light irradiation, up to 18 mol % of polyethylene **63.1** was xanthylated using 1 equiv of **63.2** (relative to the number of repeat units) in trifluorotoluene at 25°C. Functionalization in the absence of solvent proceeded equally well. The sole side product was the ethyl xanthate dimer, which could be easily removed by polymer precipitation. A

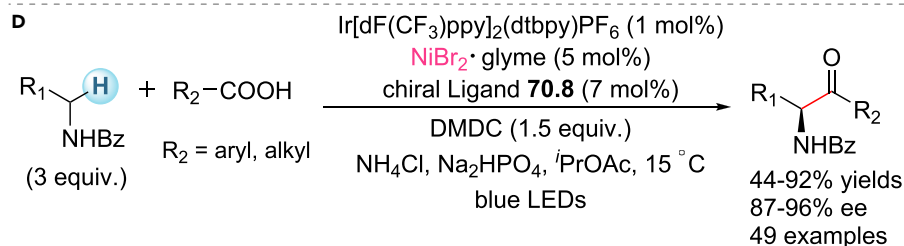
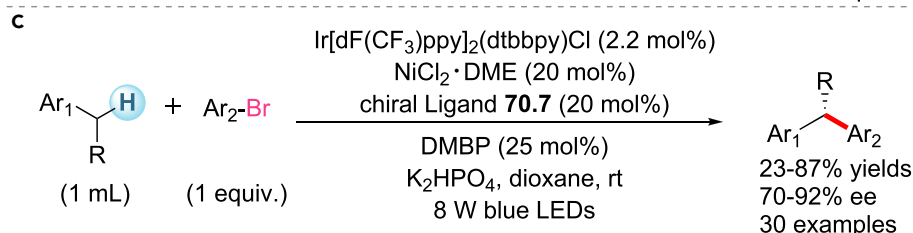
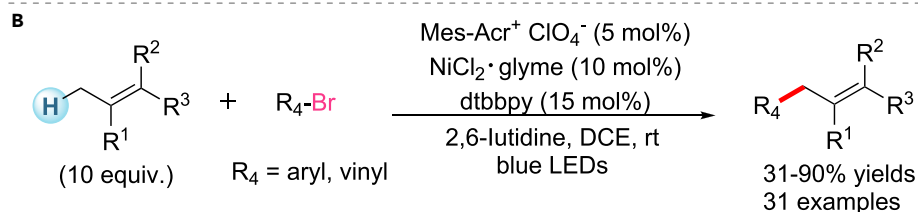
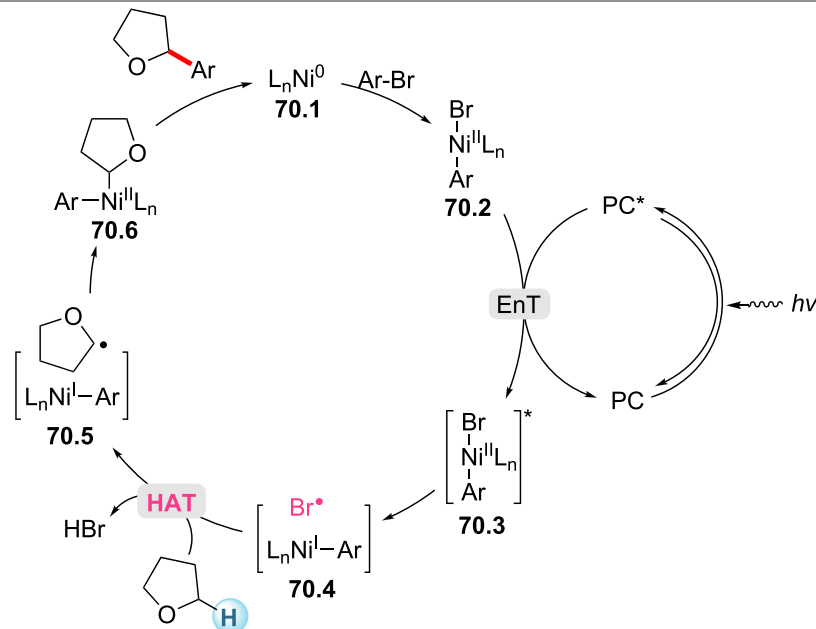
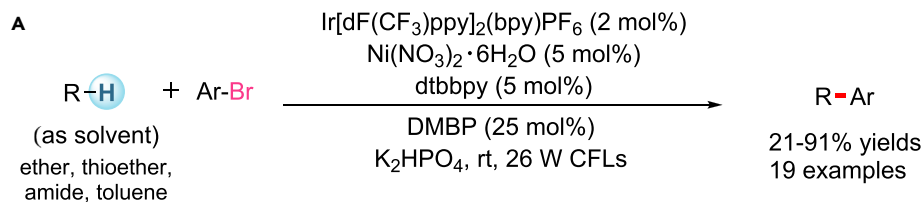


Scheme 69. Photoinduced C(sp³)-H borylation via chlorine radicals

ratio of approximately 2:1 for the secondary over primary C-H xanthylation was observed, and the sterically hindered tertiary C-H bonds of polyolefin were untouched, which prevented possible chain scission and degradation. Importantly, the xanthate group provided facile access to various functionalities (e.g., 63.4, 63.5) and could be used as handles for polymer cross-linking (63.6) and grafting (63.7).

The xanthylamide reagent 64.2 was also utilized in the O-H bond activation of carboxylic acids (Scheme 64).¹²⁴ The key step was a slightly exergonic ($\Delta G = -1.68$ kcal/mol) HAT process between the carboxylic acid O-H bond (BDE for O-H ~111 kcal/mol) and the amidyl radical derived from xanthylamide (BDE for N-H ~111 kcal/mol), which was evidenced by control experiments and kinetic and computational studies. A variety of natural products and pharmaceutical compounds can be derivatized with this method.

N-containing hypervalent iodine(III) reagents such as the Zhdankin azidoiodinane reagent could also serve as precursors to N-centered radicals through single electron



Scheme 70. Nickel/photoredox-catalyzed C(sp³)-H cross-coupling via bromine radicals

- (A) C(sp³)-H arylation with aryl bromides.¹³⁸
(B) Allylic C(sp³)-H arylation and vinylation.¹³⁹
(C) Enantioselective benzylic C(sp³)-H arylation.¹⁴⁰
(D) Enantioselective α -amino C(sp³)-H acylation.¹⁴¹ DMDC, dimethyl dicarbonate.

reduction, as reported by the group of Bolm¹²⁵ and Liu¹²⁶ in photocatalytic benzylic C-H functionalizations.

Miscellaneous examples

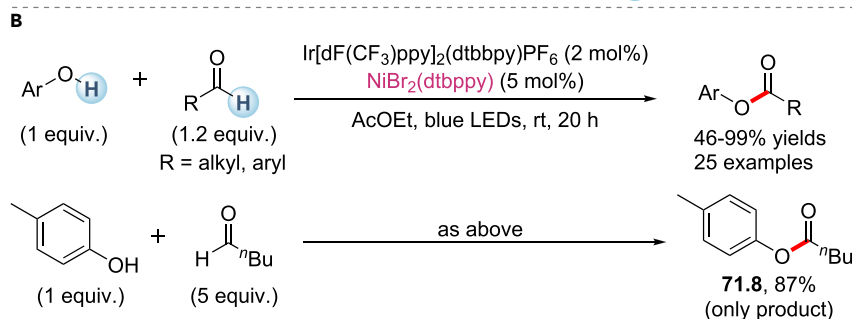
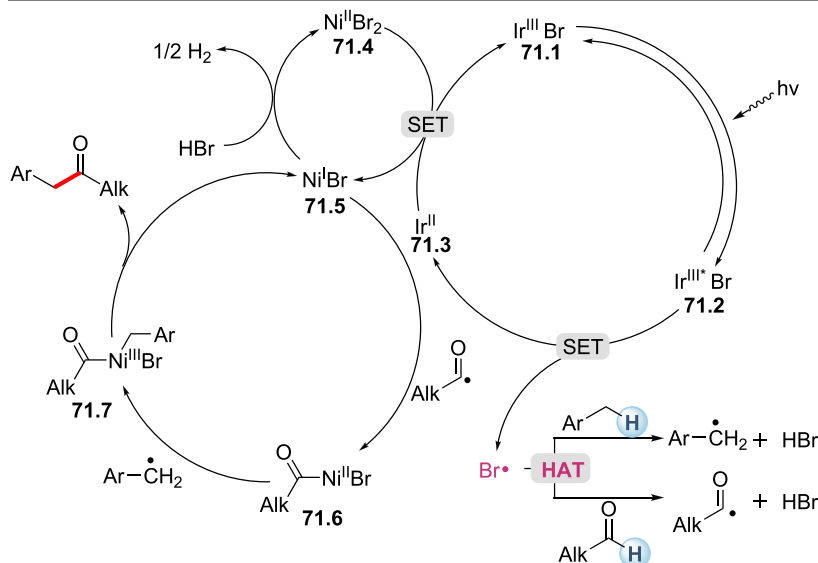
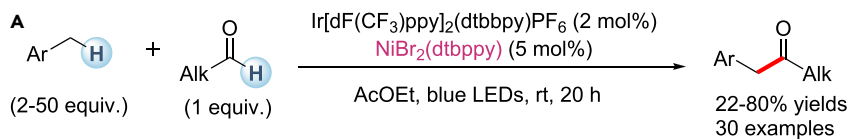
In 2020, Lambert and co-workers reported the electrophotocatalytic C-H functionalization of ethers catalyzed by a trisaminocyclopropenium cation (**65.3**) (Scheme 65).¹²⁷ Ethers underwent oxidant-free coupling with isoquinolines, alkenes, alkynes, pyrazoles, and purines selectively at the less-hindered α position. The colorless cation (**65.3**) ($E_{\text{ox}} = 1.26$ V versus saturated calomel electrode [SCE]) could be converted by anodic oxidation to the photoabsorptive radical dication (**65.5**). Photoexcitation of **65.5** then leads to intermediate **65.6** bearing aminyl radical cation character. HAT from the ether substrate to sterically hindered **65.6** affords a C radical **65.7** along with protonated dication **65.8**. The C radical (**65.7**) readily reacts with isoquinoline to produce an intermediate (**65.9**), and this was followed by a second single electron oxidation and loss of a proton to furnish the product. Meanwhile, deprotonation of the dication (**65.8**) regenerates the catalyst (**65.3**).

Cl-centered abstractors

The chlorine radical (Cl \cdot), which is classically generated by photolysis or thermolysis of chlorine gas, can react with a wide range of activated and unactivated aliphatic C-H bonds due to its electrophilic nature and the relatively large BDE of HCl (102 kcal/mol). Recent developments have focused on the photoinduced catalytic generation of chlorine radicals under mild conditions to promote selective HAT reactions.

From chloride anion

In 2018, Wu and co-workers demonstrated the use of HCl as an indirect HAT catalyst in combination with an acridinium photoredox catalyst for C-H alkylation and allylation under blue-light irradiation (Scheme 66A).¹²⁸ The utilization of microtubing reactors to maintain the volatile HCl catalyst was crucial. This protocol was effective for a variety of activated and unactivated C(sp³)-H bonds, including even ethane gas (BDE = 101.1 kcal/mol, **66.3d**). Stern-Volmer fluorescence quenching experiments suggested the HAT-active Cl \cdot could be generated from single-electron oxidation of chloride anion ($E^{\text{ox}}(\text{Cl}^-/\text{Cl}\cdot) = +2.03$ V versus SCE) by the excited acridinium photocatalyst ($E_{1/2}(\text{cat}^*/\text{cat}\cdot) = +2.06$ V versus SCE). Later, Barriault and co-workers reported the photocatalytic generation of chlorine radical from an Ir chloride complex, [Ir(dF(CF₃)ppy)₂(dtbbpy)]Cl (Scheme 66B).¹²⁹ Although this excited Ir complex is a much less effective oxidizing agent ($E_{1/2}(\text{cat}^*/\text{cat}\cdot) = +1.21$ V versus SCE), the elevated temperature and the proximity of the chloride ion could facilitate the uphill reductive quenching process. The chlorine radical formed could engage with a variety of hydridic C-H and Si-H bonds for Giese-type addition to activated alkenes. Interestingly, the observed regioselectivity for cyclopentyl methyl ether (**66.4d**) was greatly improved (from 3:1 to 10:1) toward the tertiary position by switching the reaction solvent from benzene to pyridine. Pyridine could attenuate the high reactivity of the chlorine atom through the formation of a complex (**66.5**), which represents an attractive strategy to modulate the reactivity and selectivity of HAT.



Scheme 71. Nickel/photo-catalyzed dehydrogenative coupling via bromine radicals

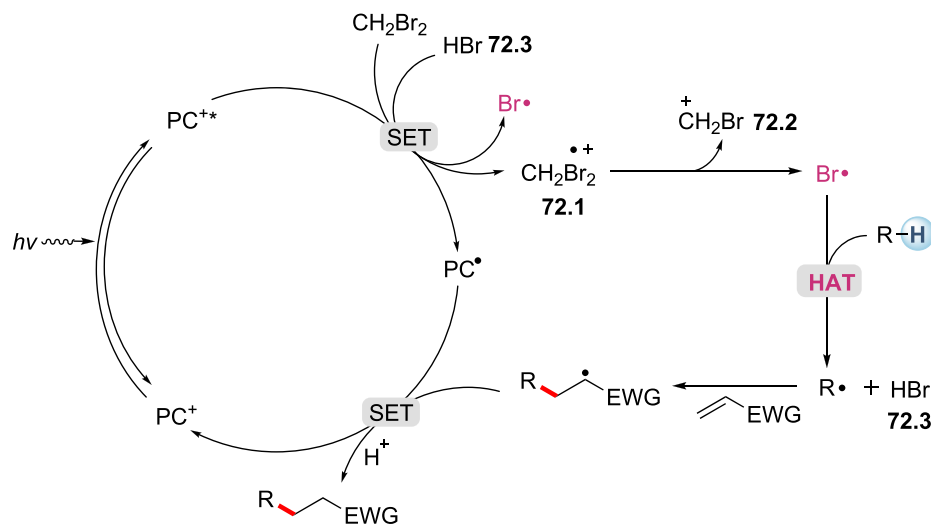
(A) Dehydrogenative coupling of benzylic and aldehydic C-H bonds.¹⁴²

(B) Dehydrogenative coupling of phenol O-H bonds and aldehydic C-H bonds.¹⁴³

Chlorine radicals also played an important role in the photoelectrochemical dehydrogenative cross-coupling of heteroarenes with aliphatic C-H bonds, as reported by Xu and co-workers.¹³⁰ Anodic oxidation of the Cl⁻ anion affords Cl₂, which produces chlorine radicals under light irradiation (392 nm). This method avoids the use of metal catalysts and chemical oxidants and demonstrates good substrate compatibility and scalability.

From Ni-Cl compounds

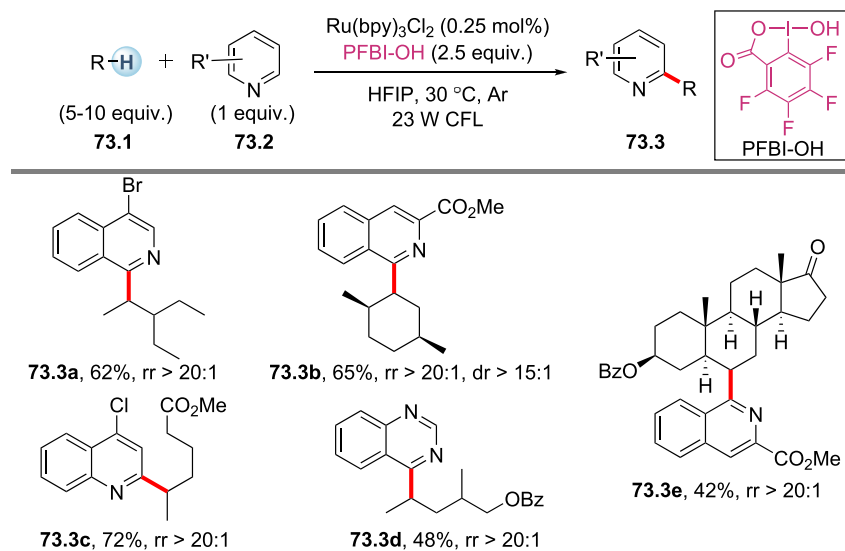
Halogen radicals can be formed by photoexcitation of high-oxidation-state transition-metal halides via dissociation from a charge-transfer excited state.¹³¹ Since 2016, Doyle and co-workers have developed a series of C(sp³)-H cross-coupling reactions based on the catalytic generation of chlorine radicals through nickel and photoredox catalysis (Scheme 67).^{132–135} Aryl or acyl chlorides serve as both cross-coupling partners and the chlorine radical source. In a typical mechanism, oxidative addition of Ni(0) 67.1 to an aryl chloride would produce the Ni(II) intermediate (67.2) (E_p = +0.85 V versus SCE), which could be oxidized by the excited Ir



Scheme 72. Photoinduced functionalizations of tertiary C(sp³)-H bonds with dibromomethane as a HAT reagent

photocatalyst ($E_{1/2} = +1.21$ V versus SCE) to produce a Ni(III) intermediate (**67.3**). Photolysis of **67.3** produces a chlorine radical and a Ni(II) species (**67.4**), and the chlorine radical readily abstracts an H atom from the ether. Reaction of the ether radical would produce the Ni(III) species (**67.6**), which affords the C(sp³)-H arylated product after reductive elimination. Finally, a single electron reduction of the resulting Ni(I) intermediate (**67.7**) ($E_p = -1.17$ V versus SCE) by the reduced Ir(II) ($E_{1/2} = -1.37$ V versus SCE) regenerates both catalysts. This catalytic system was found to be successful in C(sp³)-H arylation¹³² (Scheme 67A) and esterification¹³³ (Scheme 67C) as well as in formylation¹³⁴ (Scheme 67B) and methylation¹³⁵ (Scheme 67D) of aryl chlorides.

Chlorine radicals generated from Ni-photoredox catalysis were also employed by Wu et al. in the regioselective hydroalkylation of internal alkynes with ether and amide α -C-H bonds (Scheme 68).¹³⁶ The observed regioselectivity is complementary to that of conventional radical addition processes, and excellent regioselectivity was observed with bulkier alkyl substituents (**68.3a–68.3c**) and silyl substituents (**68.3d**). A plausible mechanism was proposed in light of the varied control experimental data. Single electron oxidation of (dtbbpy)Ni(II)Cl₂ (**68.4**) by excited Ir gives a transient Ni(III) species (**68.5**). Photolysis of the Ni(III) species (**68.5**) results in a Ni(II) species (**68.6**) and a chlorine radical, which abstracts an H atom from ether. A direct carbo-nickelation of **68.7** with alkyne is not supported by control experiments. Instead, a reductive elimination of **68.7** is proposed to deliver the ether chloride (**68.8**) and Ni(I) intermediate (**68.9**), which subsequently forms the key nickel-hydride species (**68.10**) through oxidative addition to HCl. An SET reduction of the highly



Scheme 73. Photoinduced methylene-selective arylation of alkanes via iodine-centered radical

reactive Ni(III)-H intermediate (**68.10**) by the reducing Ir(II) species affords the Ni(II)-hydride (**68.11**). Subsequent regioselective hydro-nickelation of **68.11** with the alkyne results in the less sterically hindered vinyl nickel intermediate (**68.12**-major). A final nucleophilic substitution of **68.12**-major with the ether chloride (**68.8**) generated *in situ* produces the major alkene product while regenerating the Ni(II) catalyst.

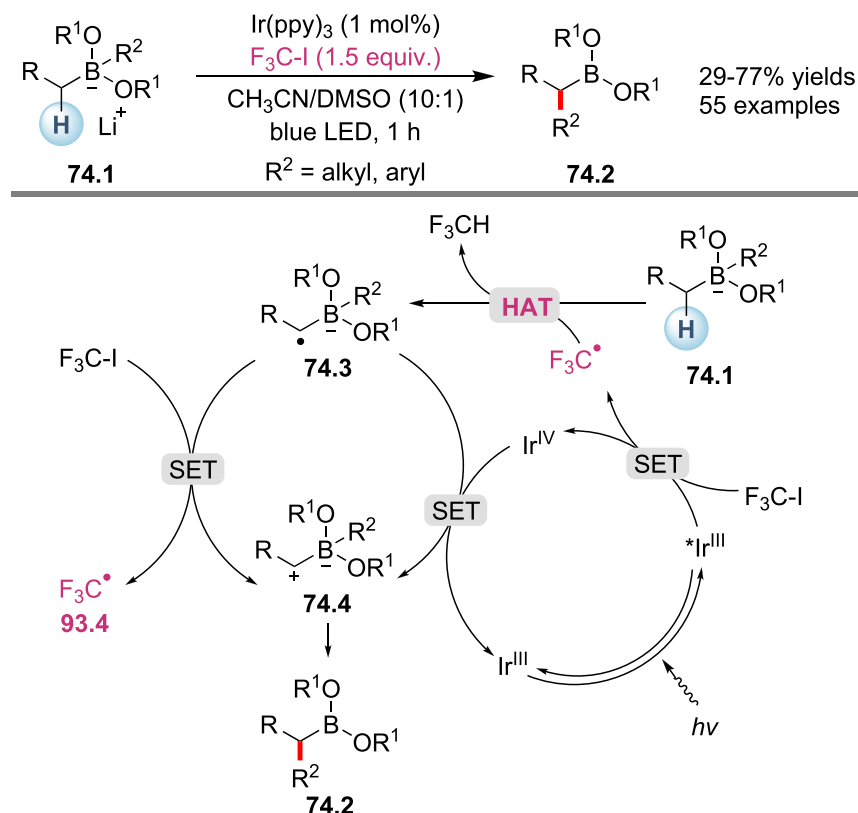
From B-Cl compounds

In 2020, Noble, Aggarwal, and co-workers disclosed a photoinduced HAT strategy for metal-free radical borylation of C(sp³)-H bonds (Scheme 69).¹³⁷ The reaction proceeded by violet-light-induced ET between an *N*-alkoxyphthalimide ester oxidant (**69.3**) and a B-chlorocatecholborane (ClBcat) HAT catalyst. With bis(catecholato)diboron ($\text{B}_2(\text{cat})_2$, **69.2**) as the limiting reagent, unactivated C(sp³)-H bonds were borylated in low to moderate yields. The products were *trans* esterified *in situ* to pinacol boronic esters owing to the instability of catechol boronic esters. Surprisingly, stronger methyl C-H bonds were borylated preferentially over weaker secondary, tertiary, and even benzylic C-H bonds (e.g., **69.4b–69.4d**). In the proposed mechanism, photoexcitation and reductive quenching of **69.3*** gives the trifluoroethoxy radical (**69.6**) after β scission. Chlorine radicals could be formed from the reaction of **69.6** with ClBcat. A sterically hindered chlorine radical-boron“ate” complex (**69.8**) was proposed as the active species for hydrogen abstraction, which accounted for the high methyl selectivity. Borylation with $\text{B}_2(\text{cat})_2$ proceeds via a radical complex (**69.9**), and cleavage of the B-B bond could be facilitated by reaction with chloride. Finally, an SET oxidation of chloride-stabilized boryl radical (**69.10**) by **69.3** regenerates **69.8**.

Br-centered abstractors

From Ni-Br

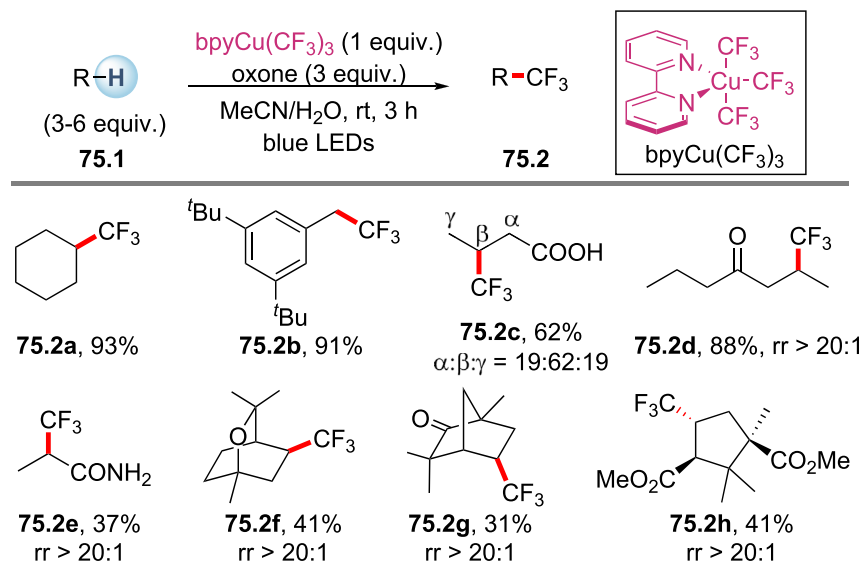
Alongside Doyle's discovery of nickel/photoredox-catalyzed C(sp³)-H arylation with aryl chlorides, Molander's group demonstrated that arylation of activated C(sp³)-H bonds could be achieved with aryl bromides through nickel catalysis and photocatalysis (Scheme 70A).¹³⁸ The reaction could proceed without the co-catalyst DMBP (4,4'-dimethoxybenzophenone), but in lower yields. Mechanistic investigations indicated a triplet-triplet EnT from excited Ir to Ni(II) species (**70.2**). A subsequent Ni-Br



Scheme 74. α functionalization of boronate complexes via trifluoromethyl radicals

homolysis of the excited-state nickel(II) complex (70.3) offers the Br radical. This is different from the generation of Cl radicals via single electron oxidation of Ni(II)-Cl and subsequent photolysis of Ni(III)-Cl (Scheme 67A). This Ni-Br strategy was utilized by Rueping and co-workers in 2018 for the cross-coupling of allylic C-H bonds with aryl- and vinylbromides (Scheme 70B).¹³⁹ More recently, enantioselective benzylic C-H arylation¹⁴⁰ (Scheme 70c) and α -amino C-H acylation¹⁴¹ (Scheme 70D) were developed using chiral bisimidazoline (70.7) and bisoxazoline (70.8) ligands, respectively.

In 2020, Ishida, Murakami, and co-workers reported photoinduced Ni-catalyzed dehydrogenative coupling between aldehydes and benzylic C-H or phenol O-H bonds (Scheme 71).^{142,143} The use of $\text{Ir}[\text{dF}(\text{CF}_3)\text{ppy}]_2(\text{dtbbpy})\text{PF}_6$ and $\text{NiBr}_2(\text{dtbbpy})$ under blue-light irradiation could provide the HAT-active bromine radicals and drive the selective cross-coupling reactions with concomitant hydrogen evolution. Anion exchange between a cationic Ir photocatalyst and nickel(II) bromide forms an Ir(III) bromide complex (71.1). When this complex is excited by light, an SET from the bromide anion to Ir(III) produces a bromine radical that could activate aldehydic and benzylic C-H bonds. The reduced Ir(II) (71.3) donates a single electron to the Ni(II) species (71.4), giving the Ni(I) species (71.5) and the Ir(III) bromide (71.1). The acyl and benzylic radicals sequentially add to the nickel(I) species (71.5) to produce a nickel(-III) complex (71.7). The following reductive elimination gives the product along with the nickel(I) species (71.5), which reacts with HBr to generate H_2 and the Ni(II)Br₂ species (71.4). Interestingly, the coupling of *p*-cresol with 5 equiv of *n*-butanal gave an



Scheme 75. Photoinduced trifluoromethylation of alkanes with $\text{bpyCu}(\text{CF}_3)_3$

ester (**71.8**) as the sole product, reflecting the lower BDE of the phenol O-H bond (~ 86 kcal/mol) compared with the benzylic C-H bond (~ 89 kcal/mol).

From dibromomethane

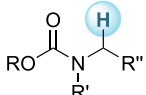
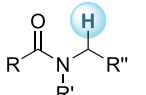
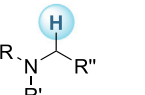
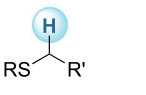
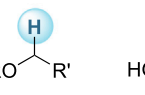
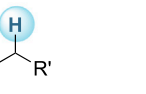
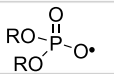
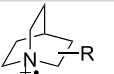
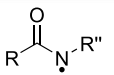
Recently, Wu and co-workers developed a visible-light-induced functionalization of unactivated $\text{C}(\text{sp}^3)\text{-H}$ bonds via the synergistic effects of an organo-photoredox catalyst and a bromine-based HAT agent (Scheme 72).¹⁴⁴ By using dibromomethane as both the solvent and the bromine radical source, the alkylation and amination of tertiary $\text{C}(\text{sp}^3)\text{-H}$ bonds were achieved in a highly selective fashion. Mechanistically, a single electron oxidation of CH_2Br_2 ($E_{1/2}^{\text{ox}} = +1.62$ V versus SCE) by an excited acridinium photocatalyst ($E_{1/2}(\text{cat}^*/\text{cat}\cdot) = +2.06$ V versus SCE) forms the CH_2Br_2 radical cation (**72.1**), which preferentially undergoes cleavage to deliver a bromine radical and a bromomethyl cation (**72.2**). Notably, because the HBr (**72.3**) generated *in situ* from the HAT process is more easily oxidized ($E_{1/2}^{\text{ox}} = +0.76$ V versus SCE) than CH_2Br_2 , HBr might act as a more reactive bromine radical source during the reaction process.

Iodine-centered abstractors

Single electron reduction or visible-light excitation of hypervalent iodine(III) reagents can generate iodine-centered radicals capable of abstracting an H atom from acyl and aliphatic C-H bonds. He et al. achieved impressive methylene selectivity in photoinduced Minisci-type alkylation reactions of *N*-heteroarenes with alkanes (Scheme 73).¹⁴⁵ More sterically accessible secondary C-H bonds were selectively arylated even in the presence of weaker tertiary C-H bonds (e.g., **73.3a**, **73.3b**, **73.3d**). The slow addition of a tertiary C radical to a heteroarene and its facile oxidation to a tertiary cation by a Ru photocatalyst may be responsible for the absence of tertiary Minisci alkylation products.

C-centered abstractors

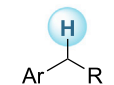
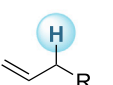
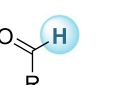
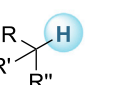
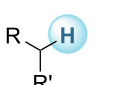
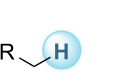
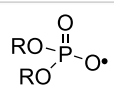

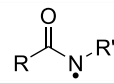
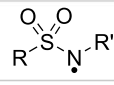
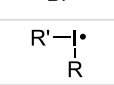
$\text{X}_3\text{C}\cdot$ radicals, where X = Br, Cl, F, could be formed via single electron reduction of $\text{X}_3\text{C-Y}$ (Y = Br, I) by excited photocatalysts. A recent example of HAT with $\text{X}_3\text{C}\cdot$ radicals was reported by Studer and co-workers, who demonstrated the α functionalization of boronated complexes (Scheme 74).¹⁴⁶ With $\text{Ir}(\text{ppy})_3$ as a photoinitiator, the

Substrate	<div style="border: 1px solid black; padding: 2px; display: inline-block;"> ✓ accessible ✓ accessible with 1 equiv. R-H </div>					
	 carbamate α -C-H	 amide α -C-H	 amine α -C-H	 thioether α -C-H	 ether α -C-H	 alcohol α -C-H
Abstractor						
benzophenone*	✓	✓	✓	✓	✓	✓
diacetyl*					✓	
neutral eosin Y*		✓	✓	✓	✓	✓
[W ₁₀ O ₃₂] ⁴⁻ *	✓	✓		✓	✓	✓
UO ₂ ²⁺ *		✓			✓	
antimony-oxo porphyrin*					✓	
PhCOO•					✓	
Alk-O•					✓	✓
	✓	✓		✓	✓	
(ROC) ₂ N-O•					✓	✓
SO ₄ ^{•-}		✓			✓	
R-S•	✓	✓	✓	✓	✓	✓
	✓	✓	✓	✓	✓	✓
	✓	✓			✓	✓
N ₃ •			✓			
Cl•	✓	✓			✓	✓
Br•		✓		✓	✓	

Scheme 76. Accessibility of activation of carbamate, amide, amine, thioether, ether, and alcohol α -C-H bonds with different hydrogen atom abstractors

electrophilic F₃C• derived from trifluoromethyl iodide could abstract an H atom from the boronate complex (74.1). This HAT process was highly selective toward the α -C-H position of the boronate complex owing to the polar effects, which is in accordance with a calculated low free energy barrier. The resulting radical anion (74.3) could be oxidized by F₃C-I to afford the zwitterion (74.4) along with the F₃C• radical. A following 1,2-alkyl/aryl migration furnishes the α -functionalized boronic ester (74.2). Alternatively, 74.3 could be oxidized by Ir(IV) species.

Very recently, Hong and co-workers took advantage of the high electrophilicity of F₃C• in the C(sp³)-H trifluoromethylation of unactivated alkanes (Scheme 75).¹⁴⁷ With 3–6 equiv of C-H substrates, various alkanes were smoothly trifluoromethylated when reacted with pica(CF₃)₃ (bpy = 2,2'-bipyridine) in the presence of Oxone

Substrate	<div style="display: flex; justify-content: space-around; align-items: center;"> ✓ accessible ✓ accessible with 1 equiv. R-H </div>					
						
Abstractor	benzylic C-H	allylic C-H	aldehyde C-H	methine C-H	methylene C-H	methyl C-H
benzophenone*	✓	✓	✓	✓	✓	
neutral eosin Y*	✓	✓	✓		✓	
[W ₁₀ O ₃₂] ^{4-*}	✓	✓	✓	✓	✓	✓
UO ₂ ²⁺			✓	✓	✓	
antimony-oxo porphyrin*			✓			
PhCOO•			✓	✓	✓	
Alk-O•	✓		✓	✓	✓	✓
	✓			✓	✓	
(ROC) ₂ N-O•	✓	✓				
SO ₄ ^{•-}			✓		✓	
NO ₃ •	✓					
R-S•	✓	✓		✓	✓	
	✓		✓	✓	✓	✓
	✓		✓	✓	✓	✓
	✓	✓				
N ₃ •	✓					
Cl•	✓	✓	✓	✓	✓	✓
Br•	✓	✓	✓	✓	✓	
	✓	✓	✓	✓	✓	
Cl ₃ C•	✓					
Br ₃ C•	✓					
F ₃ C•	✓			✓	✓	✓

Scheme 77. Accessibility of activation of benzylic, allylic, aldehyde, methine, methylene, and methyl C-H bonds with different hydrogen atom abstractors

Substrate							
	silane Si-H	phosphine oxide P-H	NHC-borane B-H	thiol S-H	sulfonic acid O-H	carboxylic acid O-H	N-sulfonyl amide N-H
benzophenone*		✓					
neutral eosin Y*	✓	✓			✓		
[W ₁₀ O ₃₂] ^{4-*}	✓						
Alk-O•		✓			✓		
							✓
R-S•	✓		✓				
	✓						
							✓
Cl•	✓						
Alk•		✓		✓			
Cl ₃ C•				✓			

Scheme 78. Accessibility of activation of Si-H, P-H, B-H, S-H, O-H, and N-H bonds with different hydrogen atom abstractors

(potassium peroxymonosulfate) under blue-light irradiation (14%–96% yields). Preference for the more hydridic and less sterically hindered methylene positions was consistently observed (75.2c–75.2h). Photoinduced homolytic cleavage of the Cu(III) complex $\text{bpyCu}(\text{CF}_3)_3$ produces $\text{F}_3\text{C}\cdot$ and a Cu(II) species, $\text{bpyCu}(\text{CF}_3)_2$. While $\text{F}_3\text{C}\cdot$ conducts HAT to give an alkyl radical, $\text{bpyCu}(\text{CF}_3)_2$ ($E^\circ_{\text{calc}} = +0.98$ V) is oxidized by Oxone ($E^\circ = +1.81$ V) to give a new Cu(III) species ($E^\circ_{\text{calc}} = +0.67$ V), which in turn oxidizes the alkyl radical to form an alkyl cation ($E^\circ_{\text{calc}} = +0.46$ V for the cyclohexyl radical). Ionic coupling of the alkyl cation with the resulting anionic Cu(II) complex that acts as a CF_3 anion source furnishes the desired product.

Apart from $\text{X}_3\text{C}\cdot$ radicals, photogenerated nucleophilic alkyl radicals are capable of abstracting hydrogen atoms from thiol S-H⁵ and phosphine P-H bonds,¹⁴⁸ while aryl radicals could cleave activated $\text{C}(\text{sp}^3)\text{-H}$ bonds through HAT.¹⁴⁹

SUMMARY OF ACCESSIBLE RADICALS AND TRANSFORMATIONS WITH DIFFERENT ABSTRACTORS

A brief summary of the patterns of R-H bonds that can be activated by certain abstractors (both direct and indirect) through photoinduced intermolecular HAT is given in Schemes 76, 77, and 78. The cases where R-H bonds are used as the limiting reagents are highlighted. Brief summaries of accessible transformations for different

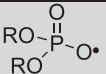
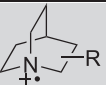
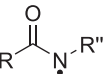
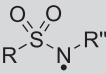
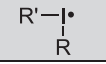
R-H bond	Available transformations through photoinduced HAT
carbamate α -C-H	<i>alkylation, allylation, arylation, alkenylation, alkynylation, cyanation, imination, azidation, oxidation, estrification</i>
amide α -C-H	<i>alkylation, allylation, arylation, alkenylation, alkynylation, acylation, cyanation, imination, thiolation</i>
amine α -C-H	<i>alkylation</i>
thioether α -C-H	<i>alkylation, allylation, cyanation, imination, thiolation</i>
ether α -C-H	<i>alkylation, allylation, arylation, alkenylation, alkynylation, acylation, cyanation, imination, carbamoylation, azidation, oxidation, estrification, fluorination, chlorination, sulfonation, thiolation, trifluoromethylthiolation, xanthylation</i>
alcohol α -C-H	<i>alkylation, allylation, arylation, alkenylation, alkynylation, cyanation, oxidation, epimerization</i>
benzylic C-H	<i>alkylation, arylation, cyanation, trifluomethylation, carboxylation, amination, azidation, oxidation, estrification, thiolation, mono-fluorination, di-fluorination, dehydrogenation</i>
allylic C-H	<i>alkylation, arylation, oxidation, thiolation</i>
aldehyde C-H	<i>deuteration, alkylation, allylation, arylation, alkenylation, amination, fluorination, trifluoromethylthiolation, difluoromethylthiolation, dehydroformylation</i>
methine C-H	<i>alkylation, allylation, arylation, alkenylation, alkynylation, cyanation, imination, amination, azidation, oxidation, estrification, thiolation, fluorination, trifluoromethylthiolation, xanthylation, chlorination, bromination, dehydrogenation</i>
methylene C-H	<i>alkylation, allylation, arylation, alkenylation, alkynylation, acylation, cyanation, imination, trifluomethylation, amination, azidation, amidation, oxidation, estrification, thiolation, fluorination, trifluoromethylthiolation, xanthylation, chlorination, bromination, dehydrogenation, borylation</i>
methyl C-H	<i>alkylation, arylation, alkenylation, trifluomethylation, amination, estrification, xanthylation, chlorination, borylation</i>
silane Si-H	<i>deuteration, alkylation, allylation, alkenylation, chlorination</i>
phosphine oxide P-H	<i>alkylation, arylation, alkenylation</i>
NHC-borane B-H	<i>alkylation, allylation, arylation, alkenylation</i>
thiol S-H	<i>alkylation, arylation</i>
sulfinic acid O-H	<i>alkylation, alkenylation</i>
carboxylic acid O-H	<i>decarboxylative xanthylation</i>
N-sulfonyl amide N-H	<i>alkylation</i>

Scheme 79. Accessible transformations of different R-H bonds through photoinduced intermolecular HAT

types of R-H bonds (Scheme 79) and different types of H atom abstractors (Scheme 80) through photoinduced intermolecular HAT are given.

SUMMARY AND OUTLOOK

Photoinduced intermolecular HAT represents a powerful and straightforward strategy for R-H (R = C, Si, etc.) bond functionalization that cannot be easily

Abstractor	Available transformations through photoinduced HAT
benzophenone*	<i>alkylation, allylation, arylation, alkenylation, alkynylation, cyanation, imination, carbamonylation, carboxylation, amination, azidation, oxidation, fluorination, sulfonation, chlorination, dehydrogenation</i>
diacetyl*	<i>arylation</i>
neutral eosin Y*	<i>alkylation, allylation, arylation, alkenylation, cyanation, oxidation, chlorination</i>
[W ₁₀ O ₃₂] ^{4-*}	<i>deuteration, alkylation, arylation, alkenylation, trifluoromethylation, oxidation, fluorination, dehydrogenation, dehydroformylation</i>
UO ₂ ^{2+*}	<i>alkylation, oxidation, fluorination</i>
antimony-oxo porphyrin*	<i>alkylation</i>
PhCOO•	<i>alkynylation, trifluoromethylthiolation</i>
Alk-O•	<i>alkylation, arylation, alkenylation, amination, oxidation, thiolation, chlorination</i>
	<i>alkylation, cyanation, azidation, fluorination, chlorination, bromination, trifluoromethylthiolation</i>
(ROC) ₂ N-O•	<i>alkylation, oxidation</i>
SO ₄ ^{•-}	<i>alkylation, arylation, alkenylation</i>
R-S•	<i>deuteration, alkylation, allylation, arylation, alkenylation, carboxylation, oxidation, thiolation, dehydrogenation</i>
	<i>alkylation, allylation, arylation, oxidation, fluorination, epimerization</i>
	<i>alkylation, amination, xanthylation, chlorination, bromination</i>
	<i>amination, arylation</i>
N ₃ •	<i>alkylation, oxidation</i>
Cl•	<i>alkylation, allylation, arylation, alkenylation, acylation, oxidation, esterification, borylation</i>
Br•	<i>alkylation, arylation, acylation, amination, bromination</i>
	<i>alkylation, arylation, alkenylation, azidation, chlorination, bromination</i>
Alk•	<i>arylation</i>
Cl ₃ C• Br ₃ C•	<i>alkylation, bromination</i>
F ₃ C•	<i>arylation, trifluoromethylation</i>

Scheme 80. Accessible transformations with different hydrogen atom abstractors through photoinduced intermolecular HAT

accomplished by other synthetic methods. In light of its rapid development in recent years, we strongly believe that photoinduced intermolecular HAT will make an enormous impact on the synthesis of fine chemicals, pharmaceutical compounds, and functional materials in both academic and industrial settings. Despite the impressive progress, much work is still required to advance the efficiency, selectivity, diversity, and economic profile of these processes. New catalytic modes, new SOMOphiles, new radical arrangements, and heterogeneous HAT catalysts are still in high demand. Improvement of HAT reactivity with simultaneous control of site selectivity is important for late-stage functionalization using C-H substrates as the limiting reagents. Asymmetric catalysis through photoinduced intermolecular HAT is still in its infancy, and is mainly limited to the use of chiral Lewis/Brønsted acids and nickel/chiral ligands. Nucleophilic hydrogen atom abstractors targeting non-hydridic C-H bonds have rarely been explored. More applications of photoinduced intermolecular HAT in natural product and pharmaceutical synthesis, polymer chemistry, material science, and biochemistry are expected.

ACKNOWLEDGMENTS

The authors are grateful for the financial support provided by the National University of Singapore (R-143-000-B60-114), the Ministry of Education (MOE) of Singapore (MOET2EP10120-0014), the Agency for Science, Technology and Research (A*STAR) of Singapore RIE2020 AME IRG (grant A20E5c0096), the National University of Singapore Flagship Green Energy Program (R-279-000-553-646 and R-279-000-553-731), the NUS (Suzhou) Research Institute, and the National Natural Science Foundation of China (grants 21871205 and 22071170).

AUTHOR CONTRIBUTIONS

Conceptualization, H.C. and J.W.; investigation, H.C., X.T., H.T., and Y.Y.; writing – original draft, H.C., X.T., H.T., and Y.Y.; writing – review & editing, H.C. and J.W.; project administration, J.W.; supervision, J.W.

DECLARATION OF INTERESTS

The authors declare no competing interests.

REFERENCES

- Darcy, J.W., Koronkiewicz, B., Parada, G.A., and Mayer, J.M. (2018). A continuum of proton-coupled electron transfer reactivity. *Acc. Chem. Res.* *51*, 2391–2399.
- Newhouse, T., and Baran, P.S. (2011). If C–H bonds could talk: selective C–H bond oxidation. *Angew. Chem. Int. Ed. Engl.* *50*, 3362–3374.
- Yi, H., Zhang, G., Wang, H., Huang, Z., Wang, J., Singh, A.K., and Lei, A. (2017). Recent advances in radical C–H activation/radical cross-coupling. *Chem. Rev.* *117*, 9016–9085.
- Wang, X., and Studer, A. (2017). Iodine (III) reagents in radical chemistry. *Acc. Chem. Res.* *50*, 1712–1724.
- Capaldo, L., and Ravelli, D. (2017). Hydrogen atom transfer (HAT): a versatile strategy for substrate activation in photocatalyzed organic synthesis. *Eur. J. Org. Chem.* *2017*, 2056–2071.
- Kärkäs, M.D. (2018). Electrochemical strategies for C–H functionalization and C–N bond formation. *Chem. Soc. Rev.* *47*, 5786–5865.
- Lewis, J.C., Coelho, P.S., and Arnold, F.H. (2011). Enzymatic functionalization of carbon–hydrogen bonds. *Chem. Soc. Rev.* *40*, 2003–2021.
- Shaw, M.H., Twilton, J., and MacMillan, D.W. (2016). Photoredox catalysis in organic chemistry. *J. Org. Chem.* *81*, 6898–6926.
- Stateman, L.M., Nakafuku, K.M., and Nagib, D.A. (2018). Remote C–H functionalization via selective hydrogen atom transfer. *Synthesis* *50*, 1569–1586.
- Gentry, E.C., and Knowles, R.R. (2016). Synthetic applications of proton-coupled electron transfer. *Acc. Chem. Res.* *49*, 1546–1556.
- Margrey, K.A., and Nicewicz, D.A. (2016). A general approach to catalytic alkene anti-Markovnikov hydrofunctionalization reactions via acridinium photoredox catalysis. *Acc. Chem. Res.* *49*, 1997–2006.
- Tedder, J.M. (1982). Which factors determine the reactivity and regioselectivity of free radical substitution and addition reactions? *Angew. Chem. Int. Ed. Engl.* *21*, 401–410.
- Turro, N.J., Ramamurthy, V., Ramamurthy, V., and Scaiano, J.C. (2009). *Principles of Molecular Photochemistry: An Introduction* (University science books).
- Albini, A., and Dichiarante, V. (2009). The 'belle époque' of photochemistry. *Photochem. Photobiol. Sci.* *8*, 248–254.
- Xia, J.B., Zhu, C., and Chen, C. (2013). Visible light-promoted metal-free C–H activation: diarylketone-catalyzed selective benzylic mono- and difluorination. *J. Am. Chem. Soc.* *135*, 17494–17500.
- Hoshikawa, T., and Inoue, M. (2013). Photoinduced direct 4-pyridination of C(sp³)–H bonds. *Chem. Sci.* *4*, 3118–3123.
- Fischer, H. (2001). The persistent radical effect: a principle for selective radical

- reactions and living radical polymerizations. *Chem. Rev.* **101**, 3581–3610.
- Kamijo, S., Hirota, M., Tao, K., Watanabe, M., and Murafuji, T. (2014). Photoinduced sulfonylation of cyclic ethers. *Tetrahedron Lett.* **55**, 5551–5554.
 - Kamijo, S., Tao, K., Takao, G., Murooka, H., and Murafuji, T. (2015). Ether derivatization via two-step protocol comprised of photochemical ethereal C–H bond chlorination and nucleophilic substitution. *Tetrahedron Lett.* **56**, 1904–1907.
 - Nagatomo, M., Yoshioka, S., and Inoue, M. (2015). Enantioselective radical alkylation of C(sp³)–H bonds using sulfoximine as a traceless chiral auxiliary. *Chem. Asian J.* **10**, 120–123.
 - Kamijo, S., Takao, G., Kamijo, K., Hirota, M., Tao, K., and Murafuji, T. (2016). Photo-induced substitutive introduction of the aldoxime functional group to carbon chains: a formal formylation of non-acidic C(sp³)–H bonds. *Angew. Chem. Int. Ed. Engl.* **55**, 9695–9699.
 - Allen, N.S., Hurley, J.P., Bannister, D., and Follows, G.W. (1992). Photochemical crosslinking of nylon-6, 6 induced by 2-substituted anthraquinones. *Eur. Polym. J.* **28**, 1309–1314.
 - Stache, E.E., Kottisch, V., and Fors, B.P. (2020). Photocontrolled radical polymerization from hydridic C–H bonds. *J. Am. Chem. Soc.* **142**, 4581–4585.
 - Porter, G., Dogra, S.K., Loutfy, R.O., Sugamori, S.E., and Yip, R.W. (1973). Triplet state of acetone in solution. Deactivation and hydrogen abstraction. *J. Chem. Soc. Faraday Trans.* **169**, 1462–1474.
 - Huang, C.Y., Li, J., Liu, W., and Li, C.J. (2019). Diacetyl as a “traceless” visible light photosensitizer in metal-free cross-dehydrogenative coupling reactions. *Chem. Sci.* **10**, 5018–5024.
 - Majek, M., and Jacobi von Wangelin, A. (2016). Mechanistic perspectives on organic photoredox catalysis for aromatic substitutions. *Acc. Chem. Res.* **49**, 2316–2327.
 - Fan, X.Z., Rong, J.W., Wu, H.L., Zhou, Q., Deng, H.P., Tan, J.D., Xue, C.W., Wu, L.Z., Tao, H.R., and Wu, J. (2018). Eosin Y as a direct hydrogen-atom transfer photocatalyst for the functionalization of C–H bonds. *Angew. Chem. Int. Ed. Engl.* **57**, 8514–8518.
 - Batistela, V.R., Pellosi, D.S., de Souza, F.D., da Costa, W.F., de Oliveira Santin, S.M., de Souza, V.R., Caetano, W., de Oliveira, H.P.M., Scaramino, I.S., and Hioka, N. (2011). pK_a determinations of xanthene derivatives in aqueous solutions by multivariate analysis applied to UV–Vis spectrophotometric data. *Spectrochim. Acta A.* **79**, 889–897.
 - Fan, X., Xiao, P., Jiao, Z., Yang, T., Dai, X., Xu, W., Tan, J.D., Cui, G., Su, H., Fang, W., et al. (2019). Neutral-eosin-Y-photocatalyzed silane chlorination using dichloromethane. *Angew. Chem. Int. Ed. Engl.* **58**, 12580–12584.
 - Yan, J., Cheo, H.W., Teo, W.K., Shi, X., Wu, H., Idres, S.B., Deng, L.W., and Wu, J. (2020). A radical smiles rearrangement promoted by neutral eosin Y as a direct hydrogen atom transfer photocatalyst. *J. Am. Chem. Soc.* **142**, 11357–11362.
 - Tzirakis, M.D., Lykakis, I.N., and Orfanopoulos, M. (2009). Decatungstate as an efficient photocatalyst in organic chemistry. *Chem. Soc. Rev.* **38**, 2609–2621.
 - Dondi, D., Fagnoni, M., and Albin, A. (2006). Tetrabutylammonium decatungstate-photosensitized alkylation of electrophilic alkenes: convenient functionalization of aliphatic C–H bonds. *Chem. Eur. J.* **12**, 4153–4163.
 - Laudadio, G., Deng, Y., van der Wal, K., Ravelli, D., Nuño, M., Fagnoni, M., Guthrie, D., Sun, Y., and Noël, T. (2020). C(sp³)–H functionalizations of light hydrocarbons using decatungstate photocatalysis in flow. *Science* **369**, 92–96.
 - Schultz, D.M., Lévesque, F., DiRocco, D.A., Reibarkh, M., Ji, Y., Joyce, L.A., Dropinski, J.F., Sheng, H., Sherry, B.D., and Davies, I.W. (2017). Oxyfunctionalization of the remote C–H bonds of aliphatic amines by decatungstate photocatalysis. *Angew. Chem. Int. Ed. Engl.* **56**, 15274–15278.
 - Laudadio, G., Govaerts, S., Wang, Y., Ravelli, D., Koolman, H.F., Fagnoni, M., Djuric, S.W., and Noël, T. (2018). Selective C(sp³)–H aerobic oxidation enabled by decatungstate photocatalysis in flow. *Angew. Chem. Int. Ed. Engl.* **57**, 4078–4082.
 - Ravelli, D., Fagnoni, M., Fukuyama, T., Nishikawa, T., and Ryu, I. (2018). Site-selective C–H functionalization by decatungstate anion photocatalysis: synergistic control by polar and steric effects expands the reaction scope. *ACS Catal.* **8**, 701–713.
 - Shi, D., He, C., Sun, W., Ming, Z., Meng, C., and Duan, C. (2016). A photosensitizing decatungstate-based MOF as heterogeneous photocatalyst for the selective C–H alkylation of aliphatic nitriles. *Chem. Commun.* **52**, 4714–4717.
 - West, J.G., Bedell, T.A., and Sorensen, E.J. (2016). The uranyl cation as a visible-light photocatalyst for C(sp³)–H fluorination. *Angew. Chem. Int. Ed. Engl.* **55**, 8923–8927.
 - Pirovano, P., Farquhar, E.R., Swart, M., and McDonald, A.R. (2016). Tuning the reactivity of terminal nickel (III)–oxygen adducts for C–H bond activation. *J. Am. Chem. Soc.* **138**, 14362–14370.
 - Capaldo, L., Merli, D., Fagnoni, M., and Ravelli, D. (2019). Visible light uranyl photocatalysis: direct C–H to C–C bond conversion. *ACS Catal.* **9**, 3054–3058.
 - Capaldo, L., Ertl, M., Fagnoni, M., Knör, G., and Ravelli, D. (2020). Antimony–oxo porphyrins as photocatalysts for redox-neutral C–H to C–C bond conversion. *ACS Catal.* **10**, 9057–9064.
 - Murphy, J.J., Bastida, D., Paria, S., Fagnoni, M., and Melchiorre, P. (2016). Asymmetric catalytic formation of quaternary carbons by iminium ion trapping of radicals. *Nature* **532**, 218–222.
 - Dong, J., Wang, X., Wang, Z., Song, H., Liu, Y., and Wang, Q. (2020). Formyl-selective deuteration of aldehydes with D₂O via synergistic organic and photoredox catalysis. *Chem. Sci.* **11**, 1026–1031.
 - Kuang, Y., Cao, H., Tang, H., Chew, J., Chen, W., Shi, X., and Wu, J. (2020). Visible light driven deuteration of formyl C–H and hydridic C(sp³)–H bonds in feedstock chemicals and pharmaceutical molecules. *Chem. Sci.* **11**, 8912–8918.
 - Roberts, B. (1999). Polarity-reversal catalysis of hydrogen-atom abstraction reactions: concepts and applications in organic chemistry. *Chem. Soc. Rev.* **28**, 25–35.
 - Li, Y., Lei, M., and Gong, L. (2019). Photocatalytic regio- and stereoselective C(sp³)–H functionalization of benzylic and allylic hydrocarbons as well as unactivated alkanes. *Nat. Catal.* **2**, 1016–1026.
 - Kuang, Y., Wang, K., Shi, X., Huang, X., Meggers, E., and Wu, J. (2019). Asymmetric synthesis of 1,4-dicarbonyl compounds from aldehydes by hydrogen atom transfer photocatalysis and chiral Lewis acid catalysis. *Angew. Chem. Int. Ed. Engl.* **58**, 16859–16863.
 - Li, F., Tian, D., Fan, Y., Lee, R., Lu, G., Yin, Y., Qiao, B., Zhao, X., Xiao, Z., and Jiang, Z. (2019). Chiral acid-catalysed enantioselective C–H functionalization of toluene and its derivatives driven by visible light. *Nat. Commun.* **10**, 1774.
 - Dai, Z.Y., Nong, Z.S., and Wang, P.S. (2020). Light-mediated asymmetric aliphatic C–H alkylation with hydrogen atom transfer catalyst and chiral phosphoric acid. *ACS Catal.* **10**, 4786–4790.
 - Twilton, J., Zhang, P., Shaw, M.H., Evans, R.W., and MacMillan, D.W. (2017). The merger of transition metal and photocatalysis. *Nat. Rev. Chem.* **1**, 0052.
 - Perry, I.B., Brewer, T.F., Sarver, P.J., Schultz, D.M., DiRocco, D.A., and MacMillan, D.W. (2018). Direct arylation of strong aliphatic C–H bonds. *Nature* **560**, 70–75.
 - Shen, Y., Gu, Y., and Martin, R. (2018). sp³C–H Arylation and alkylation enabled by the synergy of triplet excited ketones and nickel catalysts. *J. Am. Chem. Soc.* **140**, 12200–12209.
 - Dewanji, A., Krach, P.E., and Rueping, M. (2019). The dual role of benzophenone in visible-light/nickel photoredox-catalyzed C–H arylations: hydrogen-atom transfer and energy transfer. *Angew. Chem. Int. Ed. Engl.* **58**, 3566–3570.
 - Zhang, L., Si, X., Yang, Y., Zimmer, M., Witzel, S., Sekine, K., Rudolph, M., and Hashmi, A.S.K. (2019). The combination of benzaldehyde and nickel-catalyzed photoredox C(sp³)–H alkylation/arylation. *Angew. Chem. Int. Ed. Engl.* **58**, 1823–1827.
 - Fan, P., Lan, Y., Zhang, C., and Wang, C. (2020). Nickel/photo-cocatalyzed asymmetric acyl-carbamoylation of alkenes. *J. Am. Chem. Soc.* **142**, 2180–2186.
 - Ishida, N., Masuda, Y., Imamura, Y., Yamazaki, K., and Murakami, M. (2019). Carboxylation of benzylic and aliphatic C–H bonds with CO₂ induced by light/ketone/nickel. *J. Am. Chem. Soc.* **141**, 19611–19615.

57. Demarteau, J., Debuigne, A., and Detrembleur, C. (2019). Organocobalt complexes as sources of carbon-centered radicals for organic and polymer chemistries. *Chem. Rev.* *119*, 6906–6955.
58. West, J.G., Huang, D., and Sorensen, E.J. (2015). Acceptorless dehydrogenation of small molecules through cooperative base metal catalysis. *Nat. Commun.* *6*, 10093.
59. Abrams, D.J., West, J.G., and Sorensen, E.J. (2017). Toward a mild dehydroformylation using base-metal catalysis. *Chem. Sci.* *8*, 1954–1959.
60. Cao, H., Kuang, Y., Shi, X., Tan, B.B., Kwan, J.M.C., Liu, X., and Wu, J. (2020). Photoinduced site-selective alkenylation of alkanes and aldehydes with aryl alkenes. *Nat. Commun.* *11*, 1956.
61. Jones, G.H., Edwards, D.W., and Parr, D. (1976). A room temperature photochemical dehydrogenation catalyst. *J. Chem. Soc. Chem. Commun.* 969–970.
62. Sarver, P.J., Bacauanu, V., Schultz, D.M., DiRocco, D.A., Lam, Y.H., Sherer, E.C., and MacMillan, D.W. (2020). The merger of decatungstate and copper catalysis to enable aliphatic C(sp³)-H trifluoromethylation. *Nat. Chem.* *12*, 459–467.
63. Yahata, K., Sakurai, S., Hori, S., Yoshioka, S., Kaneko, Y., Hasegawa, K., and Akai, S. (2020). Coupling reaction between aldehydes and non-activated hydrocarbons via the reductive radical-polar crossover pathway. *Org. Lett.* *22*, 1199–1203.
64. Wang, L., Wang, T., Cheng, G.J., Li, X., Wei, J.J., Guo, B., Zheng, C., Chen, G., Ran, C., and Zheng, C. (2020). Direct C–H arylation of aldehydes by merging photocatalyzed hydrogen atom transfer with palladium catalysis. *ACS Catal.* *10*, 7543–7551.
65. Niu, L., Jiang, C., Liang, Y., Liu, D., Bu, F., Shi, R., Chen, H., Chowdhury, A.D., and Lei, A. (2020). Manganese-catalyzed oxidative azidation of C(sp³)-H bonds under electrophotocatalytic conditions. *J. Am. Chem. Soc.* *142*, 17693–17702.
66. Jin, J., and MacMillan, D.W. (2015). Direct α -arylation of ethers through the combination of photoredox-mediated C–H functionalization and the Minisci reaction. *Angew. Chem. Int. Ed. Engl.* *54*, 1565–1569.
67. Quint, V., Morlet-Savary, F., Lohier, J.F., Lalevee, J., Gaumont, A.C., and Lakhdar, S. (2016). Metal-free, visible light-photocatalyzed synthesis of benzo [b] phosphole oxides: synthetic and mechanistic investigations. *J. Am. Chem. Soc.* *138*, 7436–7441.
68. Zhang, P., Wang, Y., Yao, J., Wang, C., Yan, C., Antonietti, M., and Li, H. (2011). Visible-light-induced metal-free allylic oxidation utilizing a coupled photocatalytic system of g-C₃N₄ and N-hydroxy compounds. *Adv. Synth. Catal.* *353*, 1447–1451.
69. Yang, S., Zhu, S., Lu, D., and Gong, Y. (2019). Formylation of fluoroalkyl imines through visible-light-enabled H-atom transfer catalysis: access to fluorinated α -amino aldehydes. *Org. Lett.* *21*, 2019–2024.
70. Mukherjee, S., Maji, B., Tlahuext-Aca, A., and Glorius, F. (2016). Visible-light-promoted activation of unactivated C(sp³)-H bonds and their selective trifluoromethylthiolation. *J. Am. Chem. Soc.* *138*, 16200–16203.
71. Mukherjee, S., Garza-Sanchez, R.A., Tlahuext-Aca, A., and Glorius, F. (2017). Alkynylation of C(O)-H bonds enabled by photoredox-mediated hydrogen-atom transfer. *Angew. Chem. Int. Ed. Engl.* *56*, 14723–14726.
72. Mukherjee, S., Patra, T., and Glorius, F. (2018). Cooperative catalysis: a strategy to synthesize trifluoromethyl-thioesters from aldehydes. *ACS Catal.* *8*, 5842–5846.
73. Margrey, K.A., Czaplyski, W.L., Nicewicz, D.A., and Alexanian, E.J. (2018). A general strategy for aliphatic C–H functionalization enabled by organic photoredox catalysis. *J. Am. Chem. Soc.* *140*, 4213–4217.
74. Wakaki, T., Sakai, K., Enomoto, T., Kondo, M., Masaoka, S., Oisaki, K., and Kanai, M. (2018). C(sp³)-H cyanation promoted by visible-light photoredox/phosphate hybrid catalysis. *Chem. Eur. J.* *24*, 8051–8055.
75. McAtee, R.C., Noten, E.A., and Stephenson, C.R. (2020). Arene dearomatization through a catalytic N-centered radical cascade reaction. *Nat. Commun.* *11*, 2528.
76. Hering, T., Slanina, T., Hancock, A., Wille, U., and König, B. (2015). Visible light photooxidation of nitrate: the dawn of a nocturnal radical. *Chem. Commun.* *51*, 6568–6571.
77. McManus, J.B., Griffin, J.D., White, A.R., and Nicewicz, D.A. (2020). Homobenzylic oxygenation enabled by dual organic photoredox and cobalt catalysis. *J. Am. Chem. Soc.* *142*, 10325–10330.
78. Hu, A., Guo, J.J., Pan, H., and Zuo, Z. (2018). Selective functionalization of methane, ethane, and higher alkanes by cerium photocatalysis. *Science* *361*, 668–672.
79. An, Q., Wang, Z., Chen, Y., Wang, X., Zhang, K., Pan, H., Liu, W., and Zuo, Z. (2020). Cerium-catalyzed C–H functionalizations of alkanes utilizing alcohols as hydrogen atom transfer agents. *J. Am. Chem. Soc.* *142*, 6216–6226.
80. Denes, F., Pichowicz, M., Povie, G., and Renaud, P. (2014). Thiyl radicals in organic synthesis. *Chem. Rev.* *114*, 2587–2693.
81. Cuthbertson, J.D., and MacMillan, D.W. (2015). The direct arylation of allylic sp³ C–H bonds via organic and photoredox catalysis. *Nature* *519*, 74–77.
82. Meng, Q.Y., Schirmer, T.E., Berger, A.L., Donabauer, K., and König, B. (2019). Photocarboxylation of benzylic C–H bonds. *J. Am. Chem. Soc.* *141*, 11393–11397.
83. Jin, J., and MacMillan, D.W. (2015). Alcohols as alkylating agents in heteroarene C–H functionalization. *Nature* *525*, 87–90.
84. Zhao, L.M., Meng, Q.Y., Fan, X.B., Ye, C., Li, X.B., Chen, B., Ramamurthy, V., Tung, C.H., and Wu, L.Z. (2017). Photocatalysis with quantum dots and visible light: selective and efficient oxidation of alcohols to carbonyl compounds through a radical relay process in water. *Angew. Chem. Int. Ed. Engl.* *56*, 3020–3024.
85. Zhou, R., Goh, Y.Y., Liu, H., Tao, H., Li, L., and Wu, J. (2017). Visible-light-mediated metal-free hydrosilylation of alkenes through selective hydrogen atom transfer for Si–H activation. *Angew. Chem. Int. Ed. Engl.* *56*, 16621–16625.
86. Zhou, R., Li, J., Cheo, H.W., Chua, R., Zhan, G., Hou, Z., and Wu, J. (2019). Visible-light-mediated deuteration of silanes with deuterium oxide. *Chem. Sci.* *10*, 7340–7344.
87. Zhou, N., Yuan, X.A., Zhao, Y., Xie, J., and Zhu, C. (2018). Synergistic photoredox catalysis and organocatalysis for inverse hydroboration of imines. *Angew. Chem. Int. Ed. Engl.* *57*, 3990–3994.
88. Xu, W., Jiang, H., Leng, J., Ong, H.W., and Wu, J. (2020). Visible-light-induced selective defluoroborylation of polyfluoroarenes, gem-difluoroalkenes, and trifluoromethylalkenes. *Angew. Chem. Int. Ed. Engl.* *59*, 4009–4016.
89. Kim, J., Kang, B., and Hong, S.H. (2020). Direct allylic C(sp³)-H thiolation with disulfides via visible light photoredox catalysis. *ACS Catal.* *10*, 6013–6022.
90. Panferova, L.I., Zubkov, M.O., Kokorekin, V.A., Levin, V.V., and Dilmann, A.D. (2021). Using the thiyl radical for aliphatic hydrogen-atom transfer: thiolation of unactivated C–H bonds. *Angew. Chem. Int. Ed. Engl.* *60*, 2849–2854.
91. Ide, T., Barham, J.P., Fujita, M., Kawato, Y., Egami, H., and Hamashima, Y. (2018). Regio- and chemoselective Csp³-H arylation of benzylamines by single electron transfer/hydrogen atom transfer synergistic catalysis. *Chem. Sci.* *9*, 8453–8460.
92. Kato, S., Saga, Y., Kojima, M., Fuse, H., Matsunaga, S., Fukatsu, A., Kondo, M., Masaoka, S., and Kanai, M. (2017). Hybrid catalysis enabling room-temperature hydrogen gas release from N-heterocycles and tetrahydronaphthalenes. *J. Am. Chem. Soc.* *139*, 2204–2207.
93. Fuse, H., Mitsunuma, H., and Kanai, M. (2020). Catalytic acceptorless dehydrogenation of aliphatic alcohols. *J. Am. Chem. Soc.* *142*, 4493–4499.
94. Tanabe, S., Mitsunuma, H., and Kanai, M. (2020). Catalytic allylation of aldehydes using unactivated alkenes. *J. Am. Chem. Soc.* *142*, 12374–12381.
95. Xu, W., Ma, J., Yuan, X.A., Dai, J., Xie, J., and Zhu, C. (2018). Synergistic catalysis for the umpolung trifluoromethylthiolation of tertiary ethers. *Angew. Chem. Int. Ed. Engl.* *57*, 10357–10361.
96. Zhang, W., Carpenter, K.L., and Lin, S. (2020). Electrochemistry broadens the scope of flavin photocatalysis: photoelectrocatalytic oxidation of unactivated alcohols. *Angew. Chem. Int. Ed. Engl.* *59*, 409–417.
97. Jeffrey, J.L., Terrett, J.A., and MacMillan, D.W. (2015). O–H hydrogen bonding promotes H-atom transfer from α C–H bonds for C-alkylation of alcohols. *Science* *349*, 1532–1536.

98. Dimakos, V., Su, H.Y., Garrett, G.E., and Taylor, M.S. (2019). Site-selective and stereoselective C–H alkylations of carbohydrates via combined diarylborinic acid and photoredox catalysis. *J. Am. Chem. Soc.* **141**, 5149–5153.
99. Sakai, K., Oisaki, K., and Kanai, M. (2020). Identification of bond-weakening spirosilane catalyst for photoredox α -C–H alkylation of alcohols. *Adv. Synth. Catal.* **362**, 337–343.
100. Wang, Y., Carder, H.M., and Wendlandt, A.E. (2020). Synthesis of rare sugar isomers through site-selective epimerization. *Nature* **578**, 403–408.
101. Ye, J., Kalvet, I., Schoenebeck, F., and Rovis, T. (2018). Direct α -alkylation of primary aliphatic amines enabled by CO₂ and electrostatics. *Nat. Chem.* **10**, 1037–1041.
102. Ashley, M.A., Yamauchi, C., Chu, J.C., Otsuka, S., Yorimitsu, H., and Rovis, T. (2019). Photoredox-catalyzed site-selective α -C(sp³)–H alkylation of primary amine derivatives. *Angew. Chem. Int. Ed. Engl.* **58**, 4002–4006.
103. Shaw, M.H., Shurtleff, V.W., Terrett, J.A., Cuthbertson, J.D., and MacMillan, D.W. (2016). Native functionality in triple catalytic cross-coupling: sp³ C–H bonds as latent nucleophiles. *Science* **352**, 1304–1308.
104. Le, C., Liang, Y., Evans, R.W., Li, X., and MacMillan, D.W. (2017). Selective sp³ C–H alkylation via polarity-match-based cross-coupling. *Nature* **547**, 79–83.
105. Twilton, J., Christensen, M., DiRocco, D.A., Ruck, R.T., Davies, I.W., and MacMillan, D.W. (2018). Selective hydrogen atom abstraction through induced bond polarization: direct α -arylation of alcohols through photoredox, HAT, and nickel catalysis. *Angew. Chem. Int. Ed. Engl.* **57**, 5369–5373.
106. Zhang, X., and MacMillan, D.W. (2017). Direct aldehyde C–H arylation and alkylation via the combination of nickel, hydrogen atom transfer, and photoredox catalysis. *J. Am. Chem. Soc.* **139**, 11353–11356.
107. Yang, H.B., Fecue, A., and Martin, D.B. (2019). Catalyst-controlled C–H functionalization of adamantanes using selective H-atom transfer. *ACS Catal.* **9**, 5708–5715.
108. Hou, J., Ee, A., Cao, H., Ong, H.W., Xu, J.H., and Wu, J. (2018). Visible-light-mediated metal-free difunctionalization of alkenes with CO₂ and silanes or C(sp³)–H alkanes. *Angew. Chem. Int. Ed. Engl.* **57**, 17220–17224.
109. Yu, W.L., Luo, Y.C., Yan, L., Liu, D., Wang, Z.Y., and Xu, P.F. (2019). Dehydrogenative silylation of alkenes for the synthesis of substituted allylsilanes by photoredox, hydrogen-atom transfer, and cobalt catalysis. *Angew. Chem. Int. Ed. Engl.* **58**, 10941–10945.
110. Wang, H., Gao, Y., Zhou, C., and Li, G. (2020). Visible-light-driven reductive carboarylation of styrenes with CO₂ and aryl halides. *J. Am. Chem. Soc.* **142**, 8122–8129.
111. Rodríguez, R.I., Mollari, L., and Alemán, J. (2021). Light-driven enantioselective synthesis of pyrrole derivatives by a radical/polar cascade reaction. *Angew. Chem. Int. Ed. Engl.* **60**, 4555–4560.
112. Choi, G.J., Zhu, Q., Miller, D.C., Gu, C.J., and Knowles, R.R. (2016). Catalytic alkylation of remote C–H bonds enabled by proton-coupled electron transfer. *Nature* **539**, 268–271.
113. Tanaka, H., Sakai, K., Kawamura, A., Oisaki, K., and Kanai, M. (2018). Sulfonamides as new hydrogen atom transfer (HAT) catalysts for photoredox allylic and benzylic C–H arylations. *Chem. Commun.* **54**, 3215–3218.
114. Ohmatsu, K., Suzuki, R., Furukawa, Y., Sato, M., and Ooi, T. (2019). Zwitterionic 1,2,3-triazolium amidate as a catalyst for photoinduced hydrogen-atom transfer radical alkylation. *ACS Catal.* **10**, 2627–2632.
115. Pandey, G., and Laha, R. (2015). Visible-light-catalyzed direct benzylic C(sp³)–H amination reaction by cross-dehydrogenative coupling. *Angew. Chem. Int. Ed. Engl.* **54**, 14875–14879.
116. Ryder, A.S., Cunningham, W.B., Ballantyne, G., Mules, T., Kinsella, A.G., Turner-Dore, J., Alder, C.M., Edwards, L.J., McKay, B.S.J., Grayson, M.N., et al. (2020). Photocatalytic α -tertiary amine synthesis via C–H alkylation of unmasked primary amines. *Angew. Chem. Int. Ed. Engl.* **59**, 14986–14991.
117. Kee, C.W., Chin, K.F., Wong, M.W., and Tan, C.H. (2014). Selective fluorination of alkyl C–H bonds via photocatalysis. *Chem. Commun.* **50**, 8211–8214.
118. Xiang, M., Xin, Z.K., Chen, B., Tung, C.H., and Wu, L.Z. (2017). Exploring the reducing ability of organic dye (Acr⁺-Mes) for fluorination and oxidation of benzylic C(sp³)–H bonds under visible light irradiation. *Org. Lett.* **19**, 3009–3012.
119. Niu, L., Liu, J., Liang, X.A., Wang, S., and Lei, A. (2019). Visible light-induced direct α -C–H functionalization of alcohols. *Nat. Commun.* **10**, 467.
120. Schmidt, V.A., Quinn, R.K., Brusoe, A.T., and Alexanian, E.J. (2014). Site-selective aliphatic C–H bromination using *N*-bromoamides and visible light. *J. Am. Chem. Soc.* **136**, 14389–14392.
121. Quinn, R.K., Konst, Z.A., Michalak, S.E., Schmidt, Y., Szklarski, A.R., Flores, A.R., Nam, S., Horne, D.A., Vanderwal, C.D., and Alexanian, E.J. (2016). Site-selective aliphatic C–H chlorination using *N*-chloroamides enables a synthesis of chlorolissoclimide. *J. Am. Chem. Soc.* **138**, 696–702.
122. Czaplyski, W.L., Na, C.G., and Alexanian, E.J. (2016). C–H xanthylation: a synthetic platform for alkane functionalization. *J. Am. Chem. Soc.* **138**, 13854–13857.
123. Williamson, J.B., Czaplyski, W.L., Alexanian, E.J., and Leibfarth, F.A. (2018). Regioselective C–H xanthylation as a platform for polyolefin functionalization. *Angew. Chem. Int. Ed. Engl.* **57**, 6261–6265.
124. Na, C.G., Ravelli, D., and Alexanian, E.J. (2019). Direct decarboxylative functionalization of carboxylic acids via O–H hydrogen atom transfer. *J. Am. Chem. Soc.* **142**, 44–49.
125. Wang, H., Zhang, D., and Bolm, C. (2018). Sulfoximidations of benzylic C–H bonds by photocatalysis. *Angew. Chem. Int. Ed. Engl.* **57**, 5863–5866.
126. Wang, Y., Wang, N., Zhao, J., Sun, M., You, H., Fang, F., and Liu, Z.Q. (2020). Visible-light-promoted site-specific and diverse functionalization of a C(sp³)–C(sp³) bond adjacent to an arene. *ACS Catal.* **10**, 6603–6612.
127. Huang, H., Strater, Z.M., and Lambert, T.H. (2020). Electrophotocatalytic C–H functionalization of ethers with high regioselectivity. *J. Am. Chem. Soc.* **142**, 1698–1703.
128. Deng, H.P., Zhou, Q., and Wu, J. (2018). Microtubing-reactor-assisted aliphatic C–H functionalization with HCl as a hydrogen-atom-transfer catalyst precursor in conjunction with an organic photoredox catalyst. *Angew. Chem. Int. Ed. Engl.* **57**, 12661–12665.
129. Rohe, S., Morris, A.O., McCallum, T., and Barriault, L. (2018). Hydrogen atom transfer reactions via photoredox catalyzed chlorine atom generation. *Angew. Chem. Int. Ed. Engl.* **57**, 15664–15669.
130. Xu, P., Chen, P.Y., and Xu, H.C. (2020). Scalable photoelectrochemical dehydrogenative cross-coupling of heteroarenes with aliphatic C–H bonds. *Angew. Chem. Int. Ed. Engl.* **59**, 14275–14280.
131. Esswein, A.J., and Nocera, D.G. (2007). Hydrogen production by molecular photocatalysis. *Chem. Rev.* **107**, 4022–4047.
132. Shields, B.J., and Doyle, A.G. (2016). Direct C(sp³)–H cross coupling enabled by catalytic generation of chlorine radicals. *J. Am. Chem. Soc.* **138**, 12719–12722.
133. Ackerman, L.K., Martinez Alvarado, J.I., and Doyle, A.G. (2018). Direct C–C bond formation from alkanes using Ni-photoredox catalysis. *J. Am. Chem. Soc.* **140**, 14059–14063.
134. Nielsen, M.K., Shields, B.J., Liu, J., Williams, M.J., Zacuto, M.J., and Doyle, A.G. (2017). Mild, redox-neutral formylation of aryl chlorides through the photocatalytic generation of chlorine radicals. *Angew. Chem. Int. Ed. Engl.* **56**, 7191–7194.
135. Kariofillis, S.K., Shields, B.J., Tekle-Smith, M.A., Zacuto, M.J., and Doyle, A.G. (2020). Nickel/photoredox-catalyzed methylation of (hetero) aryl chlorides using trimethyl orthoformate as a methyl radical source. *J. Am. Chem. Soc.* **142**, 7683–7689.
136. Deng, H.P., Fan, X.Z., Chen, Z.H., Xu, Q.H., and Wu, J. (2017). Photoinduced nickel-catalyzed chemo- and regioselective hydroalkylation of internal alkynes with ether and amide α -hetero C(sp³)–H bonds. *J. Am. Chem. Soc.* **139**, 13579–13584.

137. Shu, C., Noble, A., and Aggarwal, V.K. (2020). Metal-free photoinduced C(sp³)-H borylation of alkanes. *Nature* 586, 714–719.
138. Heitz, D.R., Tellis, J.C., and Molander, G.A. (2016). Photochemical nickel-catalyzed C-H arylation: synthetic scope and mechanistic investigations. *J. Am. Chem. Soc.* 138, 12715–12718.
139. Huang, L., and Rueping, M. (2018). Direct cross-coupling of allylic C(sp³)-H bonds with aryl- and vinylbromides by combined nickel and visible-light catalysis. *Angew. Chem. Int. Ed. Engl.* 57, 10333–10337.
140. Cheng, X., Lu, H., and Lu, Z. (2019). Enantioselective benzylic C-H arylation via photoredox and nickel dual catalysis. *Nat. Commun.* 10, 3549.
141. Shu, X., Huan, L., Huang, Q., and Huo, H. (2020). Direct enantioselective C(sp³)-H acylation for the synthesis of α -amino ketones. *J. Am. Chem. Soc.* 142, 19058–19064.
142. Kawasaki, T., Ishida, N., and Murakami, M. (2020). Dehydrogenative coupling of benzylic and aldehydic C-H bonds. *J. Am. Chem. Soc.* 142, 3366–3370.
143. Kawasaki, T., Ishida, N., and Murakami, M. (2020). Photoinduced specific acylation of phenolic hydroxy groups with aldehydes. *Angew. Chem. Int. Ed. Engl.* 59, 18267–18271.
144. Jia, P., Li, Q., Poh, W.C., Jiang, H., Liu, H., Deng, H., and Wu, J. (2020). Light-promoted bromine-radical-mediated selective alkylation and amination of unactivated C(sp³)-H bonds. *Chem* 6, 1766–1776.
145. Li, G.X., Hu, X., He, G., and Chen, G. (2018). Photoredox-mediated Minisci-type alkylation of *N*-heteroarenes with alkanes with high methylene selectivity. *ACS Catal.* 8, 11847–11853.
146. Wang, D., Mück-Lichtenfeld, C., and Studer, A. (2019). Hydrogen atom transfer induced boron retaining coupling of organoboronic esters and organolithium reagents. *J. Am. Chem. Soc.* 141, 14126–14130.
147. Choi, G., Lee, G.S., Park, B., Kim, D., and Hong, S.H. (2021). Direct C(sp³)-H trifluoromethylation of unactivated alkanes enabled by multifunctional trifluoromethyl copper complexes. *Angew. Chem. Int. Ed. Engl.* 60, 5467–5474.
148. Arockiam, P.B., Lennert, U., Graf, C., Rothfelder, R., Scott, D.J., Fischer, T.G., Zeitler, K., and Wolf, R. (2020). Versatile visible-light-driven synthesis of asymmetrical phosphines and phosphonium salts. *Chem. Eur. J.* 26, 16374–16382.
149. Kang, J., Hwang, H.S., Soni, V.K., and Cho, E.J. (2020). Direct C(sp³)-N radical coupling: photocatalytic C-H functionalization by unconventional intermolecular hydrogen atom transfer to aryl radical. *Org. Lett.* 22, 6112–6116.